5th FISC

SECTION 8

STREAM MODELING

Page

ESTIMATING BED-LOAD DISCHARGE IN A COBBLE BED RIVER --
Brad R. Hall..... 8-1
COMPARISON OF SEDIMENT TRANSPORT FUNCTIONS --
Ronald R. Copeland..... 8-7
MODELING SEDIMENT DEPOSITION NEAR LOCKS AND DAMS --
Bradley M. Comes..... 8-14
MASS-WASTING ALGORITHMS IN AN ALLUVIAL CHANNEL MODEL --
Andrew Simon, William J. Wolfe and Albert Molina..... 8-22
NUMERICAL MODELING OF UNSTEADY SEDIMENT-LADEN FLOW --
Chintu Lai..... 8-30
USE OF 2-D HYDRODYNAMIC AND 1-D SEDIMENT MODELS --
James C. Thompson, David T. Williams and Jeffrey B. Bradley..... 8-38
SIMULATION OF BED TOPOGRAPHY IN A MEANDERING RIVER --
Howard Chang..... 8-46
PHYSICAL MODELING OF SEDIMENT TRANSPORT IN CHINA --
Guoren Dou..... 8-54
DESIGN OF SEDIMENT MODELS --
Cliff A. Pugh and Russell A. Dodge..... 8-61
SEDIMENT STUDIES AT UNION AVENUE DAM - DENVER, COLORADO --
Cassie C. Klumpp..... 8-69
SIMULATION OF SEDIMENT TRANSPORT NEAR STRUCTURES --
Sam S. Y. Wang, Phil Combs and Joseph Letter..... 8-77
MODELING OF SPATIALLY-VARYING VELOCITY DISTRIBUTION --
Chao-Lin Chiu, Weinzu Yu and Randy D. Crissman..... 8-85
BRI-STARS MODEL FOR ALLUVIAL RIVER SIMULATIONS --
A. Molinas and R. E. Trent..... 8-93
MODELING SEDIMENT TRANSPORT IN AN EPHEMERAL RIVER --
David W. Hynman, Richard A. Roberts and Robert H. Webb..... 8-101
ESTIMATING VELOCITIES AND SCOUR DEPTH IN RIVER CHANNEL BENDS --
Drew C. Baird and David G. Achterberg..... 8-109
NUMERICAL SIMULATION OF TRANSIENT SEDIMENT LADEN FLOW IN
AN ALLUVIAL CHANNEL --
Jinn-Chuang Yang and Kuan-Ping Chiu..... 8-117

ESTIMATING BED-LOAD DISCHARGE IN A COBBLE BED RIVER

By Brad R. Hall, Research Hydraulic Engineer, Hydraulics Laboratory, US Army Engineer Waterways Experiment Station, Vicksburg, Mississippi.

ABSTRACT

The Hydraulics Laboratory, US Army Engineer Waterways Experiment Station, is quantifying the existing condition sedimentation regime of the Truckee River at Reno, Nevada, in support of channel design modifications for flood control. The sedimentation analysis was complicated by the cobble-sized bed materials found in the channel, several existing bridges in the study area that significantly affect the channel hydraulics at flood discharge, and water diversion drop structures which provide local storage zones for bed-load transport. Bed-load measurements on the Truckee River at the upstream end of the study reach were not available. The sediment inflow load was determined by calculating the equilibrium sediment transport rate for a range of flow rates for a reach of the Truckee River within the study area featuring similar hydraulic characteristics of the river channel immediately upstream of the study area. This reach of river, called the equilibrium reach, is geomorphically stable and exhibits similar characteristics in channel planform, bed material, and channel bank characteristics as that portion of the Truckee River immediately upstream of the study area. The one-dimensional sediment transport model "Sedimentation in Stream Networks" was used to quantify sedimentation processes in the study reach. Sedimentation model adjustment was completed by comparing observed rating curve changes due to channel aggradation with computed shifts in the rating curve. Average annual and design flood sediment inflow and sedimentation in the study area were quantified with the TABS-1 model.

INTRODUCTION

Study Area

The Truckee River study reach is located near Reno, Nevada, and extends from the Vista gage at approximately River Mile (RM) 43.9 to just upstream of the Booth Street bridge at RM 53.0. A map of the study area is shown in Figure 1. The Truckee River is a perennial stream characterized by pool and riffle channel morphology. Several bridge crossings and water diversion structures are found in the study reach. Man-made channel modifications have limited the amount of channel migration in the upper 3 miles of the study reach. Bed material size decreases through the reach, and the channel bed is armored at base flow discharge.

Approach

The US Army Engineer Waterways Experiment Station computer program "Sedimentation in Stream Networks," TABS-1, was used to investigate the channel conditions and quantify channel response to discharge variations. A detailed description of the assumptions, limitations, and data requirements for the TABS-1 model is provided in Appendix A of Copeland and Thomas (1989). The study combined a theoretical treatment of the sediment transport processes with observed channel morphology to quantify channel bed dynamics associated with gravel and boulder fluvial processes. In addition to quantifying

instantaneous sediment transport rates, the analysis allowed evaluation of channel response to long term hydrologic sequences.

FIELD DATA

Hydrologic and Geometric Data

Three United States Geological Survey (USGS) stream gages are operated on the Truckee River study reach. The gage locations are shown in Figure 1. Geometry was developed from channel and overbank surveys completed in 1975. Bridge geometry was surveyed in 1989 including low and high chord profiles, bridge pier location, and channel bed elevations.

Suspended Sediment

Suspended sediment concentration has been sampled on a sporadic basis in the Reno, Nevada, area. Suspended sediment concentration and discharge have been sampled on the Truckee River at Reno and points downstream as part of water quality and water supply studies. Provisional records indicate that the maximum concentration sampled for the Truckee River in the study reach is 1340 mg/l at a discharge of approximately 14,000 cfs. Sampled suspended sediment concentration versus flow rate and a power regression of the data are plotted in Figure 2.

Bed Material Samples and Gradation

Bed material samples were collected from the channel bed, bars, and bank at 15 locations along the 9-mile study reach in June 1989. In addition, Wolman count (Wolman, 1954) bed surface material gradations were collected (Water Engineering and Technology, Inc., 1989). The Wolman count provides an estimate of the surficial coverage of the channel bed by coarse grain sediments (i.e., cobbles) which are generally omitted in bulk material samples. Bed material grain diameters ranged from 512 mm to 0.0625 mm.

SEDIMENTATION ANALYSIS

Bed-load Assessment

Geomorphic analysis of the Truckee River indicates that sediment storage is progressing between RM 50.6 and RM 46.7 (Water Engineering and Technology, Inc., 1989). The sediments depositing in this reach of the river are characterized as cobble-gravel mixture, with minor amounts of interstitial sand. The mode of transport of these large sized sediments is bed-load transport. To assess the rate of bed-load deposition, an analysis of measured hydraulic changes and a numerical assessment of the bed-load transport rate through the study area were performed.

Stability of the Truckee River at Reno Stage-Discharge Curve

The stage-discharge rating curve developed by the USGS for the Truckee River at Reno, Nevada, was reviewed for any significant changes in the rating. The gage is located near the Highway 395 bridge at approximately RM 50.6. The measurements indicate a very stable stage-discharge relationship through 1977. After 1977, a slight increase in stage over time for low discharges can be

detected. The rating curves indicate that for discharges less than 1,000 cfs, the stage has increased approximately 0.5 ft at the gage. The increase in stage for a given discharge rapidly diminishes for discharges greater than 1,000 cfs.

Sedimentation Assessment

Two modifications to the TABS-1 model were developed for this study. The first modification accounts for the presence of bridge piers and spans in the geometric calculations for additional wetted perimeter and reduced flow area at bridge cross sections. The calculations are similar to the "normal bridge" method in the HEC-2 Water Surface Profile model (US Army Engineer Hydrologic Engineering Center, 1982). The second modification allows for increasing the maximum transportable grain size in the computations. The maximum transportable grain size in previous versions of TABS-1 was 64 mm. A significant amount of the bed material in the study area is of a nominal diameter much greater than 64 mm. Thirteen grain size classes between 0.0625 mm and 512 mm were used in this study.

Hydraulic Roughness

Estimates of the sediment transport potential are dependent upon the proper designation of the hydraulic roughness. The roughness coefficients used for the channel portion of the hydraulic calculations were estimated with the analytical roughness predictors contained in the "Hydraulic Design Package for Flood Control Channels (SAM)," version 2.3, dated 25 October 1989. The SAM algorithm computes a Manning's n value based on bed material grain size distribution, and the relative roughness of the bed material to the channel hydraulic conditions. The Manning's n is calculated using the roughness predictor developed by either Brownlie (1983) or Limerinos (1970). The Limerinos relationship is better suited to roughness prediction for coarse grained channels with no significant bed forms. The computed values of Manning's n are 0.029 for the river reach from Vista gage (RM 43.9) to the Steamboat Creek confluence (RM 45.2), 0.035 from Steamboat Creek to the Lake Street Bridge (RM 51.9), 0.030 from Lake Street Bridge to Arlington Street Bridge (RM 52.3), and 0.035 upstream of Arlington Street Bridge.

Determination of Inflow Sediment Load

Since bed-load measurements on the Truckee River at the upstream end of the study reach were not available, the sediment inflow load to the study area was determined by calculating the equilibrium sediment transport rate for a range of flow rates for a reach of the Truckee River within the study area that has similar hydraulic characteristics to the river channel immediately upstream of the study area. This reach of river is termed the "equilibrium reach" and the portion of the Truckee River from approximately RM 50.5 to 51.5 exhibits similar characteristics in channel planform, bed material, and channel bank characteristics to that portion of the Truckee River immediately upstream of the study area.

Determining the equilibrium bed-load quantity requires an iterative application of TABS-1 to the equilibrium reach until the estimated inflowing load for all size classes to the equilibrium reach is nearly equal to the transport capacity (by size class) at each cross section in the reach after

bed elevation changes have stabilized. Excessive scour should not be computed in equilibrium reach calculations since excessive scour indicates that the coarse bed materials are being removed from the bed and the channel is not armoring. The Wolman count bed material gradations indicate that the bed is well armored by cobble size sediments. The bed gradation at the end of the equilibrium reach calculations should be similar to the bed material gradation at the beginning of the simulation. If this condition is met, then the bed material gradation is in equilibrium with the computed transport rate. The equilibrium sediment load for discharges of 1,000, 10,000, and 30,000 cfs for a simulated duration of 30 days at 0.1-day time steps for several sediment transport relationships was computed. The bed-load transport rates predicted by the Meyer-Peter and Muller equation provided uniform bed-load transport throughout the equilibrium reach.

To properly quantify bed-load transport, the appropriate value of dimensionless critical shear stress, T_c , for coarse grained sediments must be used. Published research on T_c values for gravel transport indicates that there is a wide variability in the appropriate value. A practical application of the Meyer-Peter and Muller bed-load transport equation in a steep gravel-bed river is given in Carson and Griffiths (1989). They determined that raising T_c in the Meyer-Peter and Muller bed-load transport equation from 0.047 to 0.059 gave the best agreement for observed gravel transport on a braided gravel-bed river of channel slope 0.0048. Wiberg and Smith (1987) developed an analytical method of computing T_c for coarse, mixed grain size bed sediments. Their results indicate that T_c for sediments with the characteristics of Truckee River riffles is in the range of 0.03 to 0.06. Boulder transport due to a dambreak flood surge on the Rubicon River in California was analyzed by Scott and Gravlee (1968). They determined the maximum tractive force at several locations by measuring the water surface slope, the depth of flow, and the diameter of the maximum size boulder that was moved by the flood surge. The T_c values for boulder transport determined by Scott and Gravlee are plotted in Figure 3. Due to the variability of computed and measured values of T_c on gravel and boulder bed rivers, no reason for decreasing the recommended value of T_c of 0.047 in the Meyer-Peter and Muller bed-load transport equation for computing sediment transport could be justified for this study. The equilibrium reach bed-load transport rating curve is given in Figure 4.

Estimate of the Average Annual Bed Load

A hydrograph that approximates the average annual hydrograph for the Truckee River at Reno was simulated. The average annual hydrograph was simulated for a 9-year period to compare computed with measured shifts in the stage-discharge rating curve for the Truckee River at Reno gage. The results indicate that extensive deposition occurs at the downstream portion of the study area. The computed rating curve shift for the 9-year simulation period for the Truckee River at Reno Gage also indicates aggradation at the gage location in excess of the measured gage shift.

The 9-year simulation results using the equilibrium reach bed load indicate that the computed bed-load transport into the study area is excessive. The total bed-load transport rating curve was adjusted until a better match was obtained between computed and observed sediment deposition quantities and zones, as measured by bed elevation changes through the study area after the

9-year simulation period and reasonable changes in both magnitude and trend in the observed rating curve shift at the Truckee River at Reno gage. The sediment inflow rating curve was adjusted downward to 33 percent of the bed-load transport rate computed from the equilibrium reach.

The computed rating curve shift for the Truckee River at Reno gage using the adjusted bed-load inflow rating curve is given as follows.

Flow rate, cfs	Computed Shift, ft	Observed Shift, ft
707.	1.4	0.5
1410.	0.8	0.3
2450.	0.1	0.2
5480.	0.0	0.1

The 9-year sedimentation analysis of the study reach provides a means for estimating the average annual bed-load transport at several locations. The TABS-1 results indicate sedimentation storage between RM 47.3 and RM 44.4. The average annual bed load at the upstream study limit, RM 47.3, RM 44.4, and the downstream study limit are tabulated below. The computed average annual bed-load inflow to the study reach is approximately 51,000 tons per year. Sampled suspended sediment concentration in the study reach indicated an average annual suspended sediment discharge of 250,000 tons per year. The computed bed-load discharge is approximately 17 percent of the total sediment discharge. The computed average annual trap efficiency for bed load of the study reach is 71 percent.

Bed Load, tons per year

Location	Sand	Gravel	Cobble	Total
RM 53.1	28,960	22,040	17	51,000
RM 47.3	24,420	20,130	0	44,550
RM 44.4	14,150	2,690	0	16,840
RM 43.9	12,820	1,940	0	14,760

SUMMARY AND CONCLUSIONS

Assessment of channel stability on instantaneous hydraulic conditions (e.g., shear stress, depth-averaged velocity, and stream power) does not consider long term sediment transport conditions, and does not address the effects of sediment inflow to the study area on channel stability. Channel changes result from the balance of sediment transport into a reach, the sediment transport capacity of the reach, and the sediment availability in the reach. Simulation of the sediment transport through the project reach is required to address the sediment balance and subsequent channel stability.

Sediment transport theory was combined with evidence developed from field reconnaissance to quantify the bed-load inflow rating curve for the Truckee River at Reno, Nevada. The technique used is called the equilibrium reach method, and develops the sediment load based on sediment transport theory, channel thalweg stability, and bed material gradation stability. The bed-load inflow rating curve was adjusted downward to 33 percent of the equilibrium reach sediment inflow. TABS-1 simulation using the adjusted sediment load inflow rating curve resulted in reasonable agreement between observed and computed rating curve shifts for the time period of 1977 and 1986 for the USGS

Truckee River at Reno gage. The Meyer-Peter and Muller bed-load transport equation is a reasonable estimator of bed-load transport for the study reach. Incorporation of cobble-sized bed material in the sediment transport computations simulates the armoring and reduction of bed material availability for transport.

ACKNOWLEDGEMENTS

The tests described and the resulting data presented herein, unless otherwise noted, were obtained from research conducted under the Civil Works Program of the United States Army Corps of Engineers by the US Army Engineer Waterways Experiment Station. Permission was granted by the Chief of Engineers to publish this information.

REFERENCES

Brownlie, W. R., 1983, Flow depth in sand-bed channels. Journal of the Hydraulics Division, American Society of Civil Engineers 109, 959-990.

Carson, M. A. and Griffiths, G. A., 1989, Gravel transport in the braided Waimakariri River: mechanisms, measurements and predictions. Journal of Hydrology 109, 201-220.

Copeland, R. R. and Thomas, W. A., 1989, Corte Madera Creek sedimentation study. Technical Report HL-89-6, US Army Engineer Waterways Experiment Station, Vicksburg, Mississippi.

Limerinos, J. T., 1970, Determination of the Manning coefficient from measured bed roughness in natural channels. Water Supply Paper 1989-B, US Geological Survey, US Government Printing Office, Washington, D.C.

Scott, K. M. and Gravlee, G. C., 1968, Flood surge on the Rubicon River, California - hydrology, hydraulics and boulder transport. Professional Paper 422-M, US Geological Survey, US Government Printing Office, Washington, D.C.

US Army Engineer Hydrologic Engineering Center, 1982, HEC-2, Water surface profiles users manual. US Army Engineer Hydrologic Engineering Center, Davis, California.

Water Engineering and Technology, Inc., 1989, Geomorphic analysis of Truckee River from RM 56 to RM 43, Draft report. US Army Engineer District, Sacramento.

Wiberg, P. L. and Smith, J. D., 1987, Calculations of the critical shear stress for motion of heterogenous sediments. Water Resources Research 23, 1471-1480.

Wolman, M. G., 1954, A method of sampling coarse river bed materials. American Geophysical Union, Transactions, 35, 951-956.

COMPARISON OF SEDIMENT TRANSPORT FUNCTIONS

By Ronald R. Copeland, Research Hydraulic Engineer, Waterways Experiment Station, Vicksburg, Mississippi.

ABSTRACT

A numerical model study of the Waimea River was conducted to evaluate aggradation problems adjacent to a Corps of Engineers levee, and to determine if the flood control capability was reduced. The TABS-1 one-dimensional numerical model was used. Sediment inflow data were not available and therefore were used as an adjustment parameter in the numerical model. Model adjustments were made in an attempt to reproduce measured historical periods of both aggradation and degradation. Comparisons of multiple and single grain size sediment transport functions were made. Significantly different sediment inflow adjustments were required for the different transport functions. Longitudinal distribution of sediment deposition was also different for the different functions. Using a single grain size function, the numerical model could not be adjusted to simulate both the aggradation and degradation periods. However, the model was successfully adjusted to both historical surveys using a multiple grain size function.

INTRODUCTION

The Waimea River drains an area of approximately 85 square miles on the island of Kauai, Hawaii. Rainfall over the basin is highly variable, between 460 and 22 inches per year, and runoff in the river is flashy, with flood durations of only a few hours. The largest tributary is the Makaweli River, which joins the Waimea about 1.1 miles from its mouth and has a drainage area of about 26 square miles. The town of Waimea is located on the Waimea River's floodplain.

Flood control improvements, constructed in the early 1950's, included channel excavation and widening and construction of a levee with a grouted riprap lining along the right descending bank. In 1984, the Corps of Engineers completed an extension of the levee from the existing downstream terminus to the ocean. The project was designed to provide flood protection from the 100-year flood of 64,000 cfs.

Between channel surveys conducted in January 1979 and November 1987, about 83,500 cu yd of sediment deposited in the Waimea River. This raised concerns about the ability of the flood control project to convey the design flood. The numerical model study was performed to evaluate long-term deposition patterns in the leveed reach of the Waimea River and to predict deposition patterns during a major flood event.

The TABS-1 one-dimensional sedimentation program, developed by William A. Thomas (Thomas 1980, 1982), was used to develop the numerical model for this study. The program produces a one-dimensional model that simulates the response of the riverbed profile to sediment inflow, bed material gradation, and hydraulic parameters. The model simulates a series of steady-state discharge events and their effects on the sediment transport capacity at cross sections and the resulting degradation or aggradation.

NUMERICAL MODEL

The numerical model is constructed using geometric, hydrologic, bed material, and sediment inflow data. The study reach extended from sta 0+00 at the mouth of the Waimea River to sta 90+00. The initial channel geometry for the model was based on cross sections surveyed in January 1979. Historical hydrographs were based on data from US Geological Survey gages on the Waimea and Makaweli Rivers. Bed material gradations were developed from 22 samples collected in February 1989. Due to inadequate sampling equipment, no samples were obtained from areas where the water was more than 3 ft deep. This included the entire study reach downstream from sta 33+50, except for exposed bars at sta 0+00 and 4+70. The average of all samples was used to develop an initial bed material gradation with a median grain size of 0.65 mm and a standard deviation of 2. Sediment inflow data were not available and therefore were determined indirectly during the model adjustment phase of the study.

Adjustment Data

Surveys taken in November 1987 and March 1989 were used to determine prototype aggradation and degradation. The surveys included 12 cross sections between stations 4+70 and 60+30. Volumes were accumulated starting at station 4+70 and moving upstream. Cumulative aggradation was 83,500 cu yds between January 1979 and November 1987; 58,500 cu yd were degraded between November 1987 and March 1989.

Transport Functions

Five transport functions were considered. Single grain size functions included the Yang (1973, 1984) and Ackers-White (1973) functions. A grain size of 0.65 mm was initially used with the single grain size functions. Multiple grain size functions included Laursen-Madden (US Army Corps of Engineers Hydrologic Engineering Center 1977), a combination of the Toffaleti (1966) and Meyer-Peter-Muller (1948) functions, herein referred to as TMPM, and a modification of the Laursen (1958) equation. The modified Laursen equation, hereafter referred to as the Laursen-Copeland function, incorporates data for transport of gravels in addition to the sand data used to develop the original Laursen function (Copeland and Thomas 1989).

Adjustment to November 1987 Survey

Initial model adjustment was accomplished by varying sediment inflow at the upstream boundary until aggradation measured in November 1987 was simulated. The initial estimate for sediment inflow was determined using average hydraulic parameters at four cross sections on the Waimea River upstream from its confluence with the Makaweli River. There were no data to indicate a difference in sediment inflow contributions from the Waimea and Makaweli basins; therefore, inflow concentrations were initially assumed to be equal. The initial sediment inflow rating curves were adjusted by a constant percentage.

Adjusted sediment inflow rating curves were different for the different sediment transport functions. The Laursen-Copeland, Yang, and Ackers-White functions successfully reproduced the distribution of deposited sediment in the study reach. The TMPM and Laursen-Madden functions calculated more

sediment deposition in the upstream end of the study reach than in the prototype.

Adjustment to March 1989 Survey

The March 1989 survey indicated that 58,500 cu yd of degradation had occurred since the November 1987 survey. This left about 25,000 cu yd deposited in the channel since the 1979 survey. The majority of this deposited sediment was located upstream from sta 33+50.

The numerical model, adjusted to the January 1979-November 1987 aggradation, was tested by lengthening the historical simulation to March 1989. The predicted cumulative aggradation using the initial adjusted sediment inflow curves was significantly greater than the measured data. With the Ackers-White and Laursen-Madden functions, a slight increase in sediment deposition was calculated instead of a decrease. Using the TMPM function, some degradation in the downstream portion of the study reach was calculated, but aggradation was calculated in the upstream portion of the reach, so that there was no net change in calculated cumulative aggradation. The other functions predicted degradation that was considerably less than measured. The March 1989 survey data demonstrated that further adjustment of the numerical model was required. The Yang and Laursen-Copeland sediment transport functions were chosen for further consideration, because these functions produced results with some degradation and at least some trend toward the measured data.

A significant decrease in sediment inflow between November 1987 and March 1989 would be one possible explanation for the degradation that occurred during this period. A decrease in sediment inflow from the Makaweli River basin could be attributed to stabilization of a major landslide that occurred in 1981. The Yang single-grain-size transport function was used to test the effect of temporal change in sediment inflow. Degradation of 9000 cu yd between November 1987 and March 1989 had been calculated using the sediment inflow curves adjusted to the November 1987 survey. Sediment inflow after November 1987 was reduced in the numerical model by a constant percentage in three tests. In the first test, inflow from the Makaweli River was reduced by 50 percent. This resulted in a total of 18,000 cu yd of degradation between November 1987 and March 1989. In the second test, sediment inflow was also reduced by 50 percent on the Waimea River. This resulted in a total of 49,000 cu yd of degradation. Finally, sediment inflow was reduced 67 percent on both rivers. This resulted in a calculated degradation of 55,000 cu yd, which is fairly close to the measured 58,500 cu yd.

These tests did not prove or disprove the hypothesis that the degradation in the Waimea River between November 1987 and March 1989 was caused by a significant reduction in sediment inflow. It was determined, however, that reduction in sediment inflow, due to recovery from the landslide in the Makaweli alone, would be insufficient to cause the measured quantity of degradation. More than a 67 percent sediment inflow reduction in both drainage basins would be required, according to numerical model results, to account for the removal of 55,000 cu yd. It is improbable that such a reduction could occur on a long-term basis without some obvious changes in the basin. No data indicating sediment supply decreases in the Waimea basin have been reported. It was therefore concluded that long-term adjustments to the sediment inflow would be more appropriate.

The numerical model was initially adjusted to the November 1987 measured aggradation using a sediment inflow rating curve based on the assumption of equilibrium transport. That is, the sediment inflow was assumed to be determined by the channel capacity. However, sediment inflow can also be supply limited, especially at high flows. This condition was tested in the numerical model by further adjustments to the sediment inflow curves. In general, the numerical simulation using the single grain size transport function was significantly improved by increasing inflow at lower discharges and decreasing inflow at higher discharges. However, both aggradation and degradation could not be simulated with a single sediment inflow rating curve. The best result for the calculated degradation between November 1987 and March 1989 was 49,000 cu yd, which compares to the measured degradation of 58,500 (Figure 1).

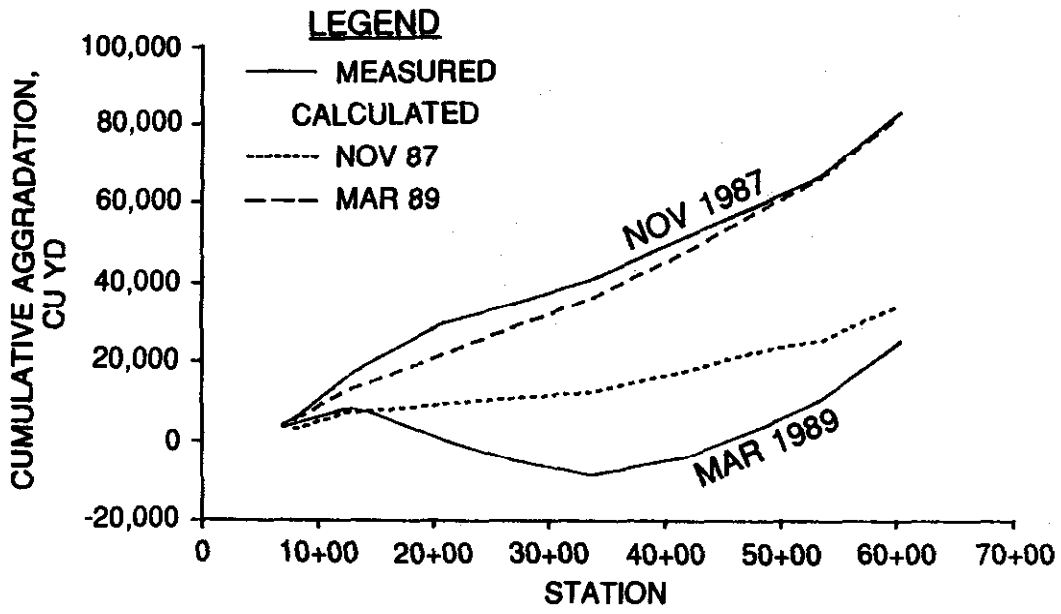

Figure 1. Comparison of measured and calculated cumulative aggradations with single grain size function

The sediment inflow curves for the Laursen-Copeland transport function were adjusted by increasing sediment inflow at low discharges and decreasing sediment inflow at high discharges. Most of the adjustment was to sand size classes. Trial and error adjustments produced a calculated degradation between November 1987 and March 1989 of 24,500 cu yd. This was an improvement over the 13,500 cu yd calculated using the original adjusted sediment inflow. The effect of adding fine sand to the sediment inflow, but not the bed material gradation, was tested. Additional adjustment to sediment inflow curves for all size classes was required. The inclusion of fine sand in the sediment inflow resulted in a significant improvement in the simulation. Calculated degradation between November 1987 and March 1989 was 68,500 cu yd. Degradation was underestimated by about 10,000 cu yd between sta 12+50 and 33+50, and aggradation was underestimated by about 20,000 cu yd between sta 33+50 and 60+30. Both the volume and distribution of sediment deposits was better with the multiple grain size transport function. A comparison of

measured and computed cumulative aggradations is shown in Figure 2.

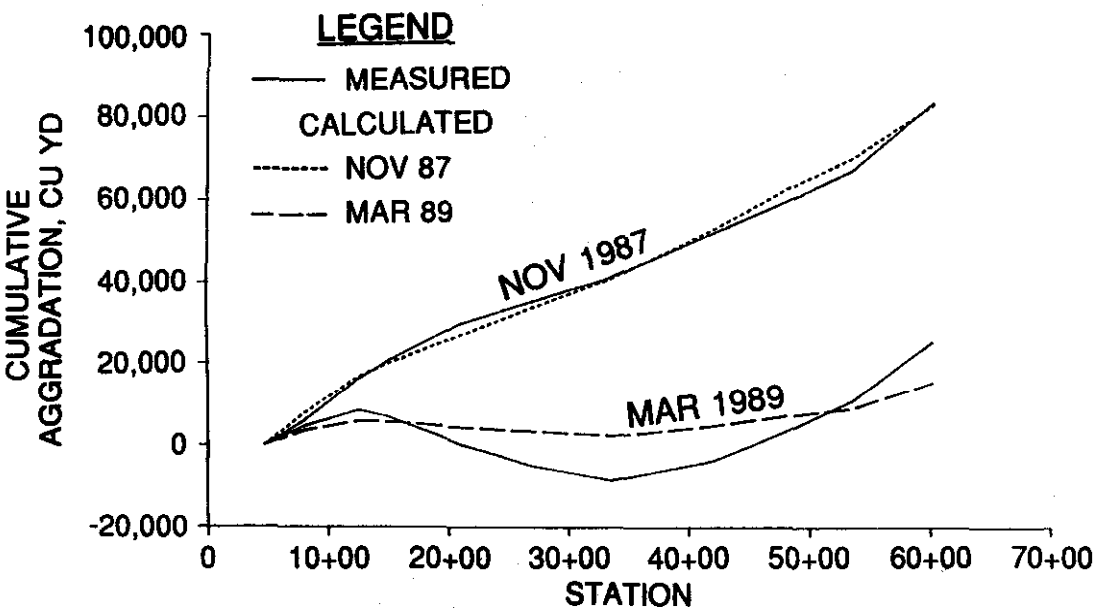

Figure 2. Comparison of measured and calculated cumulative aggradations with final adjustment of numerical model

Calculated average bed material gradations between sta 33+50 and 60+30 at different times during the historical simulation were compared. This river reach was chosen because calculated data could be compared to measured data representative of the entire channel width. The initial bed material in the numerical model had a median grain diameter of 0.65 mm based on the average from samples collected in February 1989. This average, and the envelope of sampled data, are compared with calculated bed gradations at three times during the 10-year simulation in Figure 3. On 30 October 1982, the highest flow of record during the simulation period occurred and the calculated gradation was considerably coarser with a median grain size of about 0.90 mm. On 4 November 1987, the period of highest calculated aggradation occurred and had a finer average bed gradation with a median grain diameter of 0.48 mm. Finally, the calculated and measured median grain size on 9 February 1989 was about 0.65 mm. The coarsest grain sizes were slightly underrepresented in the February 1989 calculated gradation; the sampled bed had about 13 percent gravel compared to a calculated bed that had about 10 percent gravel. The calculated bed also was composed of about 15 percent fine sand, which was not included in the initial bed material. In general, the numerical model performed very well in the reproduction of bed material gradation.

With the addition of fine sand to the inflow, there was a significant longitudinal variation in calculated bed gradation. Calculated median grain size in November 1987, which was the period of greatest sediment accumulation, varied between 0.60 mm at sta 60+30 to 0.19 mm at sta 4+70. This indicates that during periods of extended low flow, fine materials accumulate in the downstream portion of the channel. When calculated bed material gradations

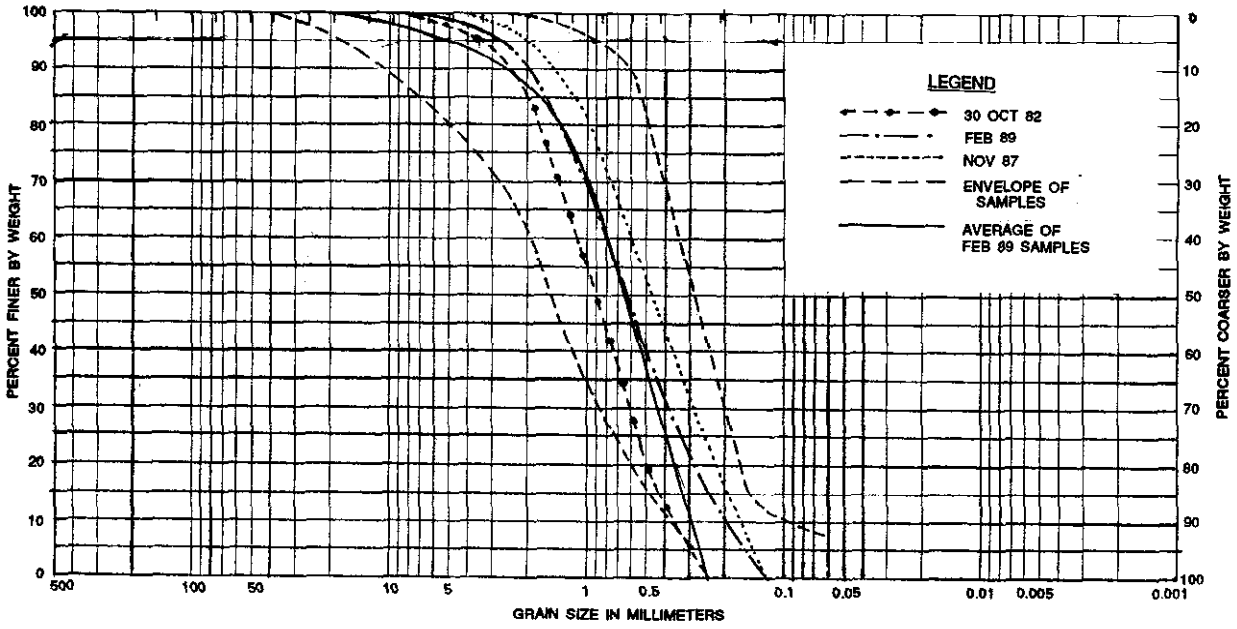

Figure 3. Calculated change in bed material between sta 65+00 and 33+50

from periods with high antecedent flow are compared, it can be concluded that finer sediments are washed out at high flows contributing to the degradation that occurs during higher flow periods. In the numerical model this result is attained independent of the initial bed material gradation assumptions.

Other Adjustments

During the course of the study several other adjustments to the numerical model were tested. Compared to the adjustment of sediment inflow, these were all found to be insignificant. Adjustments tested included reducing overbank conveyance, varying channel roughness with discharge, using a smaller grain size with the single grain size transport function, and varying the initial bed material gradation longitudinally.

CONCLUSIONS

Historical aggradation and degradation in the Waimea River were simulated with the numerical model. The model incorporated multiple grain sizes from fine sand to coarse gravel. The Laursen-Copeland multiple grain size transport function was used. An average initial bed material gradation was used for the entire study reach. A constant roughness coefficient was used. Sediment inflow rating curves were not varied with time.

The adjustment phase of the numerical model study indicated that sediment supply limitations of finer sediments at high flows were the principal cause of degradation at high flow. The historical simulation indicated that the Waimea River bed is dynamic and can be expected to fluctuate with changes in discharge. Long periods of low flow will result in more aggradation. Major storm events will tend to wash material out of the flood control channel.

ACKNOWLEDGMENTS

The tests described and the resulting data presented herein, unless otherwise noted, were obtained from research conducted for the US Army Engineer Division, Pacific Ocean, by the US Army Engineer Waterways Experiment Station, Vicksburg, Miss. Permission was granted by the Chief of Engineers to publish this information.

REFERENCES

Ackers, P., and White, W. R., 1973, Sediment transport: new approach and analysis. Journal, Hydraulics Division, American Society of Civil Engineers 99, HY11, 2041-2060.

American Society of Civil Engineers, 1975, Sedimentation Engineering. ASCE Manuals and Reports on Engineering Practice-No. 54, Vito A. Vanoni, ed., New York, p.40.

Copeland, R. R., and Thomas, W. A., 1989, Corte Madera Creek sedimentation study; numerical model investigation. Technical Report HL-89-6, US Army Engineer Waterways Experiment Station, Vicksburg, Miss.

Laursen, Emmett M., 1958, The total sediment load of streams. Journal, Hydraulics Division, American Society of Civil Engineers 84, HY1, 1530-1 to 1530-36.

Meyer-Peter, E., and Muller, R., 1948, Formulas for bed load transport. Report on Second Meeting of International Association for Hydraulic Research, Stockholm, Sweden, 39-64.

Thomas, William A., 1980, Mathematical modeling solutions. Applications of Stochastic Processes in Sediment Transport, H. W. Shen, H. Kikkawa, ed., Water Resources Publications, Littleton, Colo.

_____, 1982, Mathematical modeling of sediment movement. Gravel Bed Rivers, R. D. Hey, J. C. Bathurst, and C. R. Thorne, ed., Wiley, New York.

Toffaleti, F. B., 1966, A procedure for computation of total river sand discharge and detailed distribution, bed to surface. Committee on Channel Stabilization, US Army Corps of Engineers, Washington, DC.

US Army Engineer District, Honolulu, 1980, Waimea River flood control study; detailed project report and final environmental statement, (revised 26 February 1982). Honolulu, Hawaii.

US Army Engineer Hydrologic Engineer Center, 1977, Users manual HEC6 generalized computer program scour and deposition in rivers and reservoirs. US Army Corps of Engineers, Davis, Calif.

Yang, C. T., 1973, Incipient motion and sediment transport. Journal, Hydraulics Division, American Society of Civil Engineers 99, HY10, 1679-1704.

_____, 1984, Unit stream power equation for gravel. Journal, Hydraulics Division, American Society of Civil Engineers 110, HY12, 1783-1797.

MODELING SEDIMENT DEPOSITION NEAR LOCKS AND DAMS

By Bradley M. Comes, Research Hydraulic Engineer, US Army Engineer Waterways Experiment Station, Vicksburg, Mississippi.

ABSTRACT

The Red River Waterway Project will provide a navigation route from the Mississippi River and its junction with Old River via the Old and Red Rivers to Shreveport, Louisiana. The project will provide a minimum 200-ft-wide by 9-ft-deep channel with a system of five locks and dams. Lock and Dam No. 1, opened in the fall of 1984, experienced deposition of fine sediments in the upstream and downstream lock approach channels. The US Army Engineer Waterways Experiment Station (WES) used the TABS-2 two-dimensional numerical modeling system to address the sediment deposition problem at this lock, as well as to identify potential sedimentation problems at the planned Lock and Dam Nos. 2 (John H. Overton Lock and Dam), 3, 4, and 5. The report outlines the numerical modeling studies that were performed in the upstream pools at Lock and Dam Nos. 2 and 3. The two designs were very similar but the investigation revealed that significantly different deposition patterns would occur.

INTRODUCTION

Purpose and Scope

This report describes the results of two numerical modeling studies conducted to predict the locations and magnitudes of fine sediment deposition near Lock and Dam Nos. 2 and 3 on the Red River, Louisiana. Lock and Dam No. 1 on the Red River was opened in the fall of 1984. Deposition of fine sediment in the upstream and downstream lock approach channels was much greater than anticipated. Dredging was required at the entrance to the upstream approach channel and throughout the downstream approach channel. Sediment deposition at the downstream miter gate was severe enough to prevent operations. The lock chamber eventually had to be dewatered and the deposited sediment cleaned out. Two-dimensional numerical model studies were employed by the US Army Engineer District (USAED), Vicksburg, and WES to address the fine sediment problem at Lock and Dam No. 1 (Little 1985, Copeland and Thomas 1988). As a result of these studies, design modifications were recommended and constructed at Lock and Dam No. 1. After 2 years of operations these modifications appeared to have significantly reduced the fine sediment problems in the lock approach channels. Prior to the construction of Lock and Dam Nos. 2 and 3, the same two-dimensional numerical approach was employed to identify potential sedimentation problems at these sites.

The Models

The numerical modeling of these sites was divided into four models, a model upstream and downstream of each dam (Comes, Copeland, and Thomas 1989). In addition to these numerical model studies, three physical model studies of the sites were conducted at WES: a fixed-bed navigation study (Wooley, in preparation); a movable-bed sedimentation study (O'Neal, in preparation); and a hydraulic structures model study (Maynord and Markussen, in preparation). This report presents results from the two upstream numerical models only. The

numerical studies were conducted using the TABS-2 modeling system (Thomas and McAnally 1985). This system provides two-dimensional solutions to open-channel sand sediment problems using finite element techniques. A two-dimensional depth-averaged hydrodynamic numerical model, RMA-2V, was used to generate the current patterns. The current patterns were then coupled with the sediment properties of the river and used as input to a two-dimensional fine-grained sedimentation model, STUDH. Although TABS-2 may be used to model unsteady flow, only steady-state conditions were simulated in this study. Sediment is represented by a single grain size, and a transport potential is calculated using the Ackers-White equation (Ackers and White 1973). The numerical investigations addressed only the portion of the suspended sediment that would deposit in areas with very little to no hydraulic conveyance. The movement of bed-load particles and the larger suspended load materials were investigated with other models.

INITIAL CONDITIONS

Lock and Dam No. 2 is located in a river cutoff at 1967 river mile 87.4, which is about 44 river miles upstream from Lock and Dam No. 1. It consists of a single lock on the left descending side of the cutoff, a 348-ft-long dam with five 60-ft-wide gates and a 250-ft-long overflow weir on the right descending side with crest at elevation (el) 66.0 ft National Geodetic Vertical Datum (NGVD). The lock chamber has a usable length of 685 ft and is 84 ft wide with upstream and downstream miter gate sill elevations of 40.5 and 25.0 ft NGVD, respectively. The lock chamber floor is at el 23.0 ft NGVD. The river channel upstream from the lock and dam is about 600 ft wide and has a design invert elevation of 34.0 ft NGVD. The upstream lock approach channel is separated from the spillway entrance channel by a 700-ft-long ported guard wall. The ported guard wall was numerically modeled as a submerged weir with the overflow area equal to the area of the submerged ports. Hydraulic roughness was adjusted until the flow distribution along the wall (weir) matched distributions from measurements taken from the 1:50-scale physical model. The intake manifolds for the filling system are located in a 170-ft-long lock approach section between the downstream end of the ported guard wall and the miter gates. Figure 1 shows the plan view of the Lock and Dam No. 2 site from approximately 1,000 ft upstream of the axis of the dam to approximately 1,700 ft downstream of the axis of the dam. The upstream numerical model of Lock and Dam No. 2 extended approximately 2 miles upstream from the dam. Uniform lateral velocity distributions were specified at the upstream boundary of the model, and water-surface elevations from the design rating curve were specified at the spillway gates. The uniform lateral velocity distribution became fully developed upstream of the area of interest. This was verified using normalized velocity measurements from the 1:80V, 1:120H movable-bed physical model. Outflow distributions through the spillway gates were verified using measurements from the 1:50 structures model.

Lock and Dam No. 3 is located in a river cutoff at 1967 river mile 141.0, which is about 54 river miles upstream from Lock and Dam No. 2. The design of the lock, spillway gates, and overflow weir is functionally the same as the Lock and Dam No. 2 design with two exceptions; the upstream ported guard wall at Lock and Dam No. 3 is 100 ft longer, and the lock is separated from the first spillway gate by an additional 116 ft. The upstream numerical model of Lock and Dam No. 3 extended approximately 0.5 mile upstream from the dam. The lateral velocity distributions at the upstream end of the model were specified based on measurements taken from the 1:100-scale navigation physical

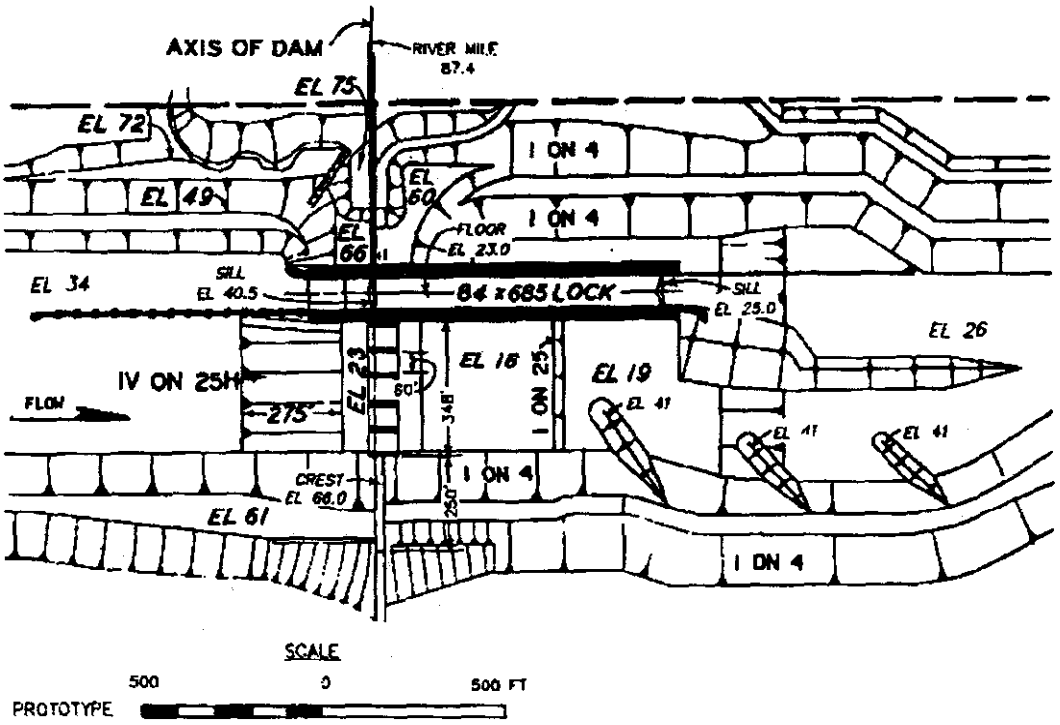

Figure 1. Plan of Lock and Dam No. 2

model, and water-surface elevations from the design rating curve were specified at the spillway gates.

The system of five dams on the Red River is designed to be operated as run-of-the-river dams. The spillway gates hold minimum pool elevations (64.0 ft NGVD for Lock and Dam No. 2) passing the daily discharge until the flows reach a magnitude that requires all gates to be removed from the water (90,000 cfs for Lock and Dam No. 2). At this point, the dams are operated as if open river existed until the flow subsides and the gates are lowered back into the water to hold the specified minimum pool. Lock and Dam No. 3 is the only exception to this mode of operation. It utilizes a "hinged-pool" concept. Lock and Dam 3 holds a normal pool elevation of 95.0 ft NGVD until a high flow rate is anticipated on the river. In anticipation of the high flow rate, the spillway gates are raised until the normal pool is drawn down to a minimum elevation of 88.0 ft NGVD. The discharge is 80,000 cfs when the minimum pool elevation is reached. As the high flow rate arrives, water is stored in the dam until the pool reaches el 89.0 ft NGVD. At this point, the dam is operated as an open river case until the flow subsides and the gates are lowered back into the water to hold the normal pool elevation.

Two steady-state discharges were chosen to investigate each site. For the Lock and Dam No. 2 investigation, 90,000 and 145,000 cfs were selected. These two discharges were selected because they both had the potential to move sediment into the slack-water areas and being used in the navigation physical model tests. The former discharge is the maximum discharge with normal pool elevation (64.0 ft NGVD) and the latter is the maximum discharge at which navigation is allowed to operate on the river. At Lock and Dam No. 3, 80,000 and 145,000 cfs were selected. The discharge of 80,000 cfs is the discharge

at which the maximum drawdown (minimum pool elevation) occurs. Many designs were tested for both sites at both discharges until an acceptable design was formulated. The final design was tested with an average annual hydrograph constructed by linking many stepwise steady-state discharges together. For the purposes of this paper, comparisons of test results from Lock and Dam Nos. 2 and 3 will be presented using the steady-state discharge of 90,000 cfs at Lock and Dam No. 2 and 80,000 cfs at Lock and Dam No. 3. A representative grain size of 0.07 mm, taken from samples of the fine-grained deposits in the lock approach of Lock and Dam No. 1, and sediment concentrations of 850 and 780 mg/l, respectively, were used.

TEST RESULTS

Lock and Dam No. 2

The Lock and Dam No. 2 investigation was performed prior to the Lock and Dam No. 3 investigation. As part of the Lock and Dam No. 2 investigation, cross-checking between the three physical models and the numerical models, the evaluation of field data, and monitoring the performance of the Lock and Dam No. 1 site were exercises that played a role in the selection of the numerical coefficients. Figure 2 shows velocity vectors generated from the hydrodynamic numerical model for the downstream one-half mile of the upstream pool. Each vector originates from a location where a node existed in the finite element grid. Notice that the ported guard wall has little effect on reducing the flow rate into the lock approach channel. Using these velocity patterns, the numerical sedimentation model was used to simulate a 10-day period. The results indicated that approximately 4 ft of the fine-grained sediments would deposit at the lock miter gates. The deposit was small in volume extending from the miter gates upstream to the most downstream port in the ported guard wall (170 ft). Figure 3 shows velocity vectors for the same condition except the guard wall was modeled as a solid wall. Notice the large outdraft near the upstream end of the guard wall. The 10-day sedimentation tests indicated that a larger deposit would occur extending from the lock miter gates

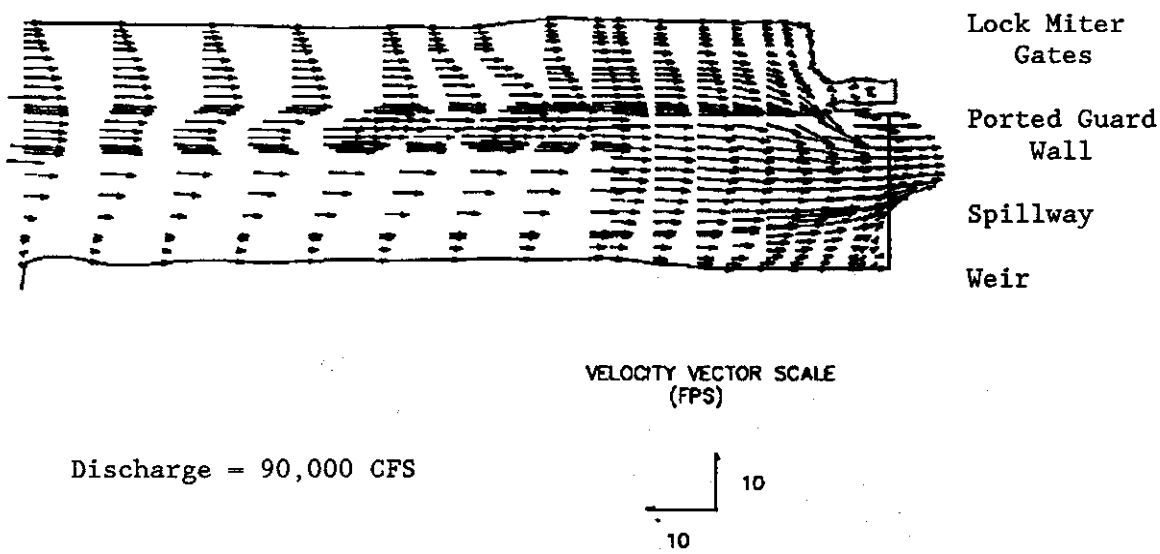

Figure 2. Lock and Dam No. 2 Velocity Vectors, Ported Guard Wall

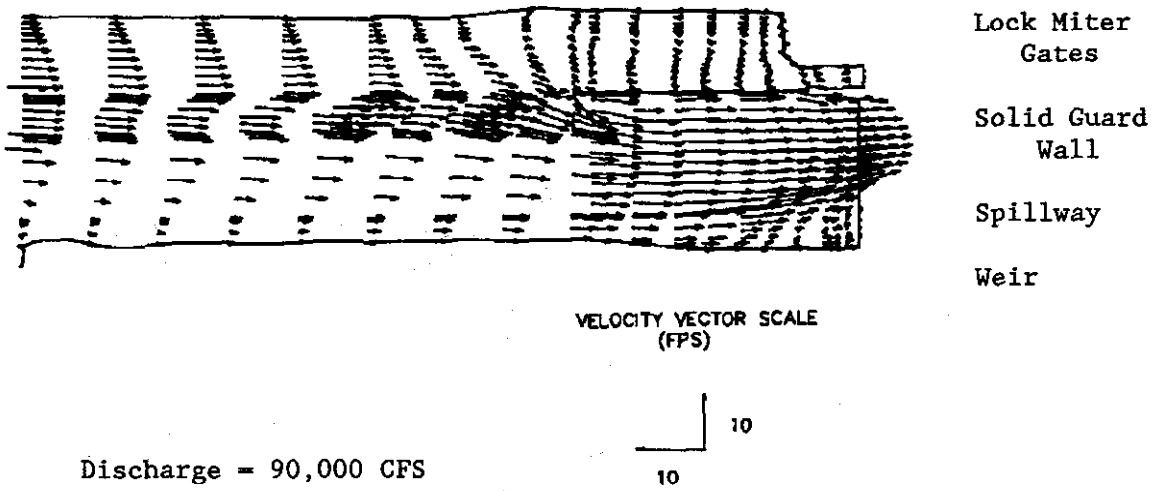

Figure 3. Lock and Dam No. 2 Velocity Vectors, Solid Guard Wall

upstream approximately 1,500 ft. The peak of the deposit (4 ft) occurred near the upstream end of the guard wall and tapered to approximately 1 ft deep at the lock miter gates. The solid guard wall moved the deposit to a more desirable location but produced an excessive outdraft for navigation at the upstream end of the guard wall as well as increased the volume of the deposit. The ported guard wall was kept in the design, and a jet pump system was installed to resuspend the material that deposited in front of the miter gates.

Lock and Dam No. 3

The numerical coefficients and hydraulic roughness parameters that were selected for the Lock and Dam No. 2 investigation were also used for the Lock and Dam No. 3 investigation. A new finite element grid was generated to account for differences in the approach channel geometry, the longer ported guard wall, and the additional spacing between the lock and the first spillway gate. Figure 4 shows velocity vectors for the reach extending 1,000 ft upstream from the dam. The descending right-hand overflow weir, not shown in this figure, is a nonovertopping weir at this flow rate. This design had slightly smaller velocities in the lock approach channel, and flow was not as nearly parallel to the guard wall as in the Lock and Dam No. 2 investigation. Notice the direction of the flow vectors near the upstream portion of the ported guard wall as compared to Figure 2. The flow patterns at Lock and Dam No. 3 produced a sediment deposit near the lock miter gates similar to the one predicted at Lock and Dam No. 2 but about one-half as deep; however, the Lock and Dam No. 3 deposit extended approximately 1,500 ft upstream and filled the left descending one-half of the lock approach channel. A detailed investigation of the differences between the Lock and Dam No. 2 design and the Lock and Dam No. 3 design was initiated since the extensive left bank deposit did not occur in the Lock and Dam No. 2 tests. Both models indicated that approximately 16 percent of the total discharge would flow behind each respective ported guard wall through a cross section located at the upstream end of the wall but that only 8 percent would flow through a cross section located near the downstream end of the wall at Lock and Dam No. 3 as compared to 14.0 percent

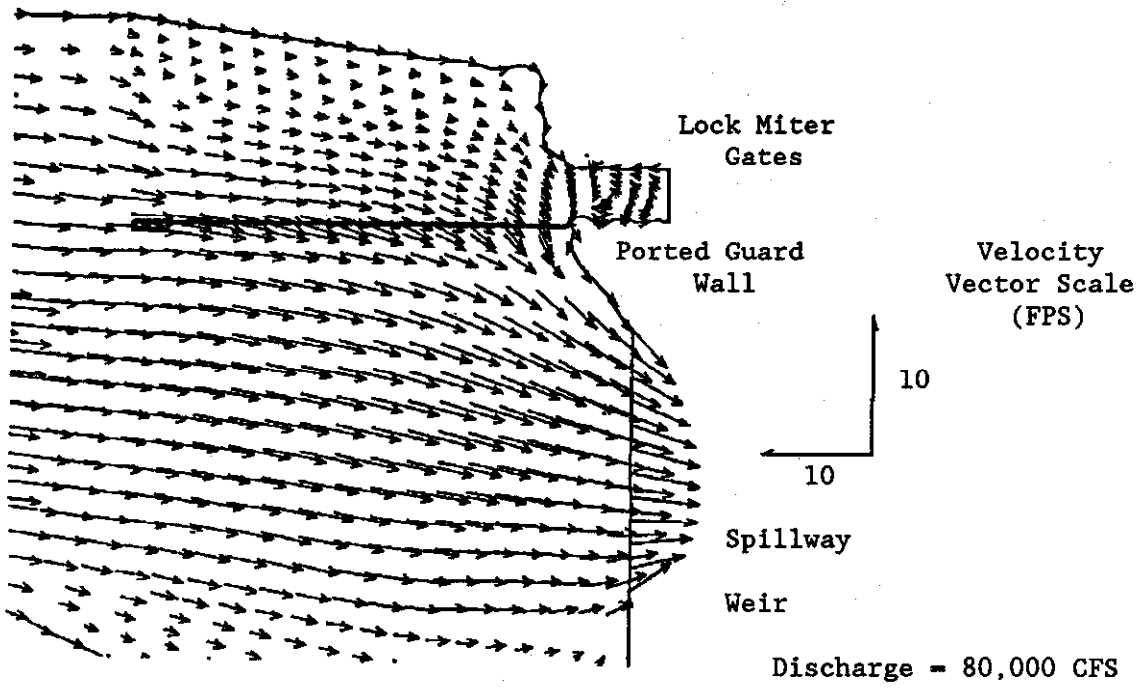

Figure 4. Lock and Dam No. 3, Lock and Spillway Separated

at Lock and Dam No. 2. Investigations of velocity and bed shear stress distributions indicated that the flow was migrating toward the spillway gates farther upstream in the Lock and Dam No. 3 design due to the tapered descending left bank line and the additional separation between the lock and the first spillway gate. A comparison of the left descending bank line in Figures 2 (Lock and Dam No. 2, ported guard wall) and 4 (Lock and Dam No. 3, lock and spillway separated) indicates that the Lock and Dam No. 2 left descending bank line is parallel to the ported guard wall and that the Lock and Dam No. 3 bank line is tapered toward the guard wall. A test was conducted modeling the upstream one-half of the guard wall as a solid wall and the downstream one-half as ported, but this design change had little effect on reducing sediment deposition behind the guard wall. Another test was conducted changing the boundary specification on the wall separating the lock and the spillway from a slip type boundary to a water-surface elevation allowing water to flow out of this portion of the boundary. Figure 5 shows the resulting velocity vectors. Notice that compared to Figure 4, the flow vectors in Figure 5 are parallel to the guard wall for almost its entire length. This test indicated a reduction in the sediment deposit along the left bank line but increased the depth of the deposit near the miter gates (similar to the Lock and Dam No. 2 test results).

SUMMARY

A two-dimensional numerical modeling system was utilized to predict locations and magnitudes of fine sediment deposition near Lock and Dam Nos. 2 and 3 on the Red River, Louisiana. Three physical models and two numerical models of each site were constructed and utilized throughout the design process. This report details only the numerical model investigations upstream of each lock and dam. The numerical models were used to investigate the deposition of fine sediments in areas with very little hydraulic conveyance.

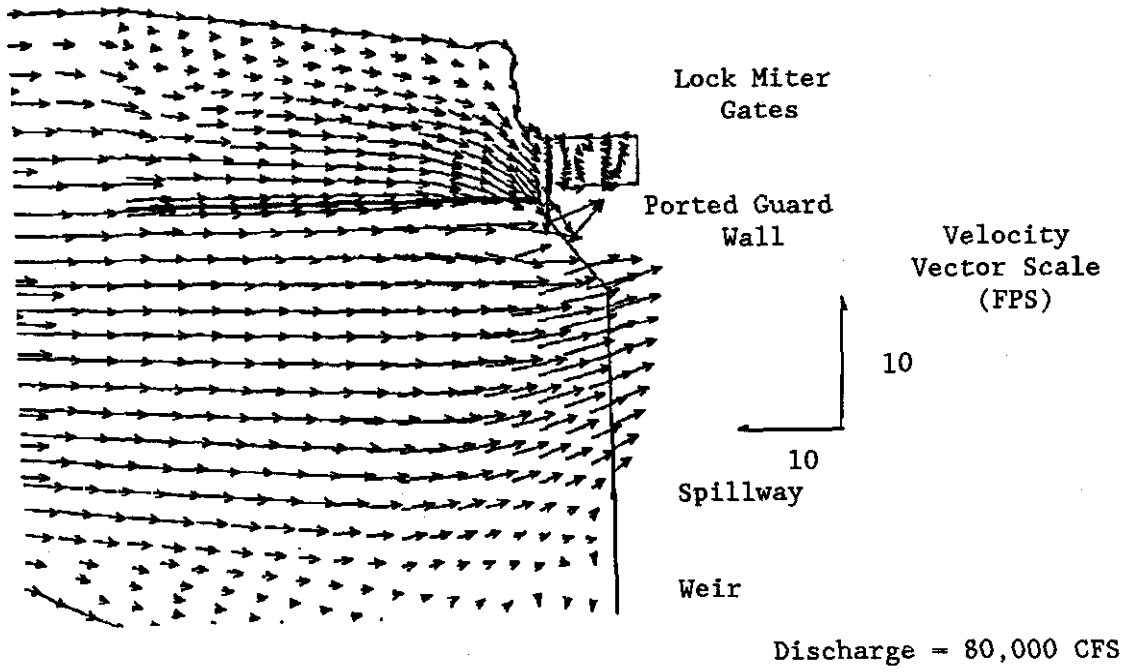

Figure 5. Lock and Dam No. 3, Lock and Spillway Together

The Lock and Dam No. 2 design has very good navigation entrance conditions (little outdraft at the upstream end of the guard wall) but produces approximately 4 ft of deposition near the lock miter gates in 10 days at an intermediate discharge. The ported guard wall brings large quantities of sediment-laden flow close to the lock gates. Study results indicate that sediment deposition at the lock gates would be essentially eliminated by constructing a solid guard wall; however, this design produces undesirable navigation conditions near the upstream end of the guard wall. The existing design with the ported guard wall presently utilizes a jet pump system to resuspend the material that is deposited in front of the miter gates.

The Lock and Dam No. 3 design had slightly lower velocities in the lock approach channel. More flow exited the upper end of the ported guard wall than in the Lock and Dam No. 2 design. An additional 116 ft of separation between the lock and the first spillway gate, coupled with a tapering bank line in the lock approach channel, directed the flow away from the left descending bank line. The resulting flow distribution caused a large band of sediment to deposit on the left descending bank of the lock approach channel. Also, approximately 2 ft of material deposited near the lock miter gates for a 10-day simulation at an intermediate discharge. Additional tests were conducted simulating a guard wall with the upper one-half solid and the lower one-half ported, but this did not reduce the deposition in the lock approach channel. Finally, a simulation representing the addition of a spillway gate between the lock and the tested spillway was conducted. This test reduced the deposition along the left descending bank line but increased deposition near the miter gates.

ACKNOWLEDGMENTS

The tests described and the resulting data presented herein, unless otherwise noted, were obtained from research conducted for the US Army Engineer District, Vicksburg, by the US Army Engineer Waterways Experiment Station. Permission was granted by the Chief of Engineers to publish this information.

REFERENCES

Ackers, P., and White, W. R., 1973, Sediment transport: new approach and analysis, J. Hyd. Div. ASCE 99, Paper No. 10167, 2041-2060.

Comes, Bradley M., Copeland, Ronald R., and Thomas, William A., 1989, Red River Waterway, John H. Overton Lock and Dam. Technical Report HL-89-16, US Army Engineer Waterways Experiment Station, Vicksburg, MS.

Copeland, Ronald R., and Thomas, William A., 1988, Red River Waterway sedimentation study, downstream from Lock and Dam No. 1; numerical model investigation. Technical Report HL-88-15, US Army Engineer Waterways Experiment Station, Vicksburg, MS.

Little, C. D., Jr. 1985, Use of a two dimensional modeling system to evaluate lock channel shoaling on Lock and Dam No. 1 on the Red River Waterway. Proceedings of 15th Mississippi Water Resources Conference, 27-28 February 1985, Jackson, MS, Mississippi Water Resources Research Institute, Mississippi State University, Starkville, MS.

Maynord, S. T., and Markussen, J. V., Red River Waterway, John H. Overton Lock and Dam, stilling basin, riprap, and hydropower requirements; spillway and hydropower hydraulic model study (in preparation). US Army Engineer Waterways Experiment Station, Vicksburg, MS.

O'Neal, C. W., Red River Waterway, John H. Overton Lock and Dam, sedimentation conditions; hydraulic model investigation (in preparation). US Army Engineer Waterways Experiment Station, Vicksburg, MS.

Thomas, William A., and McAnally, William H., Jr., 1985, User's manual for the generalized computer program system: open-channel flow and sedimentation, TABS-2. Instruction Report HL-85-1, US Army Engineer Waterways Experiment Station, Vicksburg, MS.

Wooley, R. T., Red River Waterway, John H. Overton Lock and Dam, navigation alignment conditions; hydraulic model investigation (in preparation). US Army Engineer Waterways Experiment Station, Vicksburg, MS.

MASS-WASTING ALGORITHMS IN AN ALLUVIAL CHANNEL MODEL

By **Andrew Simon**, U.S. Geological Survey, Cascades Volcano Observatory, Vancouver, Washington; **William J. Wolfe**, U.S. Geological Survey, Nashville, Tennessee; and **Albert Molinas**, Colorado State University, Ft. Collins, Colorado

ABSTRACT

Channel widening by mass-wasting processes is an important mechanism of channel adjustment in alluvial streams. At present (1990), computerized alluvial channel model generally ignore bank failure mechanisms. A general framework for several mass wasting algorithms is described here. The algorithms are directly incorporated into the BRI-STARS alluvial channel model. The modified model evaluates several possible failure mechanisms and selects the mass-wasting process with the minimum factor of safety. If this value is less than 1.0, the algorithm simulates bank failure and updates the channel cross section according to the properties of the failed material and the hydraulics during the given time step. Modifications to the analysis of wedge-type failures of stream banks are also discussed. The modifications include: (1) the destabilizing effect of excess pore pressures, (2) the stabilizing effect of confining pressures at the bank toe, and (3) relaxation of the assumption that a failure must intersect the bank toe. Continuity of failed bank material is achieved by conceptually transforming it to bed material, bed material load, or wash load during the time step following failure. In total, these modifications offer a stronger physical basis for the analysis of mass bank failures and permit a numerical solution for an important process in adjusting alluvial channels.

INTRODUCTION AND PURPOSE

Existing alluvial-channel models typically assume that channel banks are rigid, or adjust their geometry to minimize stream energy dissipation (Fan, 1988). These approaches do not account for an important process that may dominate alluvial channel adjustment: mass wasting. Many studies have shown that major channel widening occurs by mass bank failures, rather than by particle-by-particle erosion of the channel banks (Daniels, 1960; Thorne and others, 1981, Simon and Hupp, 1986; Simon, 1989a). Commonly, mass wasting and particle-by-particle erosion act in concert; fluvial erosion scours the toe of the bank, and mass failure follows. This process is particularly important on the outside of meander bends.

Channel-bed processes are often modeled by numerically solving deterministic equations of hydraulics and sediment transport. A similar approach, based on rigorous physical principles, has rarely been applied to modeling bank processes in alluvial channels. Notable exceptions include studies of riverbank stability by Alonso and Combs (1986), Osman and Thorne (1988), and Thorne and Osman (1988). Given the lack of bank-failure algorithms in process-oriented alluvial channel models, the U.S. Geological Survey designed a study to: (1) develop a set of physically based mass-wasting algorithms to model channel-widening processes in alluvial channels under a variety of channel geometries and material strengths, and (2) incorporate the algorithms into an existing alluvial channel model. This paper reports results of this study to date.

BACKGROUND AND SCOPE

To estimate rates of bank retreat by mass-wasting processes, Pizzuto (1989) proposed a model using simple planar grain flow of coarse, non-cohesive bank sediments at the angle of repose. Alonso and Combs (1986), and Osman and Thorne (1988) modeled wedge-type failure of cohesive channel banks. Both these studies assume failure through the bank toe, and neither considers the stabilizing effects of confining pressure provided by the water in the channel or the destabilizing effect of excess pore pressures during rapid drawdown (on the recessional limb of storm hydrographs). The study by Osman and Thorne (1988) represents an important contribution because it is one of the first detailed treatments that combine the effects of fluvial erosion and bank stability in the context of analyzing bank retreat.

Several studies have provided a general framework for analyzing the relative role of mass-wasting processes over the course of a major fluvial-adjustment cycle. In studies of streams greatly destabilized by channelization, Simon (1989a, 1989b) related factors of safety (FS), probability of failure, and specific bank-failure mechanisms (planar or rotational) to six-stage models of bank-slope development and channel evolution. Work by Thorne and others (1981) in channelized streams of northern Mississippi gave detailed accounts of the magnitude and spatial scale of mass wasting. Combined with standard slope-stability equations,these earlier studies offer a starting point for incorporating mass-wasting algorithms into a deterministic alluvial channel model.

The focus of this paper is on the general operating framework for mass wasting algorithms within an existing alluvial channel model. The mass-wasting algorithms reported here consider only planar failures of homogeneous channel banks with relatively simple geometries. The framework developed here can be extended to more complex channel geometry and stratigraphy, as well as rotational failure mechanisms. Extending the approach to more complex situations will permit its application over a wide range of temporal and spatial scales.

THE PROCESSES AND THE MODEL

Mass-Wasting Processes on Alluvial-Channel Banks

Bank failures that occur along alluvial channels include the following:

(1) wedge or slab failure with a steep to vertical planar failure surface, often caused by fluvial erosion or pop-out failure at the bank toe;
(2) shallow (relative to length of failure plane) planar failure parallel to ground surface, generally in materials of limited cohesion (infinite-slope model);
(3) rotational failure, occurring typically in high, low-angle banks of cohesive materials; and
(4) pop-out failure, caused by seepage forces where the pressure gradient is steep, generally near the bank toe.

Only wedge and shallow planar failures are given detailed treatment in this paper.

The stability of riverbanks can be analyzed in a number of ways depending on the assumed shape of the failure surface, the composition and stratigraphy of the channels banks, and the form of the desired solution. In a dynamic computer model, two types of solutions are computed: critical conditions and factor of safety (FS). Critical conditions of the channel bank (bank height and angle) are used to initiate iterative mass-wasting subroutines. FS is used to determine whether a given bank fails or remains stable. The preferred mode of failure is a function of (1) the components of shear strength that combine to offer resistance to failure and (2) the fluvial processes (such as scour and degradation) that influence channel geometry during a given time step. Banks of equal total strength may not fail in similar ways owing to differences in cohesive and frictional strengths, bank profiles, and pore pressure distributions.

Selection of an Alluvial Channel Model

Selection of an alluvial channel model was based on applicability to a wide range of alluvial conditions and the detail and accuracy of model results relative to data input and calibration requirements. After reviewing several models, the 'Bridge Stream Tube Model for Alluvial River Simulation' (BRI-STARS) was selected (Molinas, 1989). This model provides essentially two-dimensional (2-D) results without the excessive data requirements of true 2-D models. BRI-STARS is a stream tube computer model used to simulate the routing of water and sediment through alluvial channels. The model is composed of three major components: (1) backwater computations, (2) stream tube computations, and (3) sediment routing computations (fig. 1). Stream tubes serve to divide the channel into a preselected number of flow regions. The bed elevation is permitted to move vertically in each tube as a function of the sediment transport conditions in that tube. During a given time step, one stream tube may simulate erosion, and another may simulate deposition.

GENERAL DESCRIPTION OF THE MODIFIED MODEL

Addition of Mass-Wasting Subroutine--General

In its simplest form, modification of the existing BRI-STARS model to accommodate mass-wasting algorithms entails: (1) modifying the data input modules to accept data on physical properties of the channel banks, notably stratigraphy, shear strength, and particle-size distribution; (2) the addition of a fourth major component or subroutine that contains the bank-failure algorithms and rule sets; and (3) the establishment of a 2-D, soil-data matrix to track soil data and levels of the phreatic surface (or pore pressure ratio) in the channel banks. This sub-routine, which includes the computational procedures to simulate bank failures, is added to the end of the existing flow chart shown in figure 1.

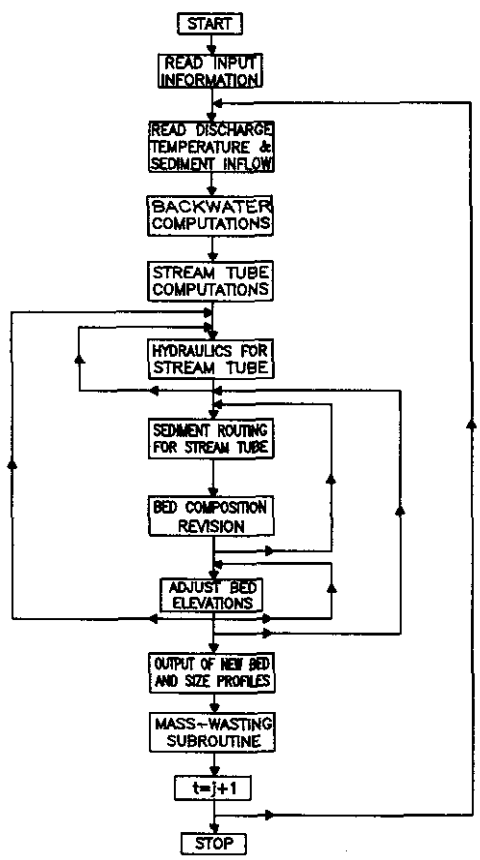

Figure 1. Flow chart for the existing BRI-STARS model showing operation during timestep t = j. (Modified from Molinas, 1989, used with permission).

For each time step, the model will accept input data, run all hydraulic and sediment transport computations, adjust the geometry of the cross sections, and then loop to the mass-wasting subroutine to test for the stability of the channel banks. If no failure is indicated by the algorithms, the model advances to the next time step and hydraulic computations begin again. If bank failure of some type is indicated, the model simulates the bank failure and either deposits the material downslope according to its physical properties and the geometry of the bank, or treats the failed material as a lateral inflow of sediment during the next time step (fig. 2). Both channel geometry and the soil-data matrix are then adjusted accordingly.

Continuity of the failed material is a paramount consideration in the development of this model. The flowchart in figure 2a shows the disposition of failed material relative to its physical properties and the hydraulic characteristics during time steps 'j' and 'j + 1'. By allowing a given volume of sediment to become bank material, bed material, or bed-material load during a specific time step, the model can transfer this material between the mass-wasting algorithms and the sediment-transport equations by simply updating the 2-D soil-data matrix. Thus, sediment that is bank material during time step 'j' and is involved in mass failure at the end of time step 'j', may become bank material, bed material, wash load, or bed-material load during time step 'j + 1' (fig. 2b).

In most instances, a potential user will not have information concerning the dynamic nature of the phreatic surface and must use a pore pressure ratio (Skempton, 1954) to account for excess pore pressures. The most critical condition for channel banks is bank saturation with extremely low flows in the channel, resulting in a maximum pore-pressure ratio of 0.5 (Huang, 1983). Use of a pore pressure ratio of 0.5 will assure the user that the most critical case is considered (Simon, 1989b). However, values less than 0.5 can be used as well as empirical measurements of the height of the phreatic surface. Values of the pore pressure ratio for other than the most critical conditions are obtained from stability charts that account for the relation between the elevation of the water surface, and the elevation of the assumed phreatic surface (Morgenstern, 1963).

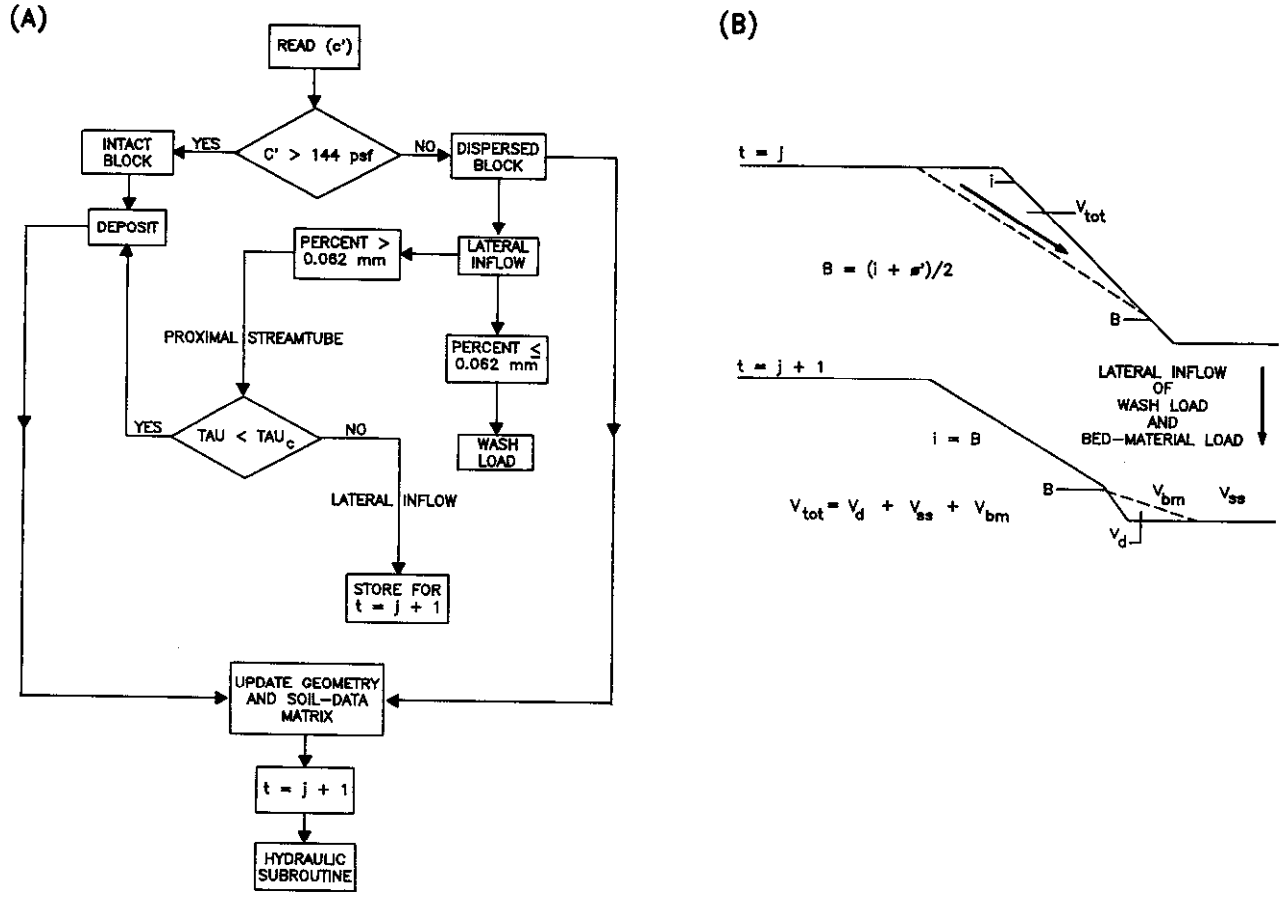

Figure 2. (A) Flow chart showing disposition of failed material during timestep t = j; Material is distributed according to its cohesion (c'), size distribution, and the shear stress (tau) on the channel bed. Tau_c is the critical shear stress needed to move material greater than 0.062 mm in equivalent diameter. (B) Conceptual representation of a given volume of sediment (V_{tot}) undergoing transformation during timestep t = j from bank material to either bed deposition (V_d), wash load (V_{ss}) or bed-material load (V_{bm}) in the next timestep.

RULE SETS AND DETAILS OF MASS-WASTING ALGORITHMS

Rule Sets

As a preface to the individual computational algorithms, the model calculates possible instabilities with worst-case conditions of: (1) minimum values of cohesion (c') and friction angle (ø'); and (2) maximum values of bank angle (i), saturated unit weight (U), and bank height (H) to solve for the critical (maximum-stable) height of the channel banks (H_c). Confining pressure afforded by flow in the channel is assumed to be zero (extremely low flow) to simulate the loss of support at the toe of the bank. A dimensionless stability number (N_s) equation is used to ascertain the most critical bank condition in the study reach (Carson and Kirkby, 1972):

$$\frac{UH_c}{c'} = N_s = \textit{function}\ (\phi', i) \qquad (1)$$

where U = saturated unit weight,
Ns = dimensionless stability number obtained from published stability charts (Chen, 1975), and
c', ø', and i are as previously defined.

For a planar failure surface equation 1 becomes (Lohnes and Handy, 1968):

$$\frac{UH_c}{c'} = N_s = \frac{4 \sin i \cos \phi'}{[1 - \cos (i - \phi')]} \qquad (2)$$

A lower N_s value (indicating lower stability) is obtained if a curved failure surface is used instead of a planar one. The plane-slip analysis can, therefore, lead to overestimates of slope stability with errors increasing as slope angle decreases (Taylor, 1948). Dimensionless stability charts for log-spiral (curved) failures through the toe (Chen, 1975), are a reliable means for assessing general bank stability and critical conditions (Thorne and others, 1981; Simon, 1989b). If the bank configuration for a given time step exceeds the critical conditions for the specified material strength ($H \geq H_c$), the mass-wasting algorithms are initiated for that time step.

The initial test for stability of the stream banks, described above, represents the beginning of the mass-wasting subroutine. Individual algorithms that drive the different failure mechanisms in the subroutine are shown in figure 3. The model evaluates different possible failure mechanisms, and then selects the process with the minimum FS. Wedge failure is initially investigated before rotational failure (fig. 3). Planar failures tend to be more critical early in the degradation process (Skimpton, 1953), while rotational failures become more critical in cohesive materials after maximum amounts of degradation have occurred (Simon 1989b). Ultimately, the mass-wasting subroutine will adjust the channel bank following a wedge failure and then, using the updated bank profile, test for the stability of the bank for rotational failures. In this way, the effect of removing the load represented by the wedge failure, will be incorporated into the analysis (fig. 3).

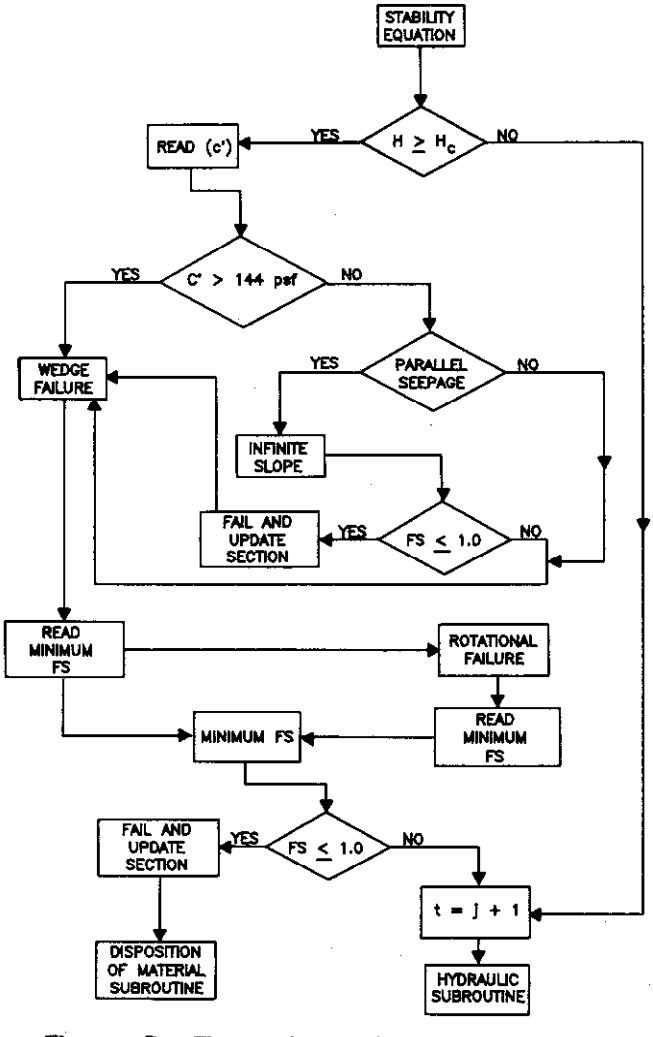

Figure 3. Flow chart showing sequence of algorithms in the mass-wasting subroutine during timestep t = j. c' is cohesion, H_c is critical bank height, and FS is the factor of safety.

Wedge Failures

Wedge-type failures have been used to simulate bank erosion in alluvial channels by Alonso and Combs (1986), and Thorne and Osman (1988). Both use similar approaches and predict failure of an unstable channel bank at an angle $B = (i + \phi')/2$. Standard wedge-type failure analysis is also used in this study, but with three important changes:

(1) incorporating the effects of pore-water pressures in the analysis, using either a phreatic surface or a pore-pressure ratio,
(2) using a search procedure to identify the lowest FS, a failure can intersect the bank surface at any location; and
(3) accounting for confining pressures exerted on the bank toe by the water in the channel.

These modifications represent a departure from the conventional analysis of wedge-type failures along stream banks. In particular, the approach used here relaxes the assumption that the failure plane must pass through the toe of the bank. This approach is justified theoretically by the stabilizing effect of confining pressures on the bank toe, and empirically by

widespread observations of planar slips following the recession of storm hydrographs (Simon, 1989b). Ample empirical evidence indicates that mass failures can occur well above the bank toe, and above the water surface (Thorne and others, 1981; Simon and Hupp, 1986).

The three modifications are incorporated into the standard wedge failure analysis given by Huang (1983):

$$F_s = \frac{c' H \csc(B) + (W_{fb}[1 - r_u]\cos(B))\tan\phi'}{W_{fb}\sin(B)} \qquad (3)$$

where W_{fb} = weight of the failure block,
B = angle of the failure plane, and
r_u = pore pressure ratio (if saturated, r_u = 0.5).

Tension cracks will be accounted for by using standard approaches (Lohnes and Handy, 1968; Thorne and others, 1981).

If the location of the phreatic surface is known, pore pressure can be incorporated directly into the analysis (Huang, 1983). Otherwise, estimation of a pore-pressure ratio (r_u) is based on the degree of bank saturation and the level of surface-water stage. High surface-water stages can result in values for r_u greater then 0.5 for fully saturated, partly submerged failure blocks (fig. 4).

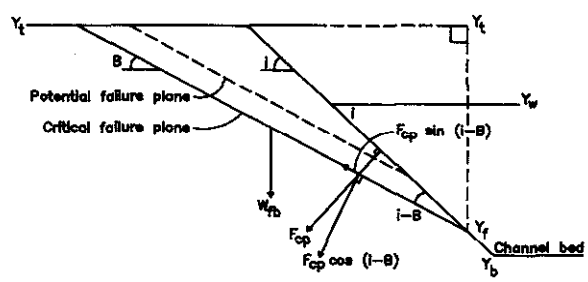

Figure 4. Representation of analysis of wedge-type failure showing search for potential failure plane, and the incorporation of surface-water confining pressure. Failure geometry is showin in terms of bank angle (i), failure plane angle (B), and the elevations of the top of bank (Y_t), the water surface (y_w), the intersection of the failure surface with the toe (y_f), and the bank toe (y_b). U_{sat} is saturated soil unit weight, and U_w is the unit weight of water.

Assuming Unit Thickness,

Volume of Failure Block (V_{fb}):
$V_{fb} = ½ (y_t - y_f)^2 (\cot B - \cot i)$

Volume of Surface Water (V_{sw}):
$V_{sw} = ½ (y_w - y_f)^2 \cot i$

For Fully Saturated Banks,

Weight of Failure Block (W_{fb}):
$W_{fb} = V_{fb} U_{sat}$

Pore Pressure Ratio (r_u):

$$r_u = \frac{(V_{fb} + V_{sw}) U_w}{V_{fb} U_{sat}} \approx \frac{V_{fb} + V_{sw}}{2 V_{fb}}$$

Resultant of Confining Pressure (F_{cp}):
$F_{cp} = ½ (y_w - y_f)^2 \csc(i) U_w$

The search procedure takes 10 equal increments of bank height (H), projects them to the bank surface, and from each point, projects a potential failure plane (at angle B) through the flood-plain surface. After locating a minimum FS, the search procedure then divides the original increment of H (0.1 H), by 10 again, and makes five incremental searches above, and five incremental searches below the initial minimum FS.

Surface water exerts a confining pressure force (F_{cp}) on a partially submerged failure block (fig. 4). Incorporating F_{cp} into equation 3 yields:

$$FS = \frac{c' L + [W_{fb} (1-r_u) \cos B + F_{cp} \cos (i - B)] \tan \phi'}{W_{fb} \sin B - F_{cp} \sin (i - B)} \quad (4)$$

where L = the length of the failure plane.

The effects of confining pressure are to (1) increase the normal, resisting force, and (2) to decrease the driving force parallel to the failure plane. Clearly, these adjustments will tend to decrease the frequency of modeled failures during moderate channel flows (fig. 4).

Shallow (Infinite Slope) Failures

The infinite slope method is generally used to perform stability analyses on materials of low cohesion where the failure is depth is small relative to its length, and where seepage parallel to the slope can be assumed. This is often true in accreted bank sediments. If $c' = 0.0$, the FS for a sliding mass is given by:

$$FS = \left[1 - \frac{U_w}{U}\right] \frac{\tan \phi'}{\tan i} \quad (5)$$

where U_w = unit weight of water, and $U_w / U = r_u$ (Skempton and Delory, 1957).

For FS $\leq$ 1.0, imminent failure is predicted at angle B (substituted for 'i' in equation 5) as a function of the degree of saturation (r_u) of the slope. The amount of bank retreat from such a failure is calculated from where the failure plane intersects the flood-plain surface.

SUMMARY AND CONCLUSIONS

Algorithms that describe mass-wasting processes can be logically assimilated into the framework of an existing alluvial channel model. The mass-wasting algorithms are placed after the sediment transport subroutine and a dimensionless stability equation is used to initiate the bank failure computations. With data about the characteristics of the bank material, channel geometry, and the ongoing fluvial processes, the model determines the most probable mode of failure based on comparison of two or more factors of safety. This paper focuses on planar failures in banks of homogeneous material and simple geometry. However, the framework developed here can be expanded to incorporate more complex stratigraphy, geometry, and failure mechanisms.

Proposed modifications to modeling planar failures offer a stronger physical basis for analysis of these types of failures. These modifications include incorporation of pore and surface-water pressures and relaxation of assumptions regarding the location of the failure plane. The flowchart and idealized representation showing the disposition of failed bank material (figs, 2a and 2b) identifies the method for maintaining continuity of the failed material from one time step to the next.

REFERENCES

Alonso, C. V., and Combs, S. T., 1986, Channel width adjustment in straight alluvial channels. Proc. 4th Federal Interagency Sedimentation Conf. 2, 5-31 - 5-40.

Carson, M. A., and Kirkby, M. J., 1972, Hillslope form and process. London, Cambridge University Press, pp. 475.

Chen, W. F., 1975, Limit analysis and soil plasticity. New York, Elsevier Sci. Publishing Co., pp. 638.

Daniels, R. B., 1960, Entrenchment of the Willow Drainage Ditch, Harrison County, Iowa. Am. J. of Sci. 258, 161-176.

Fan, Shou-shan, 1988, (ed.) Twelve selected computer stream sedimentation models developed in the United States. Subcommittee on Sedimentation, Federal Energy Regulatory Commission, U.S. Govt. Printing Office, pp. 552.

Huang, Y. H., 1983, Stability analysis of earth slopes. New York, Van Nostrand, Reinhold Co., pp. 305.

Lohnes R. L., and Handy, R. A., 1968, Slope angles in friable loess. J. Geol. 76, 247-258.

Molinas, Albert, 1989, User's manual for BRI-STARS. National Cooperative Highway Research Program, Project No. HR15-11, Ft. Collins, Co., Hydrau-Tech Engineering & Software, pp. 156.

Morgenstern, Norbert, 1963, Stability charts for earth slopes during rapid drawdown. Geotechnique. 13, 121-131.

Osman, A. M., and Thorne, C. R., 1988, Riverbank stability analysis. I: Theory. J. Hydraul. Eng. ASCE. 114, 2, 134-150.

Pizzuto, J. E., 1989, Numerical simulation of gravel river widening (Abs.). EOS, Trans. Amer. Geophy. Union. 70, 15, pp. 329.

Simon, Andrew, 1989a, A model of channel response in disturbed alluvial channels. Earth Surface Processes and Landforms. 14, 1, 11-26.

Simon, Andrew, 1989b, Shear-strength determination and stream-bank instability in loess-derived alluvium, West Tennessee, USA, in Applied Quaternary Res., De Mulder and Hageman (eds.). Balkema, Rotterdam. 129-146.

Simon, Andrew, and Hupp, C. R., 1986, Channel widening characteristics and bank-slope development along a reach of Cane Creek, West Tennessee, in Selected Papers in the Hydrol. Sci. U.S. Geol. Survey Water-Supply Paper 2290. 113-126.

Skempton, A. W., 1953, Soil mechanics in relation to geology. Proc. Yorkshire Geol. Soc. 29, 33-62.

Skempton, A. W., 1954, The use of pore-pressure coefficients in practice. Geotechnique. 4, 148-152.

Skempton, A. W., and Delory, F. A., 1957, Stability of natural slopes in London Clay. 4th Internat. Conf. on Soil Mechanics and Foundation Eng. 2, 378-381.

Taylor, D. W., 1948, Fundamentals of soil mechanics. New York, John Wiley & Sons, pp. 700.

Thorne, C. R., and Osman, A. M., 1988, Riverbank stability analysis. II: Applications. J. of Hydraul. Eng. ASCE. 114, 2, 151-172.

Thorne, C. R., Murphey, J. B., and Little, W. C., 1981, Bank stability and bank material properties in the bluffline streams of northwest Mississippi, in Stream Channel Stability. Appendix D. U.S. Dept. of Agric. Sed. Lab. Oxford, Mississippi. pp. 257.

NUMERICAL MODELING OF UNSTEADY SEDIMENT-LADEN FLOW

By Chintu Lai, Research Hydrologist, U.S. Geological Survey, Reston, Virginia.

ABSTRACT

As continuing work in numerical modeling of unsteady alluvial-channel flow, three advanced multimode method-of-characteristics (MMOC) models are studied as to their mathematical development, algorithm formulation, and other numerical and modeling aspects. A dimensionless model, ND3CMB, is useful in systematic analysis of model characteristics and parameters, serves for general and unified comparison of flows, and frees variables in the model from numerical dependence upon some dimensional system. An extended model, XEUFMB, relaxes some of the restrictive assumptions and incorporates additional nonhomogeneous terms, such as lateral inflows and nonprismatic channel sections. A comprehensive model, XSUFMB, which includes all the above features of XEUFMB, is designed to handle flow reversal. The added features in those advanced models are expected to enhance the model capability and applicability in simulating unsteady, sediment-laden flow.

INTRODUCTION

Numerical modeling of unsteady, sediment-laden flow in rivers and estuaries is an important and practical branch of general computational open-channel hydraulics. Comprehensive and extensive studies on numerical modeling of unsteady flows in fixed-bed open channels have been made since the beginning of the computer era (Baltzer and Lai, 1968; Lai,1986; 1988). However, similar studies in movable-bed open channels did not start until much later. Recently, a new series of alluvial-channel flow models based on the multimode method of characteristics (MMOC) have been developed. These models (collectively called ONED3X) were outlined in a previous report (Lai, 1989), among which the basic model, called X3UFMB, was described in some detail, accompanied by a prototype example.

As research continues in this field, advanced numerical models are being implemented and simulation techniques are being investigated. In this paper a few such models are discussed as to their mathematical development, algorithmic formulation, applications of model features, and model assesment. A dimensionless model, ND3CMB, is useful in systematic analyses of model parameters and characteristics, and serves suitably for general and unified comparison of flows. An extended model, XEUFMB, relaxes some of the restrictive assumptions made in the basic model, X3UFMB, and incorporates such terms as lateral inflows and nonprismatic channels. The model XSUFMB, in addition to possessing the aforementioned features, has the capability to handle flow reversal. It is hoped that these added attributes enhance the model capability and applicability in simulating unsteady, sediment-laden flow.

REVIEW OF MODEL DEVELOPMENT

With the basic assumptions of 1-D flow, unsteady open-channel flow with a movable bed was represented by three partial differential equations (PDE), the equations of continuity for sediment-laden flow and for sediment discharge, and the equation of motion for sediment-laden flow. The sediment concentration, c_s, or the sediment carrying capacity of streamflow, was assumed to depend

on the flow velocity, u (where $u > 0$), and the flow depth, h, i.e., $c_s = c_s(u,h) = c_s[u(x,t), h(x,t)]$. In all the previous model developments by Lai(e.g., 1986; 1989; 1991), a simple power formula, $c_s = Ku^m h^n$, was used, where K is a constant and m and n are exponents. With the substitution of this expression in the equation of continuity for sediment discharge, the following three governing equaions, applicable to flow in a wide rectangular channel of uniform width, can be written:

$$J_1 = h_t + uh_x + hu_x + \zeta_t = 0 \quad (1)$$
$$J_2 = \Psi h_t + \Psi uh_x + \omega hu_t + \Omega hu_x + p'\zeta_t = 0 \quad (2)$$
$$J_3 = gh_x + u_t + uu_x + g\zeta_x + g(S_f - S_o) = 0, \quad (3)$$

in which x = longitudinal distance; t = time; ζ = thickness of sediment layer; p' = volume of sediment in a unit volume of sediment layer; g = acceleration of gravity; S_f = friction slope; and S_o = fixed-bed slope. Some coefficients appearing here are defined as: $\Psi = c_s + \psi h$, $\psi = \partial c_s/\partial h = nc_s/h$; $\Omega = c_s + \omega u$, $\omega = \partial c_s/\partial u = mc_s/u$. It is to be noted that the concept of one dimensional analysis requires that, for the basic model as well as the following three, the sediment deposition and scour take place uniformly across the width. This will be less restrictive to deposition than to scour, which tends to be more local.

The three PDE's, equations 1 to 3, were then transformed into the following set of characteristic equations: i.e., three compatibility equations (Lai, 1986; 1991)

$$S_i\frac{Dh}{Dt} + T_i\frac{Du}{Dt} + P_i\frac{D\zeta}{Dt} + F_i = 0, \qquad i = 1,2,3 \quad (4)$$

in three distinct characteristic directions specified by

$$\left(\frac{D}{Dt}\right)_i \equiv \left(\frac{d}{dt}\right)_i = \frac{\partial}{\partial t} + \left(\frac{dx}{dt}\right)_i\frac{\partial}{\partial x} = \frac{\partial}{\partial t} + \lambda_i\frac{\partial}{\partial x}, \qquad i = 1,2,3 \quad (5)$$

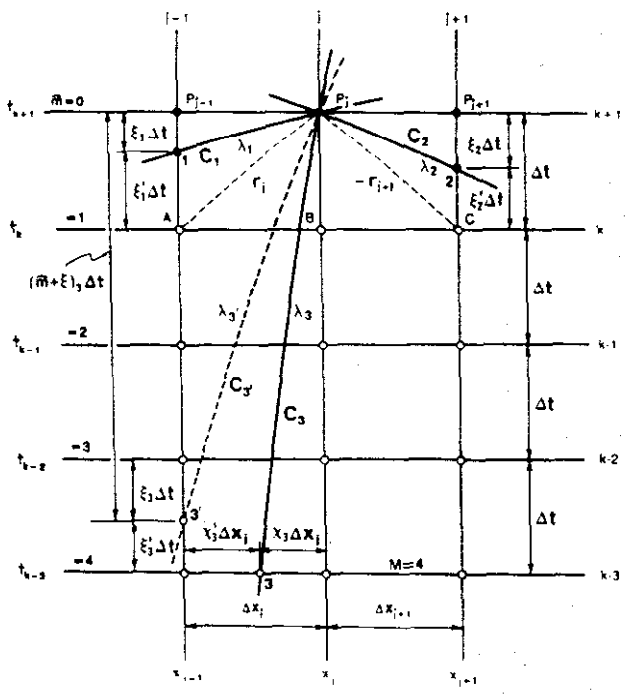

Figure 1. Multimode method of characteristics for three characteristics.

in which, $\mathrm{S}_i = (\Psi - p')\lambda_i/u, \quad \mathrm{T}_i = S_i(\lambda_i - u)/g + \omega h,$

$$P_i = S_i - \Psi + p', \text{ and } \mathrm{F}_i = S_i(\lambda_i - u)(S_f - S_o). \tag{6}$$

Numerical integrations of equations 4 along three families of characteristic curves (eqs. 5) with some specific boundary conditions lead to a numerical modeling of the corresponding movable-bed channel flow. In general, such unsteady flows are characterized by two fast propagating shallow-water waves (Characteristics C_1 and C_2, having $dx/dt = \lambda_1$ and λ_2) and one slowly moving bed-deformation wave (Characteristics C_3 or $C_{3'}$, having $dx/dt = \lambda_3$ or $\lambda_{3'}$) (see fig. 1). The MMOC provides an effective and efficient numerical solution mode commensurate with the special nature of each constituent characteristic. A typical layout of the MMOC approach that includes four numerical-solution modes is illustrated in figure 1, for which the following definitions are given: Δx, Δt = distance and time increments; M = depth of unit computational domain in number of Δt steps ($M = 4$ in the illustration); χ, ξ = spatial and temporal interpolation factors; and $C_r = |\lambda|/r = |\frac{dx}{dt}|/\frac{\Delta x}{\Delta t}$, Courant number; and $\hat{m}$ = reachback number, the number of integral Δt's a characteristic C_i (e.g., C_3) passes through between point P and point i (e.g., pt. 3). Four numerical-solution modes may be categorized as:

Implicit mode	$\hat{m} = 0,$	$M \geq 1,$	$C_r > 1$
Classical mode	$\hat{m} = 1,$	$M = 1,$	$C_r < 1$
Temporal reachback mode	$\hat{m} \geq 1,$	$M > \hat{m},$	$C_r < 1$
Spatial reachback mode	$\hat{m} = M,$	$M > 1,$	$C_r < 1$

DIMENSIONLESS MODEL: ND3CMB

Use of dimensionless equations has many advantages in flow analysis, computation, and comparison. Although the selection of base or normalizing quantities and the combination of dimensionless numbers lead to a variety of dimensionless forms and equations, the following set is considered to be practical and advantageous from programming and implementation viewpoints:

$$\begin{array}{llll} u_* = u/c_o = \mathbf{F}, & x_* = x/L, & t_* = t/T, & h_* = h/h_o = (c/c_o)^2 = c_*^2 \\ (S_o)_* = S_o/S_c, & (S_f)_* = S_f/S_c, & \zeta_* = \zeta/h_o, & p'_* = p'/C_s \\ (c_s)_* = c_s/C_s = & \frac{Ku^m h^n}{K(c_o/2)^m h_o^n} = & 2^m u_*^m h_*^n = & K_* u_*^m h_*^n \,. \end{array} \tag{7}$$

Only two base quantities are to be selected in this set: h_o = the flow depth for a typical normal flow or average flow depth; T = base time interval, such as Δt, data collection interval, and the like. Other base quantities are to be derived from the above two: $c_o = \sqrt{gh_o}$ = base speed (where $c = \sqrt{gh}$ is critical speed); $L = c_o T$ = base length; S_c = critical slope; C_s = base concentration, is the sediment concentration of the flow at $\mathbf{F} = 0.5$, depth = h_o.

From the above definitions, the following set of dimensionless equations corresponding to equations 1, 2, and 3 can be obtained (the asterisks are dropped for simplicity):

$$J_1 = h_t + uh_x + hu_x + \zeta_t = 0 \tag{8}$$

$$J_2 = \Psi h_t + \Psi u h_x + \omega h u_t + \Omega h u_x + p'\zeta_t = 0 \tag{9}$$

$$J_3 = h_x + u_t + uu_x + \zeta_x + S'_c(S_f - S_o) = 0\,. \tag{10}$$

Except the slope term, the last term in equation 10, in which $S'_c = LS_c/h_o$, the above equation set is identical with equations 1 to 3, if g is set to unity in the latter. However, the slope term in equation 10, with S_f in particular, requires a special care in its treatment.

A few previous dimensionless forms presented by Lai(1989) or Lyn(1987) had some scale factors in the equation sets involved, such as α, β, and γ, and thus, are particularly useful in theoretical discussions. The above form, on the other hand, has a special advantage in implementation, because the computer programs developed for the basic model (X3UFMB) can be used almost directly. With this feature, most of the assumptions, qualifications and characteristics attendant with the basic model are also directly transferable. The model scaling can be handled adequately through adjustment of $\Delta x, \Delta t$, and M, as α, β and γ are also functions of these parameters. However, careful I/O treatments and variable/parameter normalizations are still needed.

As a model test, a series of numerical experiments were conducted using a 20 cm wide, 22 m long laboratory flume. The channel bottom was covered by a 1 cm thick layer of uniform sand grain, having porosity $p = 0.4$ (i.e., $p' = 0.6$). The parameter values used for the concentration formula $c_s = Ku^m h^n$ were $K = 0.00145, m = 4$, and $n = -1$. A series of "experimental runs" was made on the computer model ND3CMB. For each run, the simulation was started with the initial uniform flow 5 cm deep, to which a sediment concentration of four times the carrying capacity of the initial flow was introduced at the upstream end. The two base quantities used for variable/parameter normalization were: $h_o = 0.05m$, $T = 30s$.

These simulations were generally of the form of steady water flow with unsteady sediment discharge. A few parameters such as $S_o, \Delta x$, and M, as well as the boundary conditions, were systematically changed for the model studies. Some model characteristics observed were: (a) The model performed satisfactorily in the low S_o range, but began deteriorating as S_o increased, indicating perhaps a more stringent mass conservation is needed for a steep channel (Sikonia, 1989); (b) the choice of boundary conditions also significantly affect the model behavior (Lai et al., 1989); and (c) sediment transport toward downstream, when the sediment was introduced from upstream, was extremely slow (Chang and Wang, 1972; Lyn, 1987). Figure 2 illustrates some simulation results. Details of the modeling studies will be documented separately.

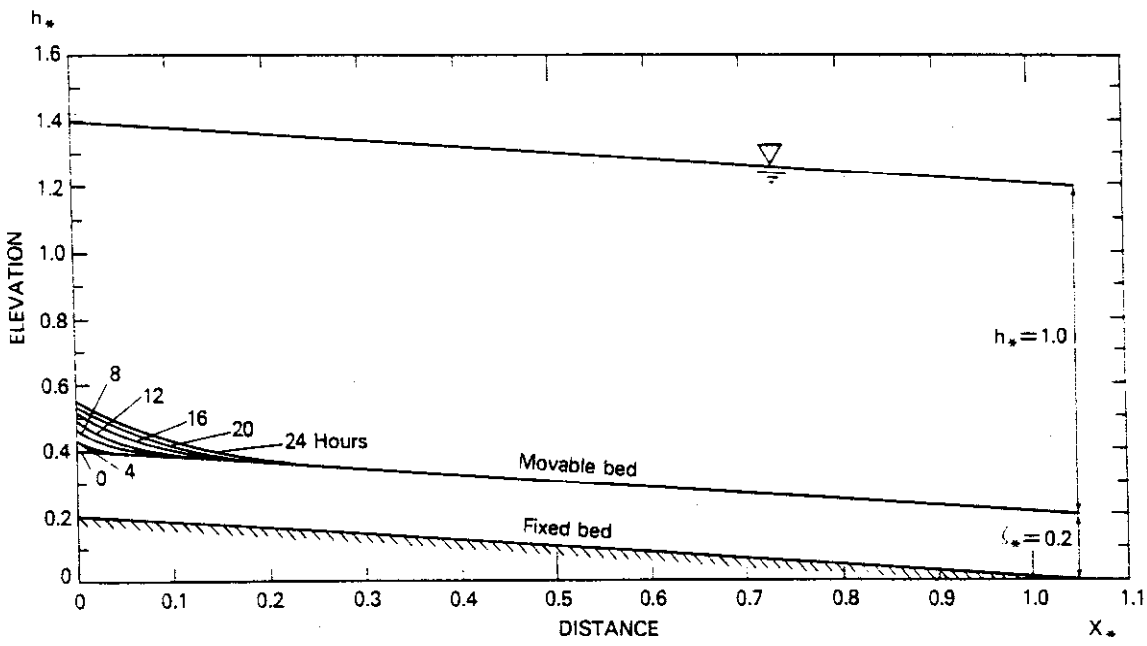

Figure 2. Time variation of bed profile for a small rectangular flume depicted using dimensionless variables.

EXTENDED MODEL: XEUFMB

By relaxing some basic assumptions, and by modifying or adding terms in the basic equation set (equations 1 to 3), extended models can be developed. A few such equation sets have been presented by Lai(1989). Among these, the following form seems to be advantageous for model building, again from implementation viewpoint, because of its proximity to the form of equations used in the basic model (cf. eqs. 1 to 3). The equation set is now valid for an arbitrary cross section, and allows lateral inflow of sediment-laden water. In particular, the form is valid for a rectangular channel, whose width can be variable and need not be wide.

$$
\begin{aligned}
J_1 &= h_t + uh_x + Hu_x + \zeta_t - \tfrac{q}{B} + \tfrac{u}{B}A_x^h = 0 \quad (11)\\
J_2 &= \hat{\Psi}h_t + \hat{\Psi}uh_x + \omega Hu_t + \Omega Hu_x + p'\zeta_t - \tfrac{q_s}{B} + c_s\tfrac{u}{B}A_x^h = 0 \quad (12)\\
J_3 &= gh_x + u_t + uu_x + g\zeta_x + \tfrac{qv}{A} + g(S_f - S_o) = 0\,, \quad (13)
\end{aligned}
$$

in which $A = A(x,h)$ and $B = B(x,h)$ are the cross-sectional area and the top width of channel, respectively, q, q_s = lateral inflow of sediment-laden water and sediment, $H = A/B$ = hydraulic (or average) depth, $A_x^h \equiv \frac{\partial A}{\partial x}|_h$ is the change of cross-sectional area in the x direction with depth h held constant ($A_x^h = 0$ for a prismatic channel), and $v = u - u'$, where u' is the lateral inflow velocity component in the x-direction. $\hat{\Psi}$, slightly different from Ψ, is defined as $\hat{\Psi} = \psi H + c_s$.

The above set, equations 11 to 13, differs from the set of equations 1 to 3, primarily in nonhomogeneous terms, which are due to the introduction of lateral-inflow and nonprismatic-channel effects. Equations 11 to 13 can likewise be transformed to characteristic equations in the same form as equations 4 and 5, with a much expanded F_i term,

$$F_i = S_i(\lambda_i - u)(S_f - S_o) + (S_i - \hat{\Psi} + c_s)\frac{u}{B}A_x^h + \left\{S_i\left[(\lambda_i - u)\frac{v}{\hat{c}^2} - 1\right] + \hat{\Psi} - c_q\right\}\frac{q}{B}\,, \qquad (14)$$

where $c_q = q_s/q$, and $\hat{c} = \sqrt{gH}$.

An equation set using Q (discharge) and Z (stage) as dependent variables is said to be in a conservation form, and may be preferred by some users for better mass conservation. Other mass conservation measures (e.g., Sikonia, 1989), if properly considered, might also improve the model accordingly. Because this model XEUFMB is largely superseded by the following model XSUFMB, further discussion will not be given here. It is documented here as one of the significant intermediate steps in the model advancement.

COMPREHENSIVE MODEL: XSUFMB

In addition to having all the features and facilities that are available with the XEUFMB model, the present model, XSUFMB, also has the capability of treating flow reversal. The case of reverse flow in a channel with a movable bed is not so simple as with a fixed bed. To begin with, it is appropriate to revisit the concentration formula $c_s = c_s(u,h) = Ku^m h^n$, which is valid only when $u > 0$. As a matter of fact, concentration is a scalar quantity depending only on flow speed and not velocity—flow direction is immaterial. Thus, in an alternate-direction flow ($u > 0$, $u < 0$), the simple power formula will make sense only if it is rewritten as $c_s = KV^m h^n$ where $V = |u|$. The partial derivatives of c_s with x and t, then give

$$\frac{\partial c_s}{\partial x} = \psi\frac{\partial h}{\partial x} + \tilde{\omega}\frac{\partial V}{\partial x}, \qquad \frac{\partial c_s}{\partial t} = \psi\frac{\partial h}{\partial t} + \tilde{\omega}\frac{\partial V}{\partial t},$$

in which $\psi = \partial c_s/\partial h = nc_s/h$, $\tilde{\omega} = \partial c_s/\partial V = mc_s/V$.

By using these relations in the equation of continuity for sediment discharge, first for $u > 0$, in which case $V = u$, then for $u < 0$, in which case $V = -u$, three partial differential equations identical to equations 11 to 13 can be derived.

Secondly, for treatment of the S_f term, the identical step used in the fixed-bed case is valid. That is, replace u^2 by $u|u|$ in the expression for S_f. Thirdly, a special computer algorithm has to be formulated for treating the unsymmetrical arrangement of boundary conditions. At the moment of flow reversal, the boundary conditions at the upstream end and at the downstream end must be interchanged. This means that one boundary condition at the upstream end and two at the downstream end must be used for the reverse flow, as against two upstream and one downstream for the normal-direction flow. The computer algorithm to implement the above concept is, in fact, much more involved than described. Worse yet, the flow does not reverse simultaneously over the entire reach; for some reaches the flow reverses only at the lower part of the reach.

The algorithm to treat reverse flow as described above was incorporated in the system, equations 11 to 13, which constitute the model XSUFMB. Because the algorithm to examine a proper alignment of the three characteristics meeting at point P on the advanced time level (i.e., two characteristics on the left side and one on the right, or vice versa) is applied grid point by grid point, including the boundary points, the concern as to nonsimultaneous or partial flow reversal may not be relevant. However, there still remains complexity associated with other aspects of flow reversal, which calls for additional considerations.

Figure 3 shows some simulation results of a Delaware River reach between Torresdale (upstream) and Delair, using the XSUFMB model. The reach has a length of 9.14 km (5.68 mi) (gage 1, G1, is at the upstream end; gage 2, G2, is 3.97 km (2.46 mi) downstream from G1; and gage 3, G3, is at the downstream end) and is normally strongly affected by tides. For the hydrodynamic boundary-value data, the time sequence of stage data of August 15 and 16, 1962 (for which a complete tidal cycle of measured discharge at Tacony-Palmyra Bridge, 4.20 km (2.92 mi) from G1, is available) (Lai, 1965; Baltzer and Lai, 1968)) at G1 and G3 were used. This period of data was repeated for a few cycles to obtain a sufficient length of time for sediment simulation. Combined with these data are the designed concentration data: During ebb flow a constant concentration with the strength four times the carrying capacity of the initial flow was imposed at the upstream end; during a period of flood flow, the maximum concentration during the preceding ebb flow was used as the boundary-value concentration at the downstream end.

The flow-sediment coupled model, XSUFMB, is capable of simulating the stage hydrograph and discharge hydrograph satisfactorily; the available measured data (i.e., for the initial 26 hours) were for most parts too close to plot in figures 3a and 3b (A few exceptions were noted on fig. 3b). Figure 3c shows substantial sediment deposition at the upstream end. Very little sediment was carried into the interior nodal points because of the periodic motion of the alternating flow.

SUMMARY AND CONCLUSIONS

Three advanced multimode method-of-characteristics (MMOC) models of unsteady alluvial-channel flow were studied as to their mathematical development, algorithm formulation, and other modeling aspects.

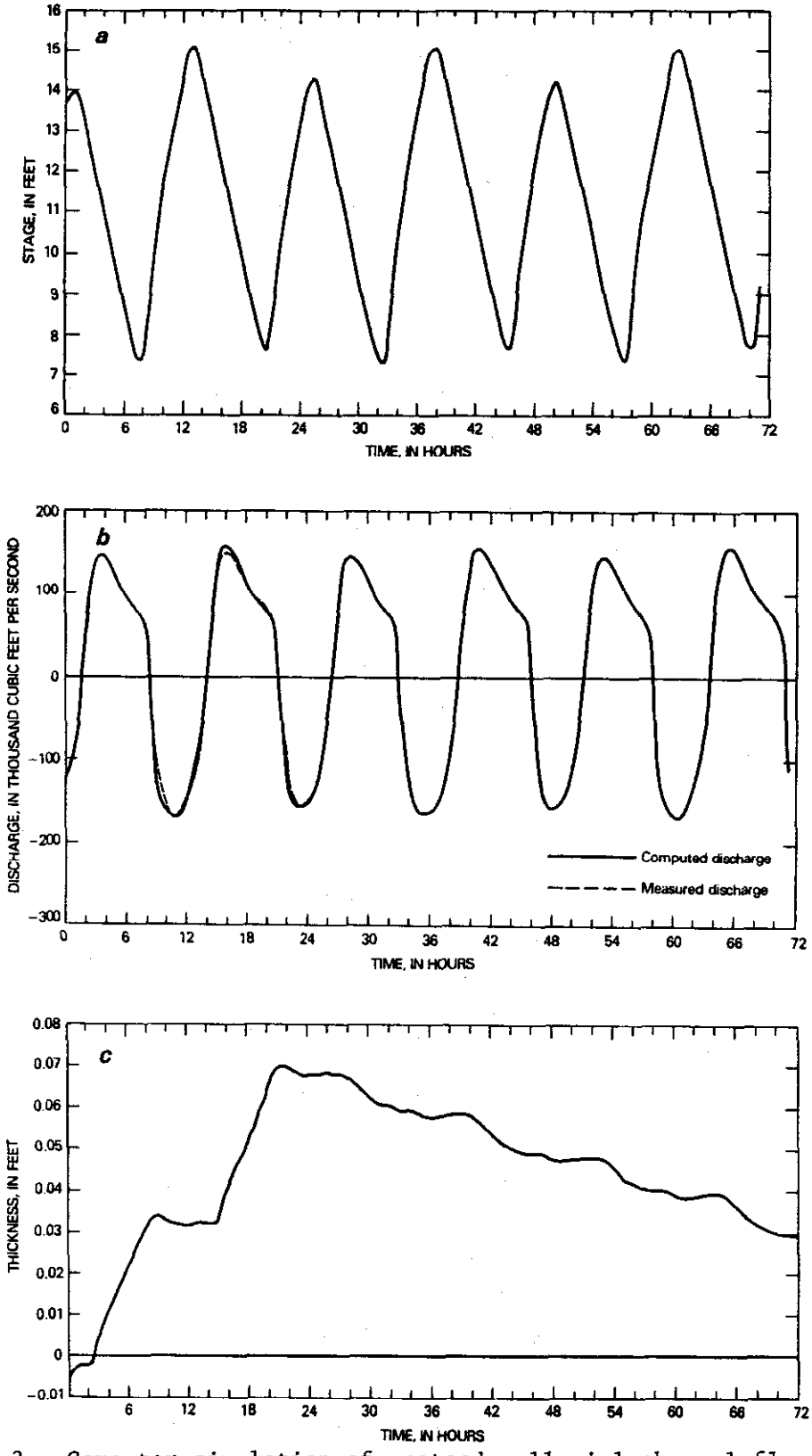

Figure 3. Computer simulation of unsteady alluvial-channel flow in a tidal reach of the Delaware River (near Philadelphia, Pa.): (a) Stage hydrograph at Gage 2, (b) Discharge hydrograph at Tacony-Palmyra Bridge, (c) Time variation of bed-layer thickness at Gage 1.

1. A dimensionless model is useful in systematic analysis of model characteristics and parameters, and serves for general and unified comparison of flows. A dimensionless model, named ND3CMB, has been developed, and is based on a set of governing partial differential equations that are nearly identical in form with the dimensional set used for the basic model X3UFMB. The model ND3CMB performed well for the aforementioned objectives.
2. An extended model, XEUFMB, includes a number of additional nonhomogeneous terms in it, thus enhancing model capability and sophistication. However, these terms increase model nonlinearity, numerical instability, computational difficulty, and programming complexity. Although several successful runs have been made using this model, further model investigations are deemed necessary and important.
3. A comprehensive model, XSUFMB, incorporates all the features and capabilities afforded by XEUFMB, and in addition, it handles the case of flow reversal. The flow reversal still remains a complex technical problem, and warrants further research and investigation.

REFERENCES

Baltzer, R. A., and Lai, C., 1968, Computer simulation of unsteady flows in waterways. J. Hydraulics Div., Amer. Soc. Civil Engr., 94(HY4), 1083-1117.

Chang, F. F. M., and Wang, T. W., 1972, Scour and fill in the Missouri River as related to the water resources planning. Completion Report for Project No. B-008-SDAK, South Dakota State University, Brookings, SD.

Lai, C., 1965, Flows of homogeneous density in tidal reaches, solution by the method of characteristics. U.S. Geological Survey Open-File Report 65-93, 58 p.

Lai, C., 1986, Numerical modeling of unsteady open-channel flow. *Advances in Hydroscience*, V. T. Chow and B. C. Yen, eds., V.14, Academic Press, Orlando, FL.

Lai, C., 1988, Comprehensive method of characteristics models for flow simulation. J. Hydraulic Engrg., Amer. Soc. Civil Engr., 114(9), 1074-1097.

Lai, C., 1989, A numerical scale model for simulating unsteady-alluvial channel flow. Tech. Rept. prepared for Sedimentation Comm., Interagency Advis. Comm. on Water Data, 72 p. –Also in *Twelve Selected Computer Stream Sedimentation Models Developed in the United States.* ed. by S. S. Fan, Chmn., Interagency Ad Hoc Sedimentation Work Group, Publ. by Fed. Energy Reg. Comm., 179-260.

Lai, C., 1991, Modeling alluvial-channel flow by multimode characteristics method. J. Engrg. Mechanics, Amer. Soc. Civil Engr., 117(1), 32-53.

Lai, C., Schaffranek, R. W., and Baltzer, R. A., 1989, Frictional resistance treatment in unsteady open-channel flow simulation. Proc., International Conf. on Channel Flow and Catchment Runoff, Centennial of Manning's Formula and Kuichling's Rational Formula, May 22-26, 1989, Univ. of Virginia, Charlottesville, VA, 688-698.

Lyn, D. A., 1987, Unsteady sediment-transport modeling. J. Hydraulic Engrg., Amer. Soc. Civil Engr., 113(1), 1-15.

Sikonia, W. G., 1989, Mass-conserving method of characteristics for streamflow modeling. U.S. Geological Survey Open-File Report 89-414, 75 p.

USE OF 2-D HYDRODYNAMIC AND 1-D SEDIMENT MODELS

By James C. Thompson, Project Engineer, David T. Williams, Chief Executive Officer, and Jeffrey B. Bradley, President, WEST Consultants, Inc., Carlsbad, California

ABSTRACT

A small run-of-the-river recreational dam on the Arkansas River has experienced significant sediment deposition since it's completion in the early 1980's. An integrated modeling approach using a two-dimensional (2-D) hydrodynamic model, FESWMS-2DH and a one-dimensional (1-D) sediment transport model, HEC-6 helped to evaluate alternative mitigation measures. The alternatives included major dredging, spot dredging, construction of smaller self-maintaining channel using river training structures or small islands, and combinations of the aforementioned.

INTRODUCTION

Zink Dam is a small recreational reservoir on the Arkansas River in Tulsa, Oklahoma. The dam, constructed in 1983, is an overflow structure of approximately twenty foot height with three small gates. It is approximately twenty miles downstream of Keystone Dam, a U.S. Army Corps of Engineer (COE) structure. Sediment sources were cutoff above Keystone after it's construction in 1963, but significant bed and bank sediments still remain as sources. Since the construction of Zink Dam, the pool has filled with sediment twice, the first time gradually over the time period 1983 - 1986. The flood of 1986 flood, which exceeded the 100 year flood event, flushed the reservoir. Since that time, again it has refilled. It is the objective of the Tulsa River Parks Authority to maintain sufficient depth in the pool to enhance boating and other recreational activities. This study is the culmination of an alternatives analysis to try to obtain that goal.

HEC-6, Scour and Deposition in Rivers and Reservoirs, is a 1-D sediment transport model originally developed by W.A. Thomas of the COE. The code used in this study was the new release by the HEC for which WEST Consultants wrote the Users Manual. The water surface and velocity field determined by FESWMS-2DH were integrated with HEC-6 to evaluate several alternatives in order to determine a solution for the Zink Dam sedimentation problem.

HEC-6 MODEL DEVELOPMENT FOR CALIBRATION

HEC-6 uses the same fundamental hydraulic relationships as the well known HEC-2 water surface profile model. The model was originally developed for use on the Ozark and Arkansas Rivers. Because it is a 1-D model, it predicts only the average bed conditions across a cross section and not the localized scour or deposition. This means that the actual cross section may have scour in one place and deposition in another but HEC-6 will only predict the net scour or deposition.

HEC-6 model calibration began with the development of a model which reflected the streambed in 1963. The calibration period was from 1963 to 1977, utilizing the hydrology for that time period. Hydraulic and sediment parameters were adjusted until the bed elevation change obtained from the model reflected the observed bed elevation change from 1963 to 1977. The observed annual sediment yields were also used in the calibration phase. In 1963, 1977 and 1988, the COE surveyed 12 sedimentation ranges (called degradation ranges) between Keystone Dam and Zink Dam. Average bed elevation changes for these time periods were computed. Since the HEC-6 model simulation required a 1963 geometry, the bed elevation changes from the 1963 - 1977 time period were subtracted from the cross sections of the 1977 HEC-2 Flood Insurance Study geometry to produce a best estimate of the actual geometric condition for 1963. This was done for cross sections from River Mile 523.8 (downstream limit of the degradation ranges) to 538.67.

The HEC-6 model calibration required the river hydrology for the 1963 -1977 time period. Mean daily discharges were obtained from WATSTORE hydrology files compiled by the U.S.G.S. for the Tulsa Gage at the 11th Street bridge (River Mile 523.7). A computer file containing these mean daily discharges was obtained from the COE. A proprietary program was used to convert the mean daily flows to an input format compatible with HEC-6. The results of the HEC-2 model for the 1977 conditions provided by the COE were used as guides for the hydraulic calibration of HEC-6 model. For the time period 1963 to 1983, the natural rating (pre-impoundment) curve at the Zink Dam site was obtained from the COE HEC-2 model. The impoundment of Zink Dam occurred in 1983 and the rating curve from the COE 1986 HEC-2 model, which included the Zink Dam geometry, was used to define the downstream boundary for 1983 to 1988. This HEC-2 model did not take into consideration hydraulic submergence losses at the dam or the use of the low flow gates at Zink Dam. A rating curve at the dam was assumed which began at elevation 612 feet (low flow gates are open) at very low flows and at elevation 618.5 (1.5 feet above the weir crest) at 10,000 cubic feet per second (cfs). Estimated submergence losses were also added to the HEC-2 rating curve for higher flows.

The bed sediment gradations for the 1963 conditions were not known. It was assumed that bed gradations taken in October 1989 just upstream of Zink Dam were indicative of the 1963 conditions for all the cross sections and were initially used in HEC-6. These gradations were then adjusted in the calibration phase. The D_{50} (diameter of particles finer than 50% by weight) of the final bed gradation used was 1 mm. Since the D_{50} of the bed ranged from 5 mm to 0.5 mm and the Arkansas River is a moderately large river with moderate slopes, the Yang's stream power sediment transport relation, an option in HEC-6, was selected for sediment transport prediction. Keystone Dam has a very high sediment trap efficiency which led to the assumption that no sediment was exiting it.

Figure 1 shows the bed elevation changes for the HEC-6 simulations for periods 1963 to 1977, which are compared to the measured changes from the degradation ranges. The general pattern of the HEC-6 simulations follows the degradation range pattern with only a few exceptions. These exceptions were not deemed excessive and would not affect the overall results.

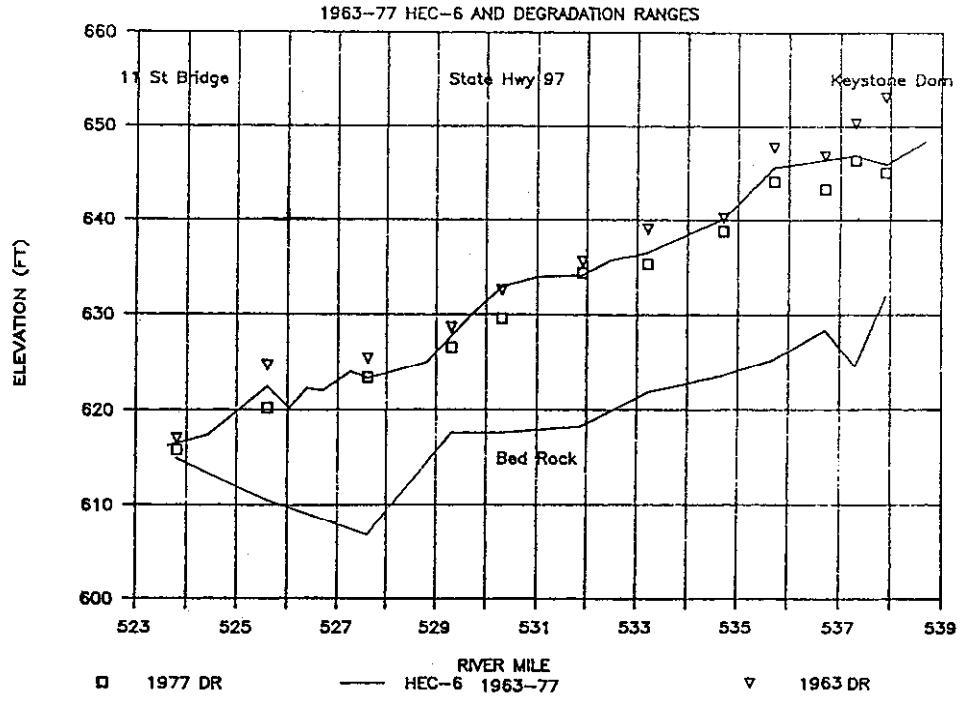

Figure 1. HEC-6 Calibration Results

HEC-6 MODEL VERIFICATION

Once a model has been calibrated, it must be verified (confirmed). The verification phase must use data not used in the calibration phase and should not require any significant adjustment of the parameters. For the confirmation test, the HEC-6 model was run from 1977 to 1988 and the resulting bed elevation change was compared to the observed bed elevation change for that period.

Figure 2 shows the HEC-6 bed elevation changes when the model is continued from 1977 to 1988 (verification period). The bed elevation changes are for the period 1963 to 1988 and are compared to the changes obtained from the degradation ranges. As in the calibration phase, the HEC-6 general pattern and relative magnitude of bed elevation changes appear to be consistent with the degradation range changes. No dependable bed gradations were available for all locations throughout the area or for the various calibration or verification time periods. As a result, the HEC-6 predicted bed gradations could not be verified; however, the 1963 to 1988 simulation predicted coarser gradations (D_{50} ranging from 2 mm to 4 mm), as expected, than originally input for the 1963 conditions.

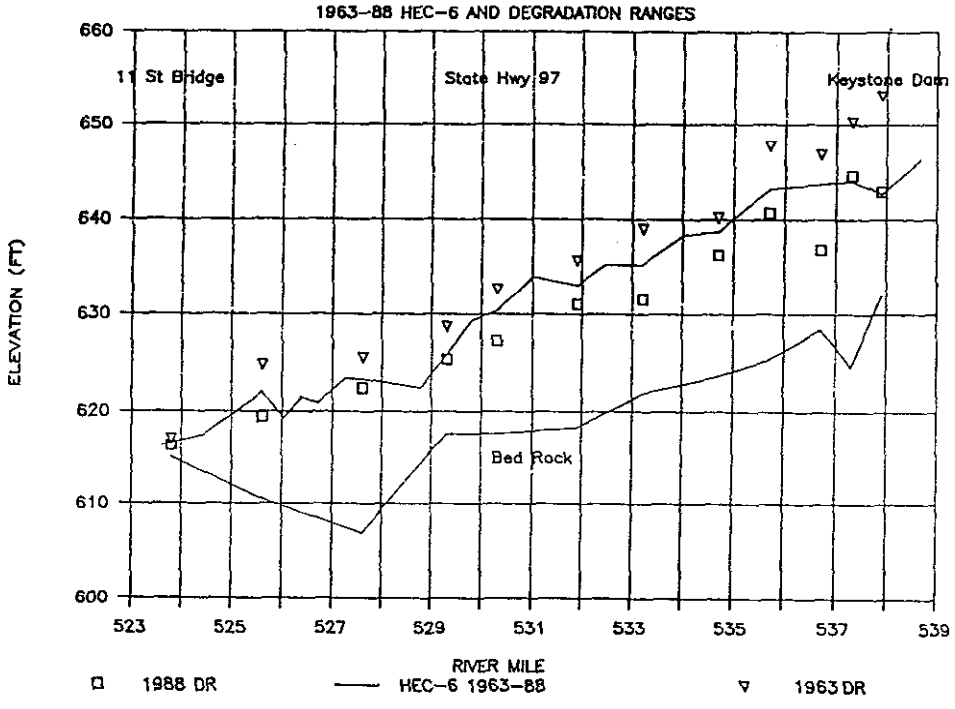

Figure 2. HEC-6 Verification Results

HEC-6 MODEL DEVELOPMENT FOR 1988 BASELINE CONDITIONS

This section deals with a detailed analysis of the baseline conditions for the reach from the 11th Street bridge to Zink Dam. Much of the information obtained in the verified model is used in the baseline conditions model. Detailed geometry of the Zink Reservoir area was not available for the 1988 (current) conditions. From the contour maps and recent aerial photographs, detailed geometry was developed and entered in an HEC-6 model. This model extends from Zink Dam (just downstream of RM 522.04) to the 11th street bridge at RM 523.69. The representative future hydrology was assumed to be the same as the historic hydrologic period of 1963 to 1988 at the Tulsa gage was used to simulate the period from 1989 to 2014.

The roughness coefficients used in the calibration/verification phases were used for the base condition. The 1963 to 1988 simulation indicated that the bed gradation coarsened such that the D_{50} of the bed increased from the 1963 input values of 1 mm to between 2 mm and 4 mm. A D_{50} of 3.3 mm was adopted as representative of the reach as shown in Figure 4 for 1988 conditions. The shape of the gradation curve was the same as that of the initial gradation. At the end of the 1963 to 1988 HEC-6 verification simulation, a series of short duration discharges of increasing magnitude were entered in the hydrology. The resulting sediment transport and sediment load gradation at RM 522.67 (upstream end of Zink Reservoir) for each discharge was used as the inflowing sediment load and gradation to the base condition model.

Baseline condition simulations are based upon the premise that the existing operation of Zink Dam will continue and constitute a "do nothing" condition. Bed elevation changes for the 1989 to 2014 simulations showed that the upper portion of the reservoir area is self maintaining and is not significantly scouring or depositing. However, the lower portion, below RM 522.9, is still depositing sediment in addition to the deposition that had occurred prior to 1988. Since HEC-6 is a 1-D sediment model, the actual deposition may be higher at one location than another along the cross section; however, the net deposition should be close to the HEC-6 results.

The 1989 to 2014 simulation showed that the sediment load entering RM 523.67 is 239 acre-feet (486,000 cu. yd.) per year, slightly higher that the verification simulation. Of this, approximately 10.8 acre-feet (22,000 cu. yd.) per year is being trapped between RM 523.67 and Zink Dam. Again, this is in addition what may have been trapped prior to 1988.

The apparent equilibrium between RM 523.67 and RM 522.9 is interesting because this area has had depositional problems. The 1988 conditions contain the two islands on the west side of the river which help to keep the sediment at the more efficient east side of the river. Deposition at a bend generally occurs at the curve's inside (west side), indicating that secondary and "vertical roller" currents are the main driving force of the sediment deposited in these areas. The primary currents, as shown by the HEC-6 results, are sufficient to keep most of the sediment moving downstream. Because of this, a general constriction of the river in this area will not significantly reduce the local deposition on the west side of the river since this action affects only the primary currents, not the secondary currents causing the deposition. A more promising alternative is a spur dike that would deflect the secondary flows away from the amphitheater and the boat ramp. Analysis of secondary currents cannot be performed by a 1-D model such as HEC-6. A 2-D hydrodynamic model is required to analyze secondary currents for existing and any proposed conditions.

TWO-DIMENSIONAL ANALYSIS USING FESWMS-2DH

FESWMS-2DH, Finite Element Surface-Water Modeling System: Two-Dimensional Flow in a Horizontal Plane, was used to determine the flow velocities and water surface elevation for existing conditions and the alternative spur dike configurations. While 1-D models, such as HEC-2, solve for a single water surface and an average velocity at each cross section, 2-D depth-averaged models allow the water surface to vary from bank to bank and allow the velocity to follow any horizontal direction. A 2-D analysis is particularly useful when evaluating the velocity field and the water surface variation under complex hydraulic conditions since local velocities and water surface elevations can be resolved. FESWMS-2DH was developed for the U.S. Federal Highway Administration by the Water Resources Division of the U.S. Geological Survey. The modeling system is able to simulate complex flow conditions which are essentially 2-D in the horizontal plane. The governing equations are the primitive form of the shallow water equations where two equations describe the conservation of momentum and one equation describes the conservation of mass. Frictional losses were modeled using Manning's equation. Turbulent effects were modeled using the Boussinesq eddy viscosity concept. Wind stress and the Coriolis force were not considered for this simulation. The resulting system of differential equations are solved by a Galerkin finite element method as described by Froehlich (1989).

The FESWMS existing conditions model extended from Zink Dam, upstream to the 11th Street Bridge. The geometry for the 2-D model was developed from contour maps, aerial photographs, site photographs and HEC-2 cross sectional data. The finite element network near the spur dikes is shown in Figure 3. The network was designed to reflect the existing conditions under a range of flows while allowing the effects of alternative spur dike configuration to be simulated. The finite element method allows a more detailed, hence more accurate, network to be used at areas of particular interest, such as near the existing islands and near the amphitheater. Special efforts were made to accurately reflect the hydraulic effects of existing bank lines, channel elevations, islands, bridges, the amphitheater, overbanks and other significant features. The entire network contains 1679 nodes and 525 elements. Elements which were dry due to low flow, islands, or spur dike configuration were not included, as such the network was customized for each flow rate and each alternative.

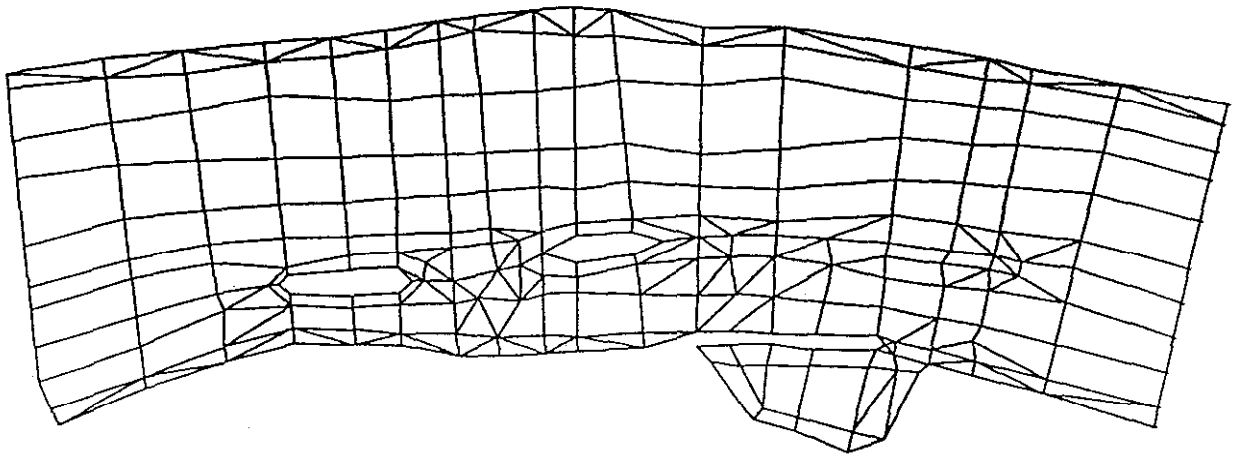

Figure 3. Finite Element Network Near Spur Dikes

The Manning's roughness coefficients, 'n', for the FESWMS model were essentially the same as for the HEC-6 model but were allowed to vary slightly with depth. Throughout most of the network the 'n' was varied through 0.033 for depths less than 10 feet to 0.027 for depths greater than 20 feet. The roughness coefficient along the overbanks and through the 21st Street Bridge was increased slightly to reflect greater frictional losses. The total flow rate was specified as the upstream boundary condition and the water surface was specified as the downstream natural boundary condition. The downstream boundary elevations of the two-dimensional model were developed from the HEC-2 model and were essentially equal to the elevations used by the HEC-6 model. A slip condition was used at all lateral boundaries. A zero order turbulence model was used to determine the appropriate eddy viscosity. The model determines the eddy viscosity as a function of the shear velocity and depth so that value of the eddy viscosity reflected the local hydraulic conditions. Typical values of the eddy viscosity were in the order of 10 ft^2/s to 20 ft^2/s.

A wide range of flow rates were simulated by the 2-D model, from 25,000 cfs (one-half the 2-year flow rate) to 305,000 cfs (the peak flow rate of the 1986 flood). This paper presents the results of an analysis of existing and alternative conditions at a flow rate of 50,000 cfs in particular since this flow rate is representative of channel forming conditions.

A complete 2-D analysis generates a tremendous amount of spatially related data and it is best to present results graphically. Figure 4 shows the flow pattern under existing conditions at a flow rate of a 50,000 cfs. Figure 5 shows the flow pattern at the same flow rate with the three spur dike alternative. The area shown in the velocity field plot extends from the 11th Street Bridge downstream to the boat ramp.

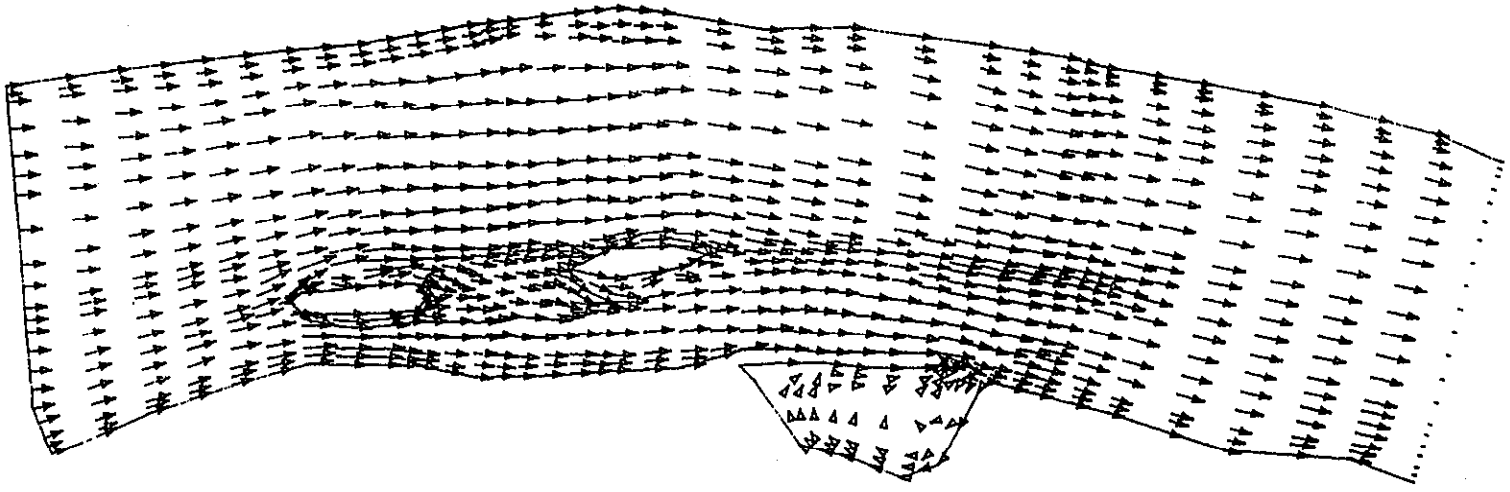

Figure 4. Velocity Vectors for Base Conditions, Q = 50,000 cfs

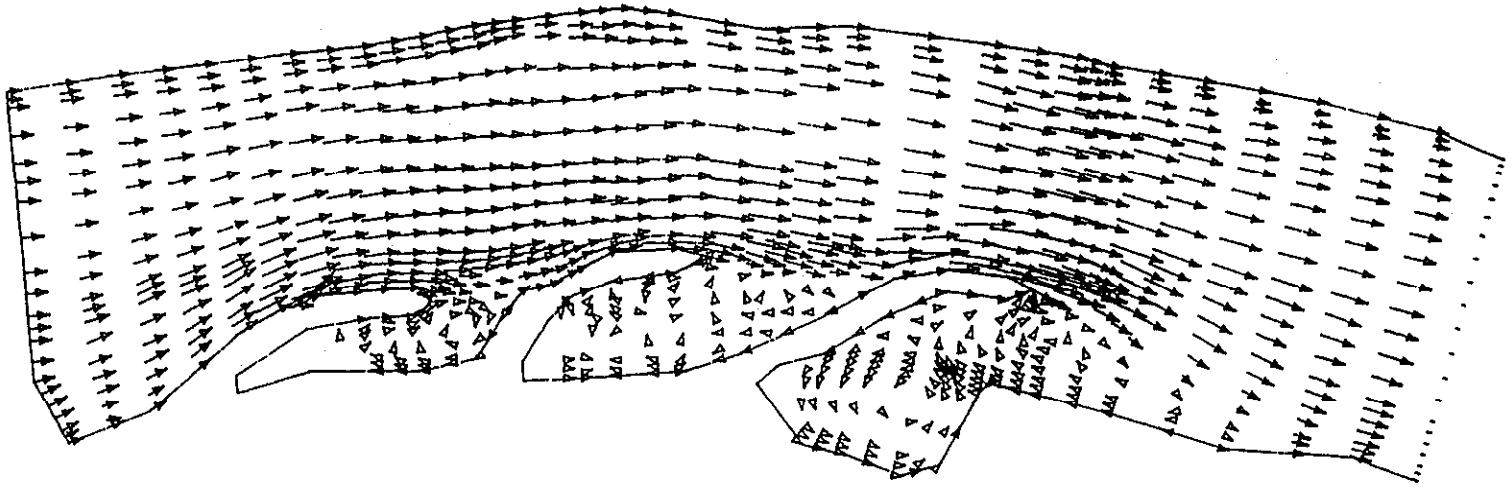

Figure 5. Velocity Vectors for 3 Spur Dike Alternative, Q = 50,000 cfs

The magnitude and direction of the velocity at each node is represented by the length and direction of the arrow or vector. Closely spaced vectors indicate closely spaced nodes and do not necessarily indicate high velocities. At a flow rate of 50,000 under existing conditions, the maximum velocity in the channel is approximately 8 ft/s. The velocity vector plot indicates that low velocity flow cross between the islands, that slow recirculating flow occurs near the amphitheater and that slow flow occurs near the boat ramp. The moderate water velocities along the west bank upstream of the amphitheater bring the sediment to the entrance and the slower velocities at the entrance allows the sediment to deposit. Fine sediment diffuses into basin is distributed by the circulation pattern in the basin. The lower velocity at the entrance to the amphitheater extend a few hundred feet downstream, where deposition near the boat ramp occurs.

Before the HEC-6 model had been fully developed, it was thought that the cause of deposition near the amphitheater entrance was due to the lack of sediment transport capability of the main channel. As a result, a three spur dikes alternative was formulated with the first and second spur dikes connected to the existing islands and the third dike would be constructed near the amphitheater basin. The philosophy of this configuration was to keep the flow and sediment along the east side of the river where the flow has greater sediment transport capacity. The third dike would serve this purpose and keep the secondary currents from the basin entrance.

The velocity vectors shown in Figure 5 indicate that some recirculation would occur near the proposed spur dikes. Slow recirculating flow would occur near the amphitheater basin. Fine tuning the geometry of the spur dike would allow continuous flushing of this basin and reduce the potential for deposition. The results indicated that at 50,000 cfs the three spur dike option would increase the water surface elevation locally by 1.0 feet along the east bank and 1.4 feet along the west bank. The increase in the water surface due to the spur dikes decreases at higher flows as the spur dikes are overtopped. The maximum velocity in the channel near the downstream spur dike would increase to about 10 ft/s which would increase the sediment carrying capacity of the channel through the constricted reach.

The HEC-6 results have shown that the reach between the 11th and 21st Street bridges is capable of transporting the inflowing sediment although deposition still occurs along the inside of the bend. All three spur dikes may not be essential since the proposed dike near amphitheater has the greatest impact and may be sufficient to reduce deposition. The results of the 2-D analysis of each dike/island alternatives were used to calibrate the hydraulics of the HEC-6 model for sediment analysis of the proposed alternatives.

HEC-6 ANALYSES OF ALTERNATIVES FOR THE LOWER REACH

The Tulsa River Parks Authority is interested in keeping enough water depth (approximately 2 feet) in the reservoir area for recreational purposes. With relatively small quantities of spot dredging, the upper reservoir area, according to the HEC-6 results, should not have any trouble maintaining such a main flow area depth which is generally at the outside of the bend. However, the lower part of the reservoir does have deposition problems and would not maintain a 2 foot water depth for low flows. Two alternatives were formulated for the lower reservoir area; dredging and maintenance of a 500 foot wide channel, and the same alternative with the construction of islands or spur dikes.

The HEC-6 model was adjusted to initially dredge a 500 foot wide channel from Zink Dam to RM 523.73 on the outside bend. For the 1989 to 2014 simulation, the program was then instructed to dredge the channel with a 1 foot overdepth whenever the water depth became less than 2 feet. The initial dredging required to reach an acceptable level is estimated to be 74,300 cubic yards with an average annual dredging requirement of 21,300 cubic yards. There are periods where no dredging is required due to a lack of sediment carrying flows or large flows which essentially clean the channel. An example of the large flow condition is the year 2012 which contains the equivalent of the 1986 flood. The years 2013 and 2014 did not require any dredging because of the cleansing effect caused

by the 2012 (1986) flood. The lack of dredging requirements from 1994 to 2001 (equivalent to 1968 to 1975) were reflective of a moderately low water yield period and resulting lack of sediment inflow.

Another alternative involved the same conditions as described above in addition to a 300 foot encroachment from the east bank by either spur dikes or islands. The encroachment would extend from Zink Dam to RM 522.73 with its elevation set 1 foot higher than the water surface elevations for a 50,000 cfs discharge. The encroachment would be inundated (probability frequency basis) of every 1 to 2 years. Again, this option assumes an initial dredging volume of 74,300 cubic yards. The results showed that the average annual dredging requirement would then be reduced to 11,200 cubic yards.

CONCLUSIONS

If no action is taken, sediment will continue to fill the pool between Zink Dam and the 21st Street Bridge. The baseline HEC-6 model indicates bed aggradation downstream of the 21st Street Bridge. Upstream of the 21st Bridge, the channel is in quasi-equilibrium, i.e., there is no net deposition or erosion. HEC-6 only evaluates average cross-sectional bed change and cannot resolve local deposition. Deposition due to secondary currents along the inside of the bend, can be observed near the amphitheater and the boat ramp. We foresee a similar magnitude problem as has been experienced in the past several years above 21st street in the no action scenario. Deposition will continue along the inside of the bend. Since primary currents on the east side or outside of the bend are sufficient to keep most material moving, a general constriction in this reach will not significantly reduce deposition. A more promising alternative is a spur dike that will defect the secondary flows away from the amphitheater and boat ramp. The existing two islands could remain as they are today. Average annual sand bed material delivery to Zink Dam is estimated at 396,000 cubic yards. The dredging required to keep the channel clean is less than this value, with no other action, because large storms (1986) will flush the reservoir. The expected dredging requirement would exceed 200,000 cubic yards.

Significant deposition has occurred downstream of the 21st Street Bridge. HEC-6 analysis indicates this area will continue to aggrade until the reservoir is filled through this reach with the occasional infrequent flood such as the 1986 event flushing deposited material from the pool.

Two sub-alternatives were investigated to alleviate depositional problems in the lower reach, a dredging option to maintain a 500 foot wide channel in which a 2-foot flow depth would be maintained, and the same option with spur dikes/islands constricting.

Spot dredging alone could only, at best, maintain the opening to the amphitheater and with the River Parks present equipment (mudcat). Spot dredging is viable if used in conjunction with the spur dike option above 21st Street. The spur dike should reduce deposition due to secondary currents, combined with spot dredging at the boat ramp and amphitheater,could become a very viable option for the upper reach. The mudcat dredge may still be insufficient to handle spot dredging.

The combined option is the one that will best mitigate sediment depositional problems. Whether the economics are viable is something that the River Parks Authority must decide. The most optimal solution would include a spur dike with local dredging above the 21st Street Bridge. Downstream it would include either the dredging alternative or the combined dredging/spur dike option.

REFERENCES

Froehlich, D.C., "Finite Element Surface-Water Modeling System: Two-Dimensional Flow in a Horizontal Plane," Vol. I. Users Manual, Federal Highway Administration, Publication No. FHWA-RD-88-177, April 1989.

U.S. Army Corps of Engineers Water Resources Support Center, "HEC-6 Scour and Deposition in Rivers and Reservoirs Users Manual," Hydrologic Engineering Center, Davis, California 1977.

SIMULATION OF BED TOPOGRAPHY IN A MEANDERING RIVER

by Howard H. Chang, San Diego State Univ., San Diego, CA

ABSTRACT

River channels are seldom straight over a length of a few channel widths. Bed topography associated with channel curvature often needs to be determined since any design for bank protection must be extended beyond the potential scour in order to prevent undercutting. The curvature-induced scour should also be tied in with aggradation and degradation invoked by any imbalance in sediment transport.

The FLUVIAL model (Chang, 1985) was developed to simulate channel-bed scour and fill together with changes induced by the curvature effect. The field data from the Fall River in Colorado was selected as a test case to evaluate the applicability of the FLUVIAL model for predicting the bed topography in curved channels with an erodible bed. The data set, at the same time, provides a means of calibrating the model. Field measurements of bend flow hydraulics and sediment characteristics in the Fall River were made at about the bankfull discharge by Thorne et al. (1985). The river channel in the study reach is highly sinuous (sinuosity 2.2) with stable banks of meander belt silts and clay.

Both transverse flow and cross-stream flow were observed in the measurement. The former refers to the velocity component normal to the primary flow. The latter is the velocity component perpendicular to the tangential direction of the river channel, resulting form the angular difference between discharge centerline and channel centerline. Because of the cross-stream flow, the transverse flow develops only in the deeper region of the curved section and it does not develop in the shallow region near the concave bank. By taking this flow pattern into consideration, general agreement between the simulation and measurement was obtained. The bed topography of the Fall river is a reflection of the flow pattern, characterized by the transverse bed slope in bends. Such bed pattern changes with the flow pattern which undergoes continuous growth and decay.

INTRODUCTION

River bank protection must be designed to contain the design discharge and withstand the velocity. It must also be extended beyond the potential scour to prevent undermining. Therefore, one needs to determine the channel bed scour in the design for channelization. Since river channels are hardly straight for a very long distance, channel bed changes are induced by the curvature effect in addition to aggradation and degradation.

The FLUVIAL model (Chang, 1985) was developed to simulate channel bed scour, considering the effects of aggradation, degradation and channel curvature. The Fall River was selected as a test case to evaluate the applicability of the FLUVIAL model for predicting the bed topography in curved channels with an erodible bed. The data set, at the same time, provides a means of calibrating the model since certain algorithms in the model require experimental calibration.

The Fall River is located in the Rocky Mountain National Park, Colorado. Field measurements of bend flow hydraulics and sediment characteristics were made at about the bankfull discharge by Thorne et al. (1985). The river channel in the study reach as shown in Fig. 1 is highly sinuous (sinuosity 2.2) with stable banks of meander belt silts and clay. The bankfull discharge is about 4 cubic meters per second on the basis of measurements. The channel slope is about 1 percent and the bed material is coarse sand moving in ripples and dunes. The average bed load transport rate was measured using the Helley-Smith sampler to be about 1.5 kg/sec. The confidence interval for this bed load is $\pm$ 50 %. The suspended load in the river is believed to be small because of the low velocity and coarse material.

DATA PREPARATION

Input data were prepared based upon the information contained in the Thorne et al. report. Such data include the cross-sectional geometry, spacing between cross sections, and radius of curvature at each cross section. The radii of curvature are measured at the channel centerline as required by the model. The measured sediment size distribution and water discharge were also used as the input in the simulation study. The water-surface elevation at the downstream section (section 9) was used as an input parameter while water-surface elevations of other sections were computed at each time step.

MECHANICS OF BEND FLOW

Sediment transport and bed topography in meander bends are related to the mechanics of flow. The characteristic flow pattern in meander bends pertaining to this study is described first and then employed to discuss the simulation results. In this discussion, the following three types of flow are considered: (1) the primary flow that is in the downstream direction, (2) the secondary flow that is normal to the primary flow and related to the flow curvature, also known as spiral flow or helical motion, and (3) the cross-stream flow resulting from the angular difference between the discharge centerline and channel centerline. The discharge centerline is defined as a line drawn on the plan view of a channel which has equal discharge of primary flow on both sides.

Much of the current bend theory has been called into question by Dietrich, et al. (1979) and by Thorne and Rais (1983) as they have found significant net cross-stream discharge in natural meanders. In the upstream vicinity of a bend apex, such as Sec. A-A in Fig. 2, the cross-stream discharge is typically 10% of the primary flow. This observation reveals a phenomenon which should be related to the development of secondary flow.

The process that characterizes the flow through meander bends is the streamwise variation of the secondary flow to which so many phenomena of river meanders are related. Bed topography are related to the streamwise growth and decay of secondary flow and its interaction with the cross-stream flow. The changing curvature of the flow path (discharge centerline) and its phase lag with the channel path (channel centerline) (see Fig. 2) have important effects on meander morphology. This changing flow curvature is in some way

related to the variation in secondary flow.

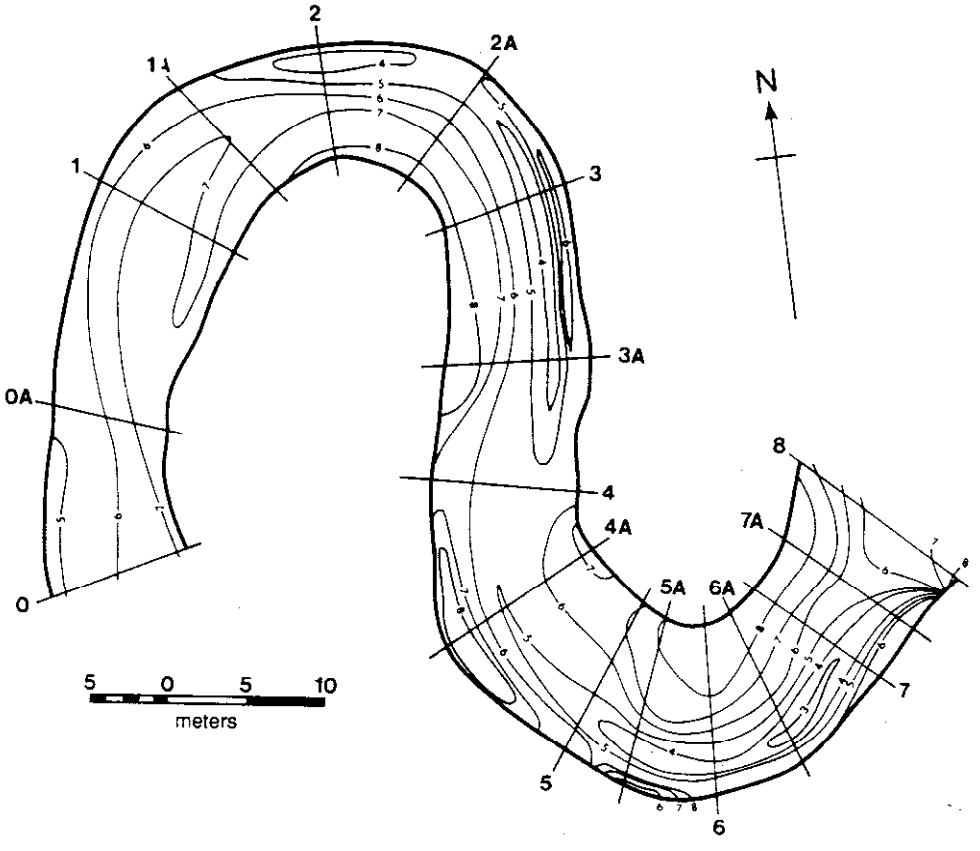

Fig. 1. Topography of Fall River with Cross-Section Lines

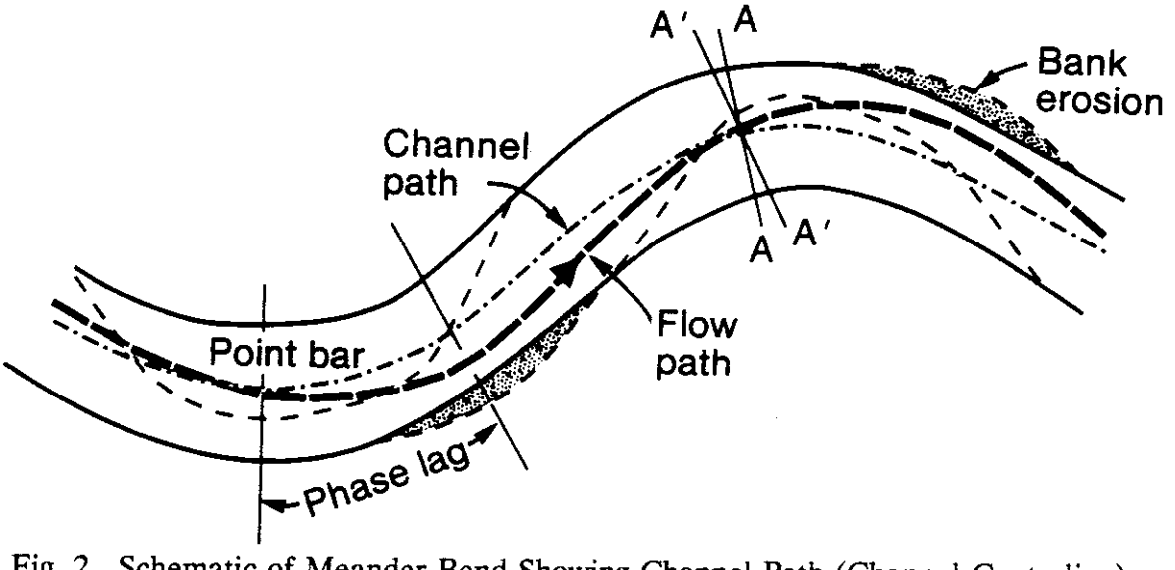

Fig. 2. Schematic of Meander Bend Showing Channel Path (Channel Centerline) and Flow Path (Discharge Centerline)

FOUNDATIONS OF MODELING FOR FALL RIVER

Physical and mathematical foundation of the FLUVIAL model are described by Chang (1985). Certain modeling features pertaining to this study are described herein, including the upstream boundary condition for sediment inflow, streamwise variation of secondary flow, and computation of transverse sediment transport.

Upstream Boundary Condition for Sediment Inflow - The rate of sediment inflow into the study reach is provided by the upstream boundary condition for sediment. It is assumed that the river channel remains unchanged above the study reach and sediment inflow rate is computed at the upstream section at each time step just like they are computed at other cross sections.

Streamwise Variation of Secondary Flow - The strength of secondary flow, or the flow curvature, varies in the streamwise direction. The variation is described by the momentum equation which in its simplified form (Chang, 1984) is

$$\underset{\mathrm{I}}{\frac{dv}{ds}} = \underset{\mathrm{II}}{\frac{u}{r_c}} - \underset{\mathrm{III}}{\frac{gS_r}{u}} - \underset{\mathrm{IV}}{\frac{\partial}{\partial z}\left(\varepsilon\frac{\partial v}{\partial z}\right)} \tag{1}$$

in which v = transverse velocity of secondary flow at water surface, s = curvilinear coordinate along the flow path, u = primary velocity at water surface, r_c = channel radius of curvature, S_r = transverse water-surface slope, z = vertical coordinate, and ε = eddy viscosity. The strength of secondary flow can be represented by the transverse surface velocity since transverse velocity profiles are similar. This equation shows that the streamwise variation of secondary flow or flow curvature (term I) is under the influence of the centrifugal acceleration from the channel curvature (term II), the transverse-water surface slope (term III), and the internal turbulent shear (term IV). The internal shear is the resistance that the flow has to overcome in changing it curvature. The secondary flow grows when the centrifugal force is greater than the resistance from the transverse water-surface slope and the internal shear; and it decays otherwise. Because of such resistance and inertia, the flow curvature does not adjust immediately to the channel curvature. This process may be considered as the delayed response of flow curvature to channel curvature (DeVriend and Struiksma, 1983) and it is responsible for the phase lag depicted schematically in Fig. 2. Phase lag is the distance the channel apex lags behind the flow apex.

Computation of Transverse Sediment Transport - Sediment transport, in the presence of transverse flow, has a component in the transverse direction. Sediment movement in the transverse direction contributes to the adjustment of transverse bed profile. In an unsteady flow, the transverse bed profile varies with time, and it is constantly adjusted toward equilibrium through scour and deposition. The transverse sediment rate is computed from the streamwise transport and the angle of deviation of bottom currents from the downstream

direction using the method developed by Kikkawa et al. (1976) and Ikeda (1982).

TEST AND CALIBRATION

The Fall River at the time of measurement is assumed to be in a state of dynamic equilibrium. Calibration of the FLUVIAL model based upon the Fall River data consisted of the following steps.

1. Determine the roughness coefficient using the measured discharge and water surface profile. Different n values were used and the value that provides the match in water-surface profile is 0.036. This value was selected for use in the simulation.

2. Select sediment transport equation based on the measured sediment rate. Sediment transport equations developed for the sand bed were tested in trial runs. The computed sediment rate was compared with the measured value of 1.5 kg/sec (with a 50 % confidence interval). The Engelund-Hansen equation was selected since its predicts a sediment rate of 1.2 kg/sec (0.3 ppm by weight). The sediment load is believed to be essentially bed load because of the coarse sediment size and low velocity.

SIMULATION RESULTS

Output from the FLUVIAL simulation are presented graphically in Fig. 3. The simulation is for a duration of 20 days which is considered long enough for the channel to adjust to an equilibrium configuration. The cross-sectional profile simulated at the end of 10 days and 20 days are plotted with the initial profile for each cross section, as shown in the figure.

The initial profile used in the simulation was measured in the field study at the bankfull discharge. Since the discharge was steady for a considerable length of time, the channel profiles may be assumed to be in a state of equilibrium. Therefore, the simulation should produce cross-sectional profiles comparable to the measured ones.

Comparisons of the measured (initial) and simulated (after 10 and 20 days) cross-sectional profiles are given in the Fig. 3. While there is general agreement, there are also variations between the measured and simulated profiles. The results are discussed in the following:

1. The transverse bed profiles is very pronounced for those sections within a meander bend. Such transverse slope is generally less pronounced or missing in a straight reach.

2. The transverse bed profile changes along the channel. It grows with the secondary currents as the flow enters a bend, it reaches a maximum near the bend exit, and it decays after leaving the bend exit.

3. The difference between the simulated and measured profiles may be significant near the convex bank, see, e.g., section 1. This discrepancy is explained below. The FLUVIAL

model considers the primary flow and the secondary currents. Each cross section used in the FLUVIAL simulation needs to be perpendicular to the primary flow. Because of the angular difference between the channel centerline and discharge centerline described in the foregoing, a cross section perpendicular to the channel centerline is not necessarily perpendicular to the primary flow direction. Also, a cross section perpendicular to the primary flow direction in a bend is usually somewhat curved instead of being straight. The cross sectional profile simulated using the FLUVIAL model is supposed to be for such a cross section. Since the cross sections used are defined by straight lines not totally perpendicular to the primary flow direction, this in part accounts for the discrepancy.

4. Other causes for the variation may be attributed to the heterogeneity in bed material, bank vegetation, and so on. The bed form may have also contributed to the difference between the measured and simulated bed profiles.

SUMMARY AND CONCLUSIONS

1. The bed topography of the Fall river is a reflection of the flow pattern, characterized by the transverse bed slope in bends. Such bed pattern changes with the flow pattern which undergoes continuous growth nd decay. The transverse bed slope and bed scour reach the maximum near the exit of a bend.

2. The scour depth is distinctly associated with channel curvature, and it is an important consideration in the design of bank protection which must extend below the potential scour.

3. There is general agreement between the simulation and measurement. Certain variations do exist. A major reason for the discrepancy is due the one-dimensionality of the FLUVIAL model. Because of the cross-stream discharge, the cross section used in the study are not exactly perpendicular to the flow direction. In order to be exactly perpendicular to the flow direction, each cross section in the bend may not be represented by a straight line, but by a slightly curved line drawn perpendicular to the primary flow.

REFERENCES

Chang, H. H., (1984). "Variation of Flow Resistance through Curved Channels," *Journal of Hydraulic Engineering*, ASCE, 110(12), 1772-1787.

Chang, H. H., (1985). "Water and Sediment Routing through Curved Channels," *Journal of Hydraulic Engineering*, ASCE, 111(4), 644-658.

Dietrich, W. E., Smith, J. D., and Dunne, T. (1979). "Flow and sediment transport in a sand bedded meander," *Journal of Geology*, 87(3), 305-315.

DeVriend, H. J., and Struiksma, N. (1983). "Flow and bed deformation in river bends," in *River Meandering*, Proc. of the Conference Rivers '83, New Orleans, Louisiana, Oct. 24-26, 810-828.

Ikeda, S., (1982). "Lateral Bed Load Transport on Side Slopes," *Journal of Hydraulic Engineering*, ASCE, 108(HY11), 1369-1373.

Kikkawa, H., Ikeda, S., and Kitagawa, A. (1976). "Flow and bed topography in curved open channels," *Journal of the Hydraulics Division*, ASCE, 102(HY9), 1327-42.

Thorne, C. R., and Rais, S. (1983). "Secondary current measurements in a meandering river," in *River Meandering*, Proc. of Conference Rivers '83, New Orleans, Louisiana, Oct. 24-26, 675-686.

Thorne, C. R., Zevenbergen, Bradley, J. B., and Pitlick, J. C., (1985). "Measurement of Bend Flow Hydraulics of the Fall river at Bankfull Stage," WRD Project Report No. 85-3, National Park Service, Colorado State University.

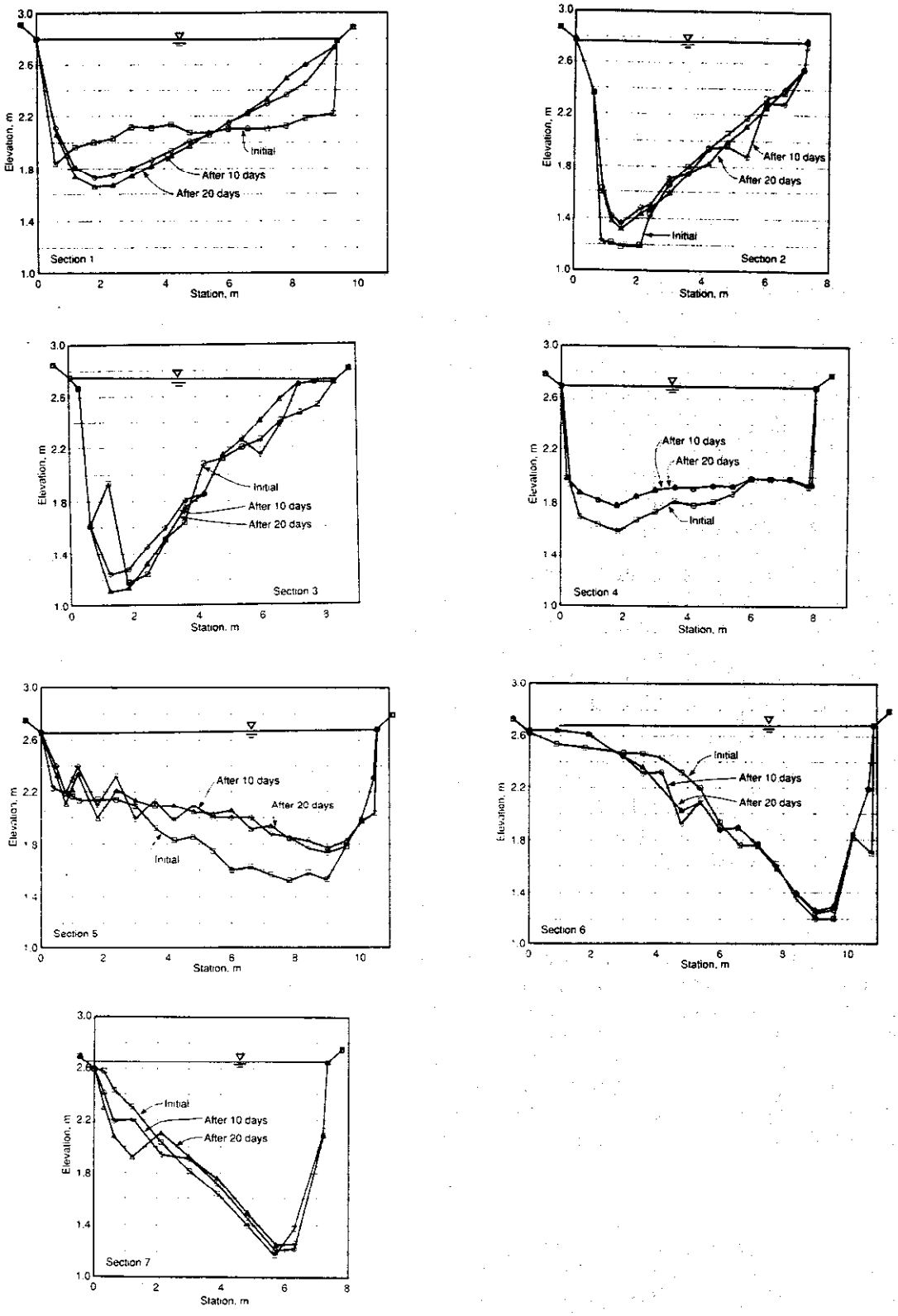

Fig. 3. Simulated Bed Profiles during Constant Discharge

PHYSICAL MODELING OF SEDIMENT TRANSPORT IN CHINA

By Dou Guoren,Prof.and Director of Nanjing Hydraulic Research Institute, Nanjing, China.

ABSTRACT

Important progress has been made in the physical modeling of sediment transport both theoretically and experimentally in China,and sedimentation problems in China's key engineering projects must be solved by conducting physical model studies, although the mathematical modeling is also widely used. In this paper, the historical development of physical modeling of sediment transport in China is reviewed first, and then the similarity theory of total sediment transport including hyperconcentration flow developed by the author is presented, and some applications of this theory including the models for Gezhouba Water Control Project, Three-Gorge Water Control Project, Xiaolangdi Water Control Project and Jinzhou Harbour Engineering Project are described.

INTRODUCTION

There are a lot of sediments transported in China's rivers, estuaries and coastal zones. The sedimentation problems become the key problem in building important water control and harbour engineering projects. Before 1960's, some big projects failed owing to the serious sedimentation. Since then, important progress has been made in the physical modeling both theoretically, and experimentally, and the sedimentation problems of important projects to be constructed in China must be solved by conducting physical model studies although the mathematical modeling is also widely used.

The sediment particle sizes in many rivers are distributed very widely, so there are both bed load and suspended load, and in some cases density current and hyperconcentration flow may occur. For such complicated conditions, it is necessary to reproduce simultaneously all particles (including so called bed-material-load and wash-load) and all forms of sediment transport in one model. The similarity theory of designing such models developed by the author and some applications of this theory will be summarized briefly in this paper.

HISTORICAL REVIEW

It is well known that China's rivers, estuaries and coastal zones are rich in sediment transport, and the success of hydraulic engineering projects depends to a great extent on the solution of sedimentation problems. Therefore, a lot of model investigations have been conducted in China. In addition to movable bed models, suspended sediment transport models were made in 1950s. Because of the complexity of conducting model studies with suspended load, the expected results could not be obtained at that time. The verification tests showed that the location of scouring and deposition caused by the suspended load in the

models could not be similar to those in the prototype. This decreased the faith in conducting physical model studies with suspended load. Since then, the model studies of this kind had not been carried out in China for near ten years. The analysis made by the authour indicated that the failure of model studies with suspended load was due to the lack of proper similarity theory, and that the theoretical basis on which those models were designed needed to be improved. By the end of 1960s, the suspended sediment transport model study was made again by the author to study the serious sedimentation in Qingshan Canal caused by suspended load and density current, and good results were obtained. Based on this model investigation, the similarity laws for suspended load were developed, and according to these laws another model was made in 1971 to solve the sedimentation problems caused by suspended load in the dam site of Gezhouba Water Control Project. The suspended load and density current were reproduced very well. However, in this model, the transport of bed load could not be considered yet. As mentioned above,in many rivers, such as the Yangtze River, there are both suspended load and bed load. So, in order to study the bed load transport, another model was made to predict the location and quantity of deposition caused by the bed load. However, it was difficult to analyze the results obtained from the two models. It was obvious that the sedimentation problems in the dam site of Gezhouba Project could not be solved properly by using the two models. It was necessary to reproduce simultaneously all forms of sediment transport in one model. The main difficulty to design models with total sediment transport is that the time scale for the model only with suspended load transport is strongly different from that for the model only with bed load transport. The analysis indicated that the difference in time scales of bed deformation was caused by that for the model with suspended load, the similarity criterion of initial movement velocity was not considered, meanwhile, for the model with bed load, the similarity criterion of settling velocity was not considered. If both similarity criteria were satisfied, the difference in time scales of bed deformation could disappear. In 1973, a similarity theory of total sediment transport modeling was developed by the author, according to which all particles and all forms of sediment transport can be reproduced simultaneously in one model. Such a model with total sediment transport was made in the same year for the Gezhouba Water Control Project. The success in conducting this model study not only led to the successful solution of sedimentation problems in the Gezhouba Project, but also encouraged engineers to use the physical models to solve sedimentation problems in various condition. Since then, a large number of models of this kind have been made in China to solve various sediment problems in rivers, estuaries and coastal zones. One of them is the model for the Three-Gorge Water Control Project. A 800-meter long model with total sediment transport was made in 1986 to study the sedimentation problems in the fluctuating backwater region of this Project, and some important results have been obtained by this model. By the end of 1980s, the physical modeling of hyperconcentration flow had been studied in connection with the construction of the Xiaolangdi Water Control Project on the Yellow River. The similarity laws of hyperconcentration flow were obtained by

the author in 1989, and according to these laws, a new physical model has been made in 1990 to further study the sedimentation problems near the dam site of the Xiaolangdi Project. Among the sediment transport models for estuaries and coastal zones, the model studies on the sedimentation problems of Dandong habour and Jinzhou habour can be mentioned. The sediment transport caused by the tidal currents was reproduced very well, and the predictions made by these models have been proved by the measurements in nature. The further study in this field is to study the similarity laws according to which the sediment transport under the combined actions of tidal currents and waves can be reproduced in the model.

SIMILARITY THEORY OF SEDIMENT TRANSPORT MODEL

The main points of the similarity theory developed by the author in 1970s and widely used in China for designing total sediment transport model are as follows. The flow in the model and in the prototype will be similar if the similarity of Froude number and resistance can be satisfied simultaneously,i.e.

$$\lambda v = \lambda_H^{\frac{1}{2}}, \quad \lambda co = \left(\frac{\lambda_L}{\lambda_H}\right)^{\frac{1}{2}}, \quad \lambda t = \frac{\lambda_L}{\lambda v}, \tag{1}$$

where λv, λ_H, λco, λ_L are scales of velocity, depth, dimensionless Chezy's coefficient and length, respectively.

The similarity scales of suspended load are determined by the two-dimentional nonequilibrium sediment transport equations developed by the author(1963), and they are

$$\lambda w = \lambda v \frac{\lambda_H}{\lambda_L}, \quad \lambda s = \lambda s_*, \quad \lambda_{t1} = \frac{\lambda \gamma_o \lambda_L}{\lambda v \lambda s} \tag{2}$$

where λw, λs, λs_* are the scales of particle settling velocity, sediment concentration and sediment carrying capacity, respectively. $\lambda \gamma_o$ is the scale of dry specific weight, λ_{t1} is the time scale of scouring and deposition caused by suspended load. The sediment carrying capacity can be determined by the author's formula(1989). In addition to (2), the initial suspension similarity should also be satisfied for suspended load

$$\lambda v_f = \lambda v \tag{2'}$$

where v_f is the velocity of initial suspension, which can be determined by the author's formula(1977). In order to meet the similarity requirement of density flow, the scale of sediment concentration should be determined by

$$\lambda s = \frac{\lambda \gamma_s}{\lambda (\gamma_s - \gamma)} \tag{2''}$$

where γ_s and γ are the specific weights of sediment particles and water, respectively.

The similarity scales of bed load are determined by the bed load discharge formula and the equation of bed deformation obtained by the author (1977,1989), and they are

$$\lambda q_s = \frac{\lambda \gamma_s \lambda^4 v}{\lambda(\gamma_s - \gamma)\lambda_{c_o}^2 \lambda w}, \quad \lambda v = \lambda v_k, \quad \lambda_{t2} = \frac{\lambda \gamma_o \lambda_H \lambda_L}{\lambda q_s} \quad (3)$$

where λq_s and λv_k are the scales of bed load discharge and initial movement velocity,respectively; λ_{t2} is the time scale of scouring and deposition caused by bed load. It is not difficult to find out that if all of the scale relations mentioned above are adopted, the time scales for suspended load and bed load will be approximate or equal, and therefore it is possible to reproduce simultaneously both suspended load and bed load in one model. it is worth pointing out that the success of conducting such model investigations depends also on the ability to maintain the required grain-size distribution of suspended load in the model flow.

For hyperconcentration flow, the following similarity requirements should be added

$$\lambda s = \lambda s_{max}, \quad \lambda \tau_B = \lambda \tau_o \quad (4)$$

where λs_{max} is the scale of the possible maximum concentration of sediments, $\lambda \tau_B$ and $\lambda \tau_o$ are the scales of the Bingham shear stress and the bed shear stress,respectively. The formulas obtained by the author for determining s_{max} and τ_B are

$$s_{max} = \frac{2\gamma_s}{3\sum p_i \left(1+2\frac{\delta}{d_i}\right)^3} \quad (4')$$

$$\tau_B = \delta_o \frac{\gamma'}{\gamma\gamma_s}\left(\sum p_i \left(\frac{\delta}{d_i}\right)^3\right)^{\frac{1}{3}} \frac{s}{(1-s/s_{max})^2} \quad (4'')$$

where p_i is the percentage of particles with diameter d_i ; δ is the thickness of water film (=0.21 $\cdot 10^{-4}$cm); δ_o is a coefficient determined by experiments (for sediments in the Lower Yellow River $\delta_o = 156 \cdot 10^3$ kg/ cm^2 , for bakelite powder $\delta_o = 47 \cdot 10^3$ kg/ cm^2); γ' and γ are the specific weights of turbid and pure water. It is not difficult to prove that the Reynolds number of Bingham fluid flow with higher value in the model will be equal to that in the prototype, if the similarity relations (1) and (4) are satisfied.

Whether a model can or not meet the above similarity requirements depends on the model sediments selected, which should have a wide range of particle sizes and good hydraulic properties and whose physical and chemical properties are to be comparatively stable. Various materials, such as natural silt, talcum powder, coal powder, coal-ashes, wood flour, granular polydichlorstyrene and bakelite, were used as the model sediment, and it is found that the best of them is the granular bakelite.

APPLICATIONS OF THE SIMILARITY THEORY

Since the beginning of 1970s, more than 40 physical models with sediment transport have been made in China. The majority of them were designed according to the similarity theory developed by the author. Here, only some typical model studies will be mentioned briefly (see Tab.1).

Tab.1

scales / Models	λ_L	λ_H	λ_V	λ_W	λ_{V_k}	λ_t	λ_S	λ_{t_1} λ_{t_2}
Gezhouba, dam site	200	100	10	5	10	20	0.46	96
Three-Gorge, backwater region	250	100	10	4	10	25	0.51	120
Xiaolangdi, Dam site	80	80	8.94	4.20	8.94	8.94	1.09	36
Jinzhou Port	800	100	10	1.25	10	80	0.5	224

Gezhouba Model

The Gezhouba water Control Project is located on the Yangtze River near Yichang city. The morphology of the river reach in the vicinity of the dam site of this project is very complicated. The average yearly quantities of suspended load and bed load are 520 million tons and 8 million tons respectively, including nearly one million tons of gravels, the diameter of which is more than 10mm. Therefore, the sedimentation problem was a key problem for the Gezhouba Project. The model studies on this problem were conducted in 1970s, and in the model both suspended load and bed load including density current and gravel transport were very well reproduced. By using this model, hundreds of tests were conducted, and a series of engineering measures against sedimentation were proposed. All of the proposals were adopted in the construction. The Gezhouba Project has been completed and put into operation, and the

engineering measures have been proved very effective, and the normal operation of power generation and navigation has been ensured. The sedimentation conditions such as the locations and quantities of deposition and the effectiveness of washing sluices and tunnels observed in the field after the operation of this project are in very good agreement with the model predictions.

Three-Gorge Model

The Three-Gorge Project is to be located on the Yangtze river at Sandouping, 44km upstream of Yichang. The pool level will vary from 145m to 175m in a year, so the fluctuating backwater region is very long, about 180km. The channel process of this river reach in the natural conditions is characterized by deposition in flood seasons and scouring in dry seasons, basically reaching an equilibrium of deposition and scouring in a year. After completing the project, the deposition in the flood seasons will continue to take place, however, the scouring in the dry season can not be realized owing to the fact that the reservoir will be impounded at the beginning of dry seasons. Therefore, the sedimentation problems in the fluctuating backwater region have to be studied seriously. For this purpose, a 800-meter long model with total sediment transport has been made to further study the sedimentation problems and engineering measures to ensure the navigation conditions in the whole fluctuating backwater region. The verification tests have been conducted, and the scouring and deposition processes of the studied river reach in a year have been reproduced in the model. Good agreements have been found between the locations and quantities of deposition and scouring observed in the whole river reach and predicted by the model. The comparison shows that the errors of the scouring and deposition quantities for all locations are less than 30%. The sedimentation conditions after 80-year reservoir operation have been predicted by the model, and the engineering measures are being studied to improve the navigation channel and the piers of shipping terminals in the whole fluctuating backwater region.

Xiaolangdi Model

Xiaolangdi Water Control Project is to be located on the Yellow River downstream of the Sanmenxia Project. The sediment concentration is very high, ranging from 10kg/ m^3 to 500kg/m^3 . When the concentration is more than 100kg/m^3 , the fluid may be considered as Bingham fluid, and the Bingham shear stress and other issues should be taken into account. Therefore, in designing the Xiaolangdi model the hyperconcentration flow similarity laws mentioned above have been adopted. The verification tests have been conducted, and good agreements have been found between the sedimentation conditions observed in the field and the model predictions. By using this model the layout of the project and the engineering measures against siltation at the dam site will be studied.

Jinzhou Harbour Model

Jingzhou Harbour is located on the northeast part of Jinzhou Bay. In order to study the siltation caused by tidal currents in the navigation channel and harbour basin to be dredged, a sediment transport model was made, in which the tidal currents and sediment movement were reproduced. The verification tests were conducted, and the tidal currents and concentration distribution in the bay were well reproduced in the model, and some engineering measures based on the model studies have been proposed to ensure the normal navigation. The Jinzhou Harbour Project has been completed, and the quantity of deposition in the navigation channel and harbour basin observed in the field are in good agreement with those predicted by the model.

CONCLUSION

Great progress has been made in the physical modeling of sediment transport both theoretically and experimentally in China. The locations and quantities of scouring and deposition in rivers, estuaries and coastal zones can be well predicted by the physical model studies. The sedimentation problems in China's key engineering projects have been solved successfully by conducting physical model studies. The development of physical modeling also provides the basis for developing mathematical models of sediment transport in China.

REFERENCES

Dou, Guoren, 1962, On the theory of initial sediment motion, Scientia Sinica, Vol.11, No. 7,(in Russian).

Dou, Guoren, 1963, Suspended sediment movement and calculation of bed deformation for tidal estuaries, Jour. of Hydraulic Engineering, No. 4, (in Chinese).

Dou, Guoren, 1977, A similarity theory of total sediment transport modeling with reference to a particular project, Report of Nanjing Hydraulic Research Institute, No. 2, (in Chinese).

Dou, Guoren, 1985,Model investigation on the flow condition and sediment problems of the Gezhouba Project, Proc. of the XXVI International Navigation Congress, Brussels.

Dou, Guoren, Wan,Shenggan, and Lu, changshi, 1987, Studies on the sedimentation problem in varying backwater zone of the Three-Gorge Project by sediment-laden flow model, Proc. of the 4th International Symposium on River Sedimentation, Beijing.

Dou, Guoren, 1989, Sediment transport in rivers and its physical and mathematical modeling, Proc.of the International Symposium on Sediment Transport Modeling, New Orleans.

Dou, Guoren, 1989, Sediment-hyperconcentration flow and its similarity laws, Proc. of the International Symposium on Sediment Transport Modeling, New Orleans.

Dong,Fengwu, Xu,Minfu and et al, 1989, Sedimentation model study of Jinzhou Harbour, Report of Nanjing Hydraulic Research Institute.

DESIGN OF SEDIMENT MODELS

by Clifford A. Pugh, Head, Hydraulic Equipment Section, and
Russell A. Dodge, Research Hydraulic Engineer
U. S. Bureau of Reclamation, Denver, Colorado

ABSTRACT

Recent physical model studies at the Bureau of Reclamation's hydraulic laboratory requiring scaling of sediment transport rates were designed with a method based on the Shields function as modified by Taylor. Taylor developed a dimensionless sediment discharge parameter, which provides nesting curves that parallel Shields' incipient motion curve at constant values of dimensionless sediment discharge. Using this method clearly demonstrates when lightweight materials are required or when the sand particle sizes can be adjusted in the model to represent the sediment transport rates. A method to adjust the sand particle sizes based on settling velocity was developed. This method appears to make the correct adjustment to fit the transport curves on the Shields diagram. The method was used for modeling the lateral scour of fuse plugs and compared well with prototype experience. The method also illustrates the limitations and applicability of sediment models. The sediment transport rates may be properly scaled in one area of a model and improperly scaled in a different area where the Reynolds number is different.

INTRODUCTION

Background

Reclamation experience with sediment models started in the early 1950's. Several predesign models were conducted for the Missouri River Basin and Middle Rio Grande diversions. The sediment used for all these studies was a fine uniform sand with a mean diameter of 0.2 mm. Settling velocity is very important in determining when a particle will remain at rest or how far it will travel once lifted into the flow. The 50-percent model sizes were scaled by settling velocity according to the Froude law, that is by the square root of the length ratio.

These models were force fed sediment to develop bed slopes sufficient to move sediment at rates estimated by sediment bedload equations. Bed slopes that were developed this way were generally exaggerated because of friction differences between model and prototype. However at diversions, flow splits occur within a short reach in the direction of flow, and the structure does not need to be distorted.

Sediment concentration was measured in all the component flows of the models. Concentration ratios of the measured delivery rate to the river concentration were used to compare the relative amount of sediment in the delivery for different trial diversion arrangements.

Carlson [1970] summarized these early studies and concluded that physical modeling of proposed diversion schemes in close liaison with design engineers results in much better sediment control than when studies are not conducted.

Some of the more recent Reclamation experience has been with steep and fast flowing mountain streams where sediment is coarser. Segregation and armoring can be important in regard to river and diversion performance. Therefore, as much of the range of sediment diameters as possible was represented by settling velocity scaling. During these later studies and during a fuse plug model study, Reclamation model design methods were reviewed and a more rational model design method was developed. The fuse plug model study results (Pugh [1985]) compared favorably with the Oxbow field data [1959].

MODELING CONSIDERATIONS

Similitude

Hydraulic models are used because of the large number of variables involved and because of complicated boundary conditions. A physical model is designed in a manner such that the flow characteristics of the model simulate in a known manner the physical behavior of the prototype.

A model and prototype must be similar geometrically, kinematically and dynamically. Geometric similarity exists when the ratios of all homologous dimensions between model and prototype are the same. The geometric scale ratio, or length ratio, is denoted by L_r which is the ratio L_m/L_p, where the subscripts m and p refer to the model and prototype, respectively. Kinematic similarity, or similarity of motion, implies that the ratios of velocities and accelerations between model and prototype are equal. Dynamic similarity requires that the ratios of homologous forces between the model and prototype be the same. Possible hydraulic forces are caused by gravity, viscosity, pressure, surface tension and elasticity.

For hydraulic modeling, the more important dimensionless parameters are dimensionless ratios formed with respect to inertia:

Froude number (inertia/gravity) $F_r = V/(Lg)^{1/2}$

Reynolds number (inertia/viscosity) $R_e = VL/\nu$

Euler number (inertia/pressure) $E_u = \rho V^2/\Delta p$

Where ν = kinematic viscosity
ρ = density
g = acceleration due to gravity
V = the average velocity
L = a characteristic length
Δp = differential pressure.

The scale relationships for open channel flow based on Froude number are as follows:

$$\text{Length} = L_r$$

$$\text{Area} = L_r^2$$

$$\text{Volume} = L_r^3$$

$$\text{Time} = L_r^{1/2}$$

$$\text{Force} = L_r^3$$

$$\text{Shear} = L_r$$

$$\text{Velocity} = L_r^{1/2}$$

$$\text{Discharge} = L_r^{5/2}$$

Similitude Deficiency of Froude Scaling

Models involving erosion of noncohesive bed material must simulate tractive shear (τ), because the tractive shear causes the drag force which overcomes the forces holding the particle in place.

The tractive shear on a particle fluctuates because of the turbulence. The drag force and the turbulence are a function of Reynolds number. Therefore, a model based on Froude law does not necessarily simulate the tractive forces and the erosion accurately. In some models, the sediment sizes must be adjusted to compensate for Reynolds number defect. Reynolds number defect (R_{ed}) of a Froude number model can be determined by the Froude scaled variables being substituted in the Reynolds number resulting in:

$$R_{ed} = L_r^{3/2} \tag{1}$$

If erosion occurs by chunking action such as cutbank scour or in a controlled manner, such as in an impervious core in a fuse plug, a model needs to include effects of elastic forces as well as gravity. Taking the ratio of gravity and elastic forces results in the structural integrity number M expressed as:

$$M = \gamma L/E \tag{2}$$

where E is the modulus of elasticity of the chunking material or the core in a fuse plug. M must be made the same in the model and prototype.

Dimensionless Unit Sediment Discharge

Vanoni [1975] used Taylor's data [1971] to show that dimensionless unit sediment discharge at low transport rates falls close to Shields curve for threshold of movement (fig. 1). To properly simulate sediment discharge, the dimensionless unit sediment discharge rate (q_s*) must be the same in the model and prototype.

For a model with a grain Reynolds number (R*) between 5 and 100, the dimensionless sediment unit discharge will be too high if the sand grain

diameters are scaled geometrically. Therefore, model sediment sizes or specific gravity should be adjusted in this range to properly simulate sediment transport.

By dimensional analysis, it has been shown that noncohesive material has a functional relationship which can be expressed as a dimensionless shear stress,

$$\tau^* = \tau/(\gamma_s - \gamma_w)d_s = \Phi(U^*d_s/\nu,\ d_s/R,\ \gamma_s/\gamma_w) \tag{3}$$

where the grain Reynolds number is,

$$R^* = U^*d_s/\nu \tag{4}$$

The shear velocity can be expressed as:

$$U^* = (\tau/\rho)^{1/2} \tag{5}$$

Where d_s = sand grain diameter
ν = kinematic viscosity of water
τ = tractive shear
ρ = density of water
R = hydraulics radius
γ_s = specific weight of sand
γ_w = specific weight of water

This function, except for the roughness ratio [the ratio of the sand grain diameter to the hydraulic radius (d_s/R)] and the relative specific weight [the ratio of the specific weight of sand to the specific weight of water (γ_s/γ_w)], is the same as the Shields function [1936]. The relative weight term is usually dropped on the basis of the same materials, water and natural sand, being used in the model as in the prototype. The relative diameter is dropped on the basis of relatively deep flow or fine grain sediment bed material. Thus, the equation reduces to Shields function. In addition, Shields' data for a large spread in particle specific weight fall within the data scatter for sand alone.

Shields developed a dimensionless diagram relating dimensionless shear to a boundary or grain Reynolds number. Shields used this diagram to define threshold of movement. This concept has been expanded by others to include transport parameters, such as number of particles moving, probability of particles moving, and dimensionless sediment discharge.

Investigators since Shields have verified that Shields' entrainment curve is a special transport case, representing nearly zero transport. Gessler [1968] shows that the probability of particles moving, used as a nesting parameter, produces curves that parallel the Shields curve. Graf and Pazis [1977], using the number of particles moving per square foot of bed as a third parameter, produced curves that also parallel Shields' curve. Taylor [1971] developed (by dimensional analysis) a dimensionless unit sediment discharge parameter:

$$q_s^* = q_s/U^*d_s \tag{6}$$

where q_s is the sediment discharge in volume per transverse flow width and U^* is the shear velocity.

Taylor's analysis, discussed by Vanoni [1975], indicates that using q_s^* as a third parameter with Shields' parameters produces curves of equal q_s^* that nearly parallel Shields' incipient motion curve. Thus,

$$q_s^* = \Phi(U^* d_s/\nu,\ \tau/(\gamma_s - \gamma_w)d_s) \tag{7}$$

These functions can be used by physical modelers to predict transport scaling, transport volume and time model defect, possible correction factors and possible model adjustments. To use Taylor's function, the data point with coordinates $[(R^*)_p, (\tau^*)_p]$ corresponding to the unit dimensionless discharge, q_s^*, is located on a plot of Shields-Taylor function. A curve is drawn through this point parallel to the Shields-Taylor curves. Then a trial model particle size and specific gravity combination is found that causes $(q_s^*)_m$ to lie on the $(q_s^*)_p$ curve. An increase in trial diameter size causes a shift of the point downward and to the right toward the target $(q_s^*)_p$ curve. A change in trial specific gravity causes the trial point to move vertically toward the target $(q_s^*)_p$ curve. If the geometrically scaled model grain diameter is adjusted in size according to the settling velocity as explained below, the correct adjustment is made to cause the value of $(q_s^*)_m$ to approximate the target value of $(q_s^*)_p$. Examples of sediment scaling for the fuse plug model study are shown in figure 1. In this study, 12.5-ft- and 25-ft-high prototype fuse plug embankments were simulated at scales of 1:25 (tests 1-6) and 1:10 (tests 7 and 8). The prototype and model data points and model adjustments are shown in the figure.

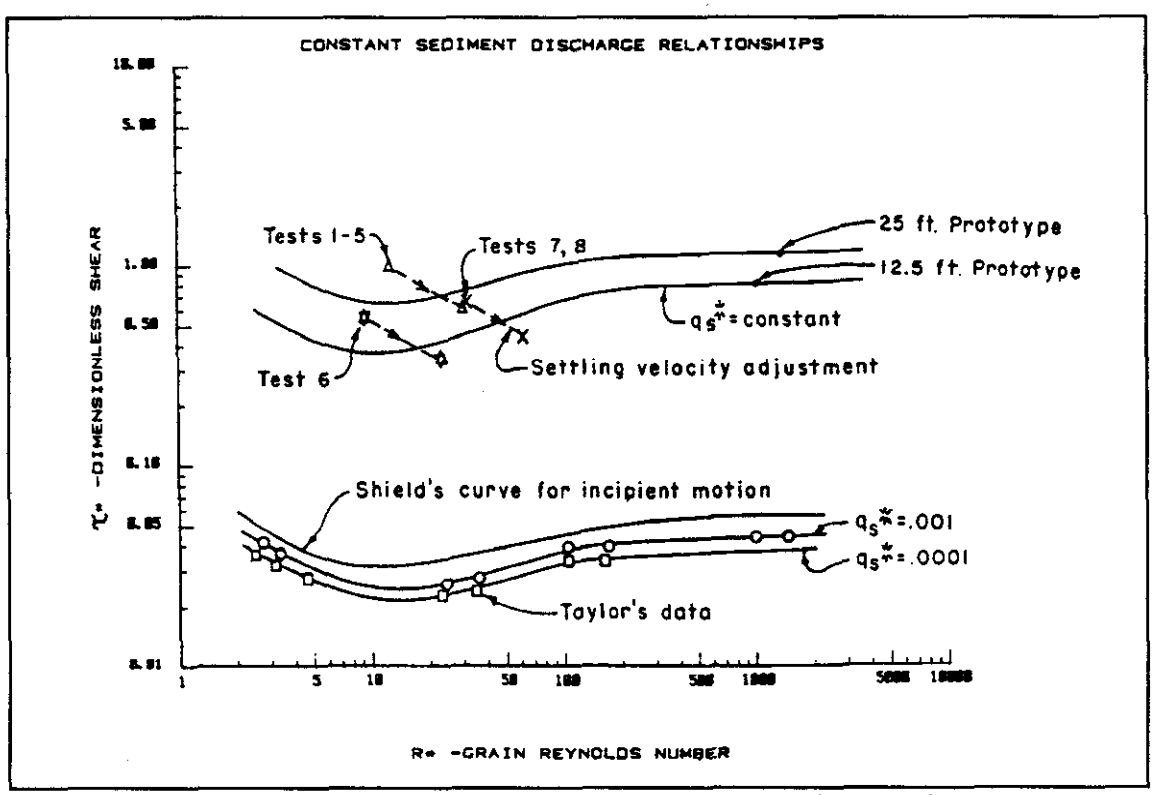

Figure 1. - Constant sediment discharge relationships.

Friction Scaling

It is sometimes convenient to use other equivalent relations for U* that are easier to work with in terms of field and the model data. These forms are

$$U^* = (gRS)^{1/2} = (\tau/\rho)^{1/2} = V(f/8)^{1/2} \quad (8)$$

To determine the Darcy-Weisbach friction factor f in an open channel, the Reynolds number R_e is computed as $4RV/\nu$ where R is the hydraulic radius and V is the average velocity at the area in question. To determine f, relative roughness is defined as $K_s/4R$ where K_s is the rugosity. Kamphius [1974] shows that K_s is equal to $2d_{90}$ where d_{90} is the particle size at which 90 percent of the grains are smaller in diameter.

The following relationship in terms of f can be used to determine τ^*:

$$\tau^* = (V^2 f/8gd)(\gamma_w/\gamma_s - \gamma_w) \quad (9)$$

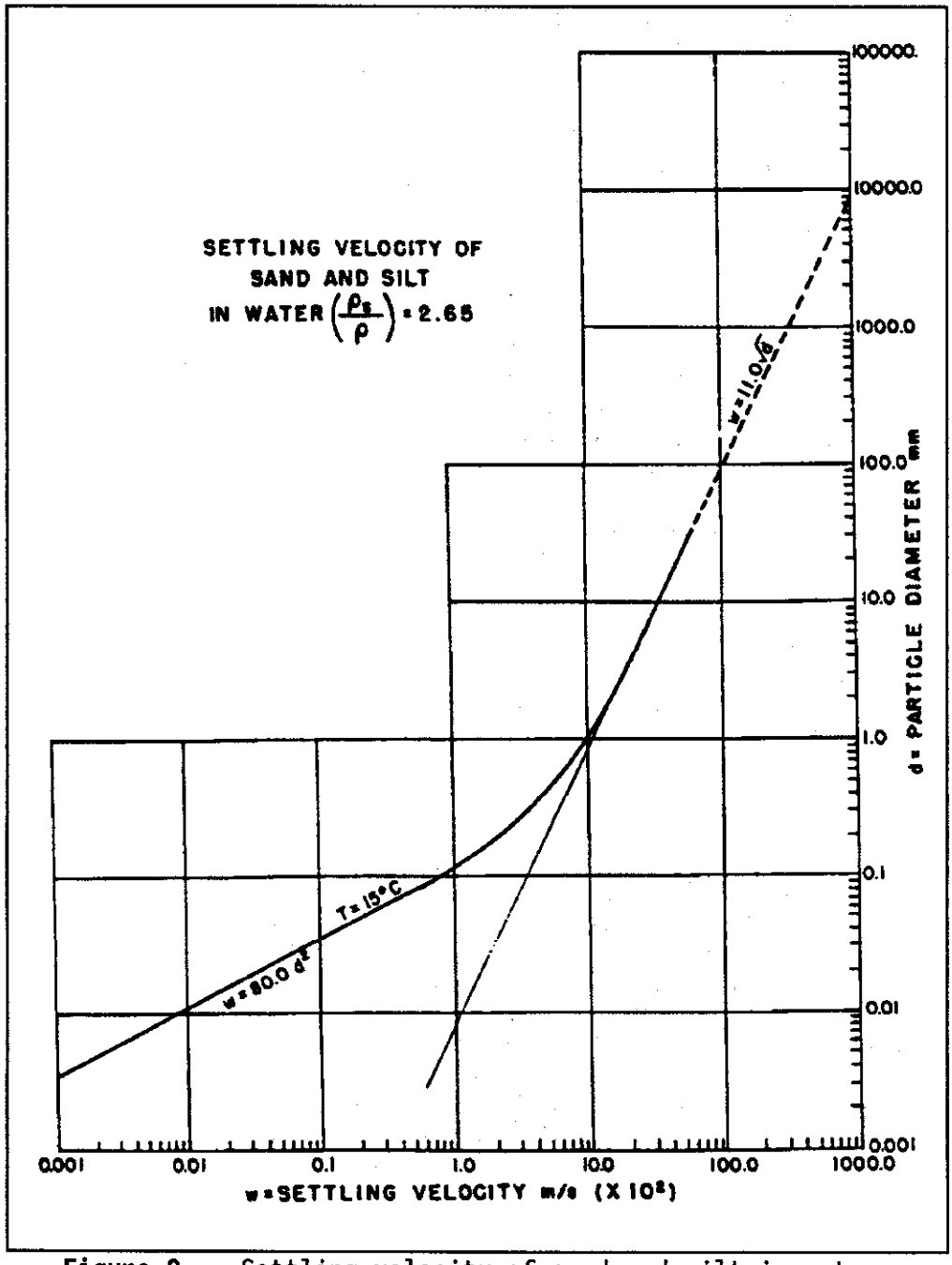

Figure 2. - Settling velocity of sand and silt in water.

Settling Velocity

Settling velocity is an important parameter that determines when a particle will remain at rest or how far it will travel once lifted into the flow. A diagram of settling velocity (w) of sand and silt particles is given in figure 2. For particles larger than 1 mm, settling velocity is a function of the particle diameter (d) raised to the 1/2 power. Also, for particles larger than 1 mm, the grain Reynolds number is generally larger than 100, and no adjustment in grain diameter is necessary to achieve the prototype value of q_s*. This is consistent with Froude scaling for velocity as discussed earlier. However, there is a defect in Froude velocity scaling for particles less than 1 mm because of fluid shear and Reynolds number defect.

By an increase of the size of a model sediment grain, the settling velocity can be corrected to the proper value for Froude scaling. For example, 1:10 scaling of a 2-mm prototype sand particle would be 0.2 mm. However, from figure 2, the settling velocity would then be 0.02 m/s when it should be 0.049 m/s according to Froude scaling. If the particle size is increased from 0.2 to 0.4 mm, the settling velocity is corrected to 0.049 m/s, the proper value for Froude scaling. This adjustment moves the location of the point plotted on the Shields-Taylor curves (fig. 1) close to the target value of the prototype unit dimensionless sediment discharge rate.

Prototype Comparison

A field test was performed in 1959 (Albrook [1959]) on a 1:2 scale model of the 8.2-m-high fuse plug used for the Oxbow Project on the Snake River in Idaho. The gradation curve for the 4.1-m-high test embankment was very close to the prototype gradation simulated in the fuse plug model study conducted at the Bureau of Reclamation's hydraulic laboratory in 1985.

The geometrically scaled sand grain diameters in the model were adjusted in size with the settling velocity adjustment correcting for the Reynolds number defect (Pugh [1985]).

The lateral erosion rate predicted by Reclamation's 1:10 scale model for the Oxbow field test was 1.66 m/min as compared to 1.71 m/min measured during the Oxbow test. The difference of 2.5 percent is well within experimental accuracies and seems to confirm the scaling technique.

CONCLUSIONS

The model design method described in this paper to simulate sediment transport in physical models compensates for the fact that the Reynolds number is generally too low to properly simulate sediment transport in a Froude scale model. The method uses an adaptation of the Taylor dimensionless unit sediment discharge curves to determine the appropriate sediment diameters or adjustment in model sediment specific gravity. Adjusting the model sediment size according to settling velocity to correct to the proper value for Froude scaling confirms the adjustment shown by the Taylor-Shields curves. Comparisons of sediment erosion rates predicted by a fuse plug model using this technique and erosion rates measured during a field test on the Oxbow Project support the validity of the technique.

REFERENCES

Carlson, E. J., "Laboratory and Field Investigations of Sediment Control Structures at Diversion Dams," International Commission on Irrigation and Drainage, Ninth Congress, 1970.

Gessler, J., "The Beginning of Bedload Movement of Mixtures Investigated as Natural Armoring in Channels," Translation T-5, Keck Laboratories, CIT, 1968.

Graf, W. H., and G. C. Pazis, " Les Phenomenes de Deposition et D'erosion Dams un Canal Alluvionnaire," Journal of Hydraulic Research, vol. 15/2, 1977.

Kamphius, J. W., " Determination of Sand Roughness for Fixed Beds," Journal of Hydraulic Research 12 (1974) No. 2.

"Oxbow Hydroelectric Development, Idaho Spillway with Fuse Plug Control, Model Studies of Fuse Plug Washout," R. L. Albrook Hydraulic Laboratory and International Engineering Company, Inc., Washington State College, Pullman, Washington, 1959.

Pugh, C. A., "Hydraulic Model Studies of Fuse Plug Embankments," Bureau of Reclamation, REC-ERC-85-7, 1985.

Shields, A. "Application of Similarity Principles and Turbulence Research to Bedload Movement," Translation CIT, Pasadena, California, 1936.

Simons, D. B., Şentürk, "Sediment Transport Technology," WRP, Fort Collins, Colorado, 1977.

Taylor,B. D., "Temperature Effects in Alluvial Streams," Report No. KH-R-27, Keck Laboratory of Hydraulics and Water Resources, CIT, Pasadena, California, 1971.

Vanoni, V. A., "Sedimentation Engineering," ASCE - Manuals and Reports on Engineering Practice - No. 54, 1975.

SEDIMENT STUDIES AT UNION AVENUE DAM - DENVER, COLORADO

By Cassie C. Klumpp, U.S. Bureau of Reclamation, Denver, Colorado

ABSTRACT

The Union Avenue Dam was constructed on the South Platte River in 1985 by the U. S. Army Corps of Engineers (COE) to provide a water supply intake for the City of Englewood and to control the grade of the South Platte River. Energy is dissipated at the base of the dam in a hydraulic jump. This type of energy dissipator is hazardous to recreational boaters.

The Colorado Water Conservation Board (CWCB) investigated the possibility of constructing a series of boat chutes at the dam to improve boater safety. The CWCB selected Wright Water Engineers to plan the project and requested assistance from the U.S. Bureau of Reclamation (Reclamation) to construct a physical model of the boat chute in their hydraulic lab.

Model tests were conducted to provide favorable flow patterns for boating. Sediment tests were made in the physical model to observe scour and deposition effects near the Englewood water intake upstream of Union Avenue and deposition and scour patterns in the pool between boat chute 1 and boat chute 2. A typical particle size distribution curve was obtained from the COE near Union Avenue Dam. Different sediment transport equations were used to estimate sediment discharge near the dam. After the sediment discharge rate was determined in the prototype, the sediment sizes were scaled down to model size and a sediment test was conducted in the physical model for 2 days. The results of the test were analyzed, and it was determined that the the changes in the Union Avenue dam would not affect the intake and the sluice. The deposition patterns in the pool between the first and second chute will change flow patterns. However, this should not adversely affect recreational boating through the series of boat chutes.

INTRODUCTION

In 1985, the COE constructed a dam 300 feet downstream of Union Avenue in Englewood on the South Platte River. The dam serves as a diversion structure for a water supply intake for the city of Englewood and also controls the grade of the South Platte River for flood control. The reinforced concrete dam is 18.5 feet high and has a 3 to 1 slope on the downstream face of the spillway. The total head drop is 15 feet to the downstream channel. The energy is dissipated in a hydraulic jump at the base of the spillway.

Recreational boating has become popular on the South Platte River in recent years (Samad et. al., 1986; Simmons et. al., 1987). The CWCB (Colorado Water Conservation Board) proposed construction of a series of boat chutes, each with a drop of 2 to 4 feet, to handle the total head drop of 15 feet. The CWCB selected Wright Water Engineers (WWE) to design the boat chutes. A 1 to 18 scale model, constructed in the laboratory, includes the Union Avenue dam, city of Englewood intake structure, radial-gate- controlled sluiceway, downstream pool, and the second boat chute (figure 1).

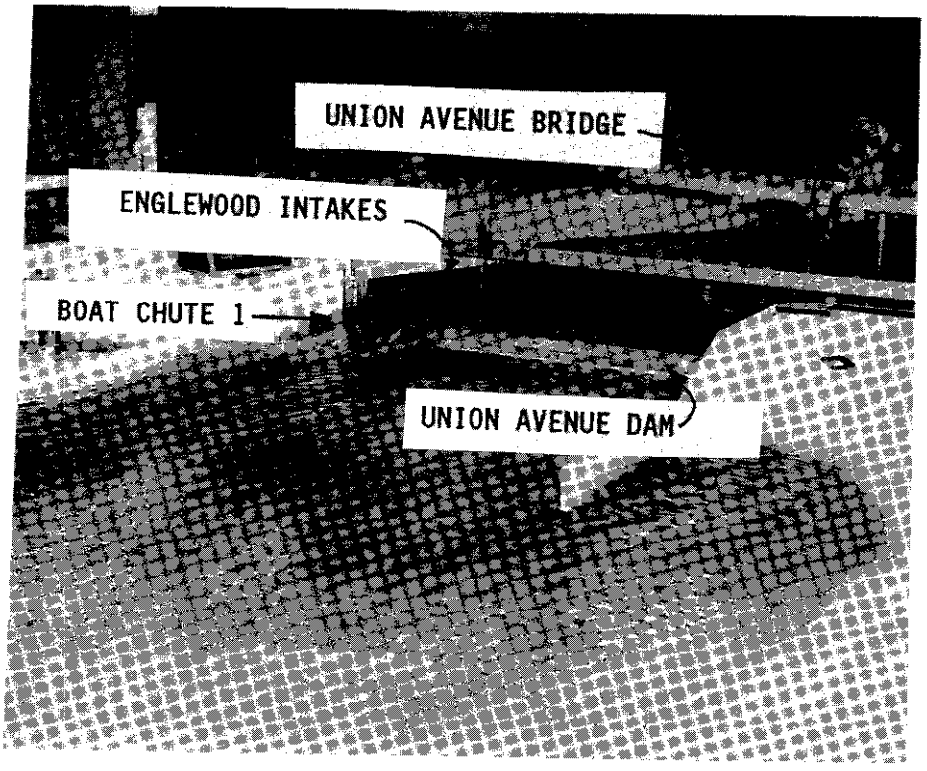

Figure 1 - Union Avenue Boat Chute Model

The model includes the river bend upstream of the Englewood dam. The model entrance at the baffle to the bridge is a fixed bed. From the bridge to the dam, the model riverbed was filled with sediment sized according to the gradation determined from scaling the prototype gradation curve. The bedform was shaped according to cross sections provided by WWE. Templates were used in the model to form the sand according to the field data.

A series of tests were conducted in the laboratory study the hydraulics of boating conditions for discharges ranging between 100 and 1,500 ft^3/s. Sediment tests were conducted for a typical spring flow of 3,000 ft^3/s to observe deposition and scour patterns as they affect the Englewood water intake structure upstream of Union Avenue dam and deposition and scour patterns in the pool between boat chute 1 and boat chute 2.

PHYSICAL MODEL

Hydraulic Similitude

Hydraulic similitude must exist between model and prototype to obtain accurate hydraulic and sediment measurements. Flow was simulated in the model by using the Froude number, a dimensionless number that relates inertial force to gravity force:

$$F_r = \frac{V}{\sqrt{Lg}} \tag{1}$$

where:

V = velocity
L = length, and
g = acceleration due to gravity

Based on the Froude number, protytype and model parameters can be determined from the following similitude equations:

$$L_r = \frac{L_p}{L_m} = 18 \tag{2}$$

$$T_r = L_r^{1/2} = 4.24 \tag{3}$$

$$Q_r = (L_r)^{2.5} = 1,375 \tag{4}$$

where:

T_r = time ratio
L_r = length ratio
and Q_r = discharge ratio.

Subscripts p and m refer to the prototype and model, and r is the ratio between model and prototype.

Sediment Scaling

Sediment models must simulate shear stress properly because shear stress creates the drag force necessary to overcome forces holding a particle in place. Shear stress on a particle will fluctuate because of turbulence. Sediment erosion is simulated properly in a model by making model and prototype dimensionless unit sediment discharge rates equal ($q_{sm} = q_{sp}$).

WWE gave Reclamation a typical prototype particle size distribution curve of the South Patte River at Oxford Avenue located near Union Avenue Dam. If the particle size distribution curve is scaled geometrically according to Froude scaling ($\tau_m = \tau_p$), then the model unit sediment discharge rate (q_{s*}) will be too great for grain Reynolds numbers ranging between 5 and 100. Model grain sizes must be adjusted to properly simulate sediment transport in this range.

Sand and silt particles usually settle according to Stokes law. Sand and silt particles less than 1 millimeter settle at slower velocities as the particles become smaller. In order to adjust the sediment discharge rate in the model, particles less than 1 millimeter are increased in size until the settling velocity is corrected to the proper velocity consistent with Froude scaling. When the model grains sizes are adjusted for settling velocity, the value of τ_* decreases while the value of R_* increases bringing the model value of unit sediment discharge closer to the prototype. The grain size distribution of bedload in the South Platte River at Oxford Avenue was simulated in the model. Figure 2 shows the prototype and model grain size distributions.

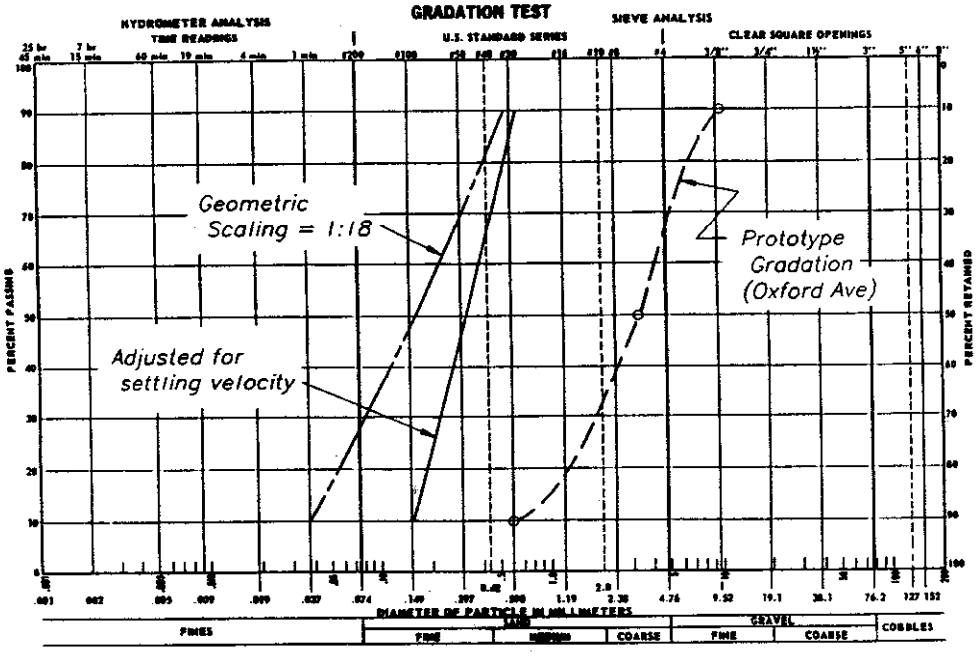

Figure 2 - Model and prototype grain size distribution for bedload.

SEDIMENT STUDIES

Sluicing flows

The model was operated initially with discharges ranging from 50 to 3,000 ft^3/s. Sand that was placed upstream of the dam spilled over the low sluice wall in front of the Englewood intakes for various operating conditions. Operating the radial gate and the sluiceway moved sand through the intake areas; however, some sand deposited near the intakes. The amount of sand deposited depends on how much water is going through the intakes and the opening of the radial gate. Good sluicing action was achieved when the radial gate was fully opened even when the city of Englewood took their maximum water right during the summer months. When the radial gate was close to fully open, the model boats were pinned against the wall or drawn into the radial gate. This condition was considered unacceptable for boating. The city of Englewood presently operates the sluice for gate settings from 25 percent to 100 percent.

To improve sluicing and reduce risk to boaters, the low wall currently in front of the intakes was increased in height to the elevation of the water intake wall (5296.5 feet). With this change in the sluice, all of the water entering the intake area was forced to enter from the upstream of the intake greatly increasing the velocity in the intake channel. The velocity originally obtained for a 100 percent gate setting was maintained with only a 25 percent gate opening.

Sediment Tests

Estimates of bedload transport rates were made for a spring flow of 3000 ft^3/s, which has a return period of 10 years (Wright Water Engineers, 1987). The particle size distribution curve for the analysis is shown in figure 2. A uniform velocity distribution was assumed with a cross-section width of 120 feet.

A prototype velocity of 7 ft/s was estimated assuming a Manning's n roughness of 0.03 for the channel and 0.04 for the overbanks. The estimated water surface slope of the channel is 0.003 ft/ft and the D50 of the bedload sediment is 3.1 mm. Based on these data, the estimated bedload transport rate that was computed from the sediment transport equations varied from 2,500 tons/day for the Meyer-Peter & Muller equation to 10,000 tons/day for the Rottner equation, averaging 3500 tons per day (Stevens and Yang, 1989). Using the discharge scale ratio ($L_{r2.5}$), the bedload discharge scaled to approximately 200 lb/hour or an application rate of 50 lb/ 15 minutes.

The sediment test was conducted for three days. Initially the test was conducted with the existing sluice wall in place at the lower elevation. At a radial gate opening of 30 percent, a large deposit of sediment formed in the Englewood intake area covering the first three water intakes. At 100 percent radial gate opening the first three water intakes were still covered although the sediment deposit was reduced.

The sediment test was continued for three days with a raised solid wall in place along the Englewood intake. Sediment was fed into the model upstream of the Union Avenue Bridge every 15 minutes. After 3 days, the deposition in the pool appeared to be stable. This was verified by taking measurements at

specified locations in the pool between boat chute 1 and boat chute 2. The sediment deposition in the pool between the two boat chutes did not change significantly for a period of a few hours.

Two photographs show the pool between boat chute 1 and boat chute 2 before and after the sediment test (figure 3 and figure 4). Prior to the sediment test, some deposition occurred in the pool at the end of the sluice channel. After the test, a large sand bar was deposited downstream of the main dam to the left of the boat chute almost to the end of the sluice wall. Another deposit formed downstream of the boat chute in the shape of an alluvial fan. Down-stream of the sluice gate a deposit formed near the submerged wall that forms part of the downstream sluice channel. However, there was no deposition in the area immediately downstream of the radial gate, therefore, not affecting the sluicing of sediment away from the water intakes upstream of the dam.

The deposits produced by the sediment test would probably occur during several years unless a relatively large flood occurred during any one year. Sediment deposits that occurred during the test affect flow patterns in the pool between boat chute 1 and boat chute 2. However, flow patterns are acceptable for boating before or after deposition. Prior to the sediment tests the flow gradually turns toward the second chute on the left bank. A back eddy forms downstream from the dam that carries boaters toward the upstream dam. Following sediment deposition the back eddy is eliminated and the flow forms a channel from boat chute 1 to boat chute 2.

Floodflows

Discharges up to to the 100 year flood of 16,400 ft^3/s were observed in the model. Model data showed the water level is contained within the stream banks up to the 100 year flood. The 100 year flood was tested in the model before and after the sediment tests. The sediment deposition in the pool between boat chute 1 and 2 also did not affect the flow during the 100 year flood (figure 5).

CONCLUSIONS

1. Boaters would be drawn into the intake area during sluicing with the present Englewood water intake design. A solid wall, the same height as the intakes was recommended in front of the Englewood primary intakes. The raised wall greatly improved sluicing capacity.

2. Sediment tests conducted in the physical model showed that the sluice would not be adversely affected by the build up of sediment in the pool between boat chute 1 and boat chute 2. The radial gate of the sluice channel is free of sediment.

3. Sediment deposition affected flow patterns in the pool. However, flow patterns are acceptable for boating both before and after the sediment tests.

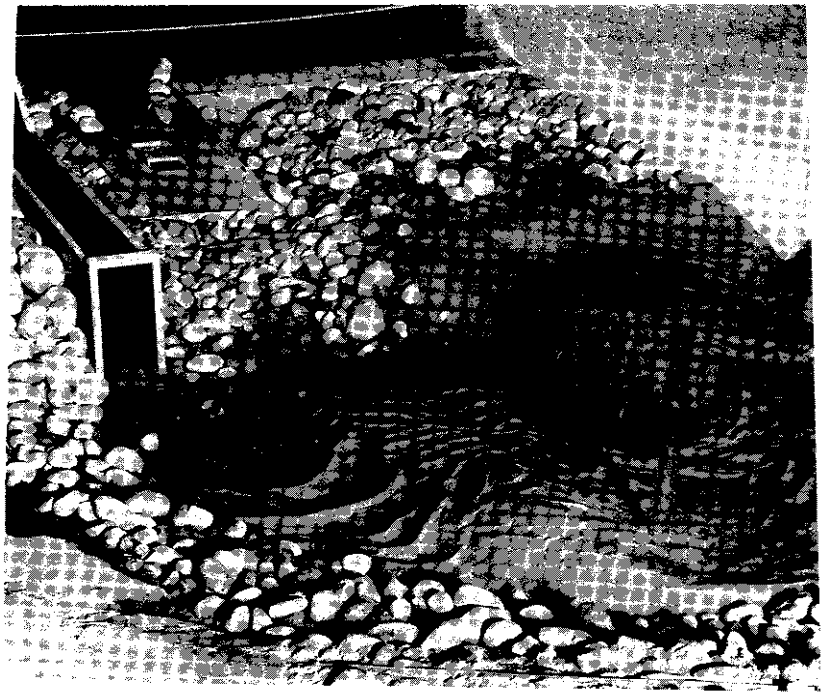

Figure 3 - Area between two boat chutes prior to sediment test.

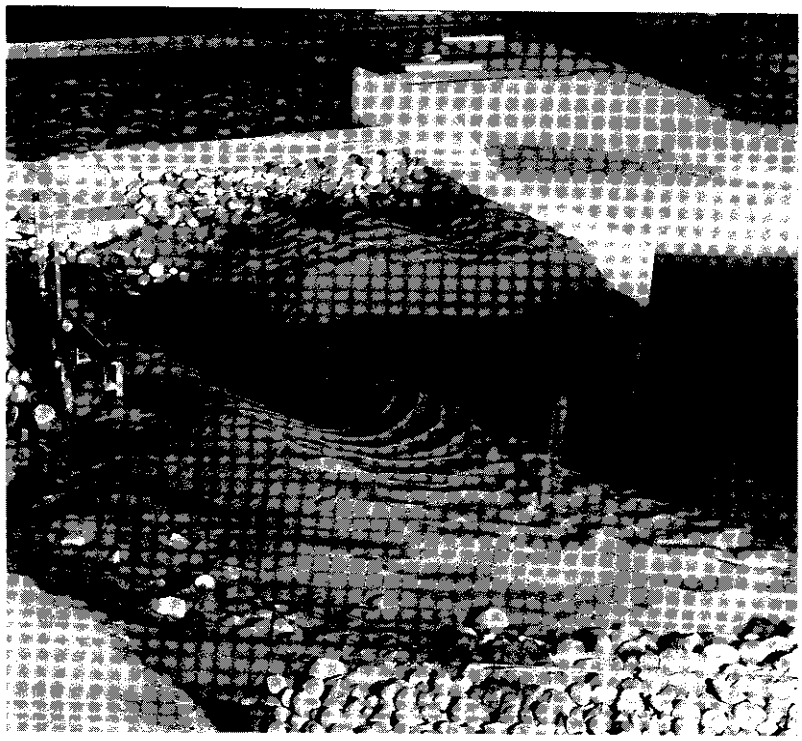

Figure 4 - Deposition after sediment test

Figure 5 - Model with flow at 16,400 ft^3/s (COE 100 year flood)

REFERENCES

Samad, Mohammed A., Ph. D., John M. Phlaum, William C. Taggart, and Richard E. McLaughlin, "Modeling of the Undular Jump for White Water Bypass," Water Forum '86, Proceedings of the American Society of Civil Engineers, July 1986.

Simmons, William P., Thomas H. Logan, Richard A. Simmons, and Richard J. Brown, "Model Studies of Denver White Water Channel," Journal of the Hyddrauics Division, American Society of Civil Engineers, July 1987.

Stevens, Jr., Herbert H. and Chih Ted Yang, "Summary and Use of Fluvial Sediment Transport Formulas," USGS, Water Resources Investigation Report Investigation Report, Pub. No. 89-4026, Lakewood, Colorado.

Wright Water Engineers, "Feasibility Study, Boat Bypass Structure at Union Avenue Dam," prepared for Coloardo Water Conservation Board, September 1987.

SIMULATION OF SEDIMENT TRANSPORT NEAR STRUCTURES

By Sam S.Y. Wang, F.A.P. Barnard Professor, and Director, Center for Computational Hydroscience and Engineering, The University of Mississippi, University, Mississippi,

Phil Combs, Chief, Hydraulics Sections, U.S. Army Corps of Engineers, Vicksburg District, Vicksburg, Mississippi, and

Joseph Letter, Hydraulic Engineer, Estuaries Division, U.S. Army Corps of Engineers, Waterways Experiment Station, Hydraulics Laboratory, Vicksburg, Mississippi.

ABSTRACT

A newly refined computational simulation model based on the Efficient Finite Element Method is presented. Its cost-effectiveness in simulating three-dimensional free surface flow, sediment transport and bed surface elevation changes is demonstrated with a typical example.

INTRODUCTION

The construction of hydraulic structures in a hydraulic system changes the flow, and thus, the sedimentation processes in the system. It is necessary to have a reasonable prediction of the bed erosion, sediment transport and deposition, so that not only the cost-effectiveness, but also the environmental impact of the proposed structure can be assessed before the design is finalized. Recently, for economic reasons, more and more of these studies are being carried out by numerical modeling. In conducting numerical simulation of the highly complicated sedimentation phenomena, research engineers are confronted by the difficulties of numerical (spurious) waves and instabilities. The Efficient Finite Element Method has been newly developed at the Center for Computational Hydroscience and Engineering at The University of Mississippi. It effectively eliminated most of these difficulties when it was applied to investigate the sedimentation phenomena in hydraulic systems.

The sedimentation phenomena of local scour and deposition around hydraulic structures are of interest and importance in all hydraulic systems. Due to the presence of structures built in alluvial channels, complications in the flow are increased, which include separations, eddies, vortices, local accelerations and decelerations, helical secondary motions and intensified turbulence. Consequently, additional fluid dynamic forces, as well as fluctuations of forces, are exerted on the sediment particles on the bed. These forces accelerate the erosion, entrainment and transportation of sediments and result in local scouring and deposition. To establish a better understanding of these phenomena, an unsteady, three-dimensional mathematical model is adopted to simulate the turbulent flow around hydraulic structures. Transient three-dimensional sediment transport equations are used to predict the suspended sediment movement and empirical relations are used to predict sediment transport in the form of bed load. To solve these sets of nonlinear partial differential equations in a region with irregular boundaries, a new numerical methodology has been developed. Early computational simulation models reported were 1-d and 2-d models, such as Thomas (1982), Adeff/Wang

(1985), Armanini/Di Silvio (1988), Cunge (1980), Kerssens (1979), Alonso/Wang (1980), Bechteler/Schrimpf (1984), van Rijn (1987), Teisson/Fritsch (1988), Wang (1989), and many others. Since this paper primarily deals with 3-d models, no details on 1-d, 2-d vertical and 2-d horizontal models shall be discussed.

To simulate a 3-d sedimentation phenomenon, one needs to solve the mathematical equations governing both the free-surface flow and the sedimentation processes. The solution of this complex phenomenon, in a highly irregular domain, is obtained numerically. Since a brief review of the recent developments in simulating free surface flows was published by Wang/Hu/Mayerle (1990), and a state of the art survey on finite element modeling of 3-d sedimentation processes was given by Wang (1990); the historical survey of these two areas is not duplicated in this short paper. Readers may refer to the two publications cited above and the references listed in those two papers, if so interested.

MATHEMATICAL MODEL

Free Surface Fluid Flow Model

The 3-d free surface turbulent flows of an incompressible fluid associated with sediment transport may be approximately by the Shallow Water Theory including hydrostatic pressure assumption. In this special case, the first two momentum equations (in x and y directions) and the continuity equation are used together with the free surface kinematic condition below, to compute the velocity and free surface elevation, $\vec{u}$ and η respectively.

$$\frac{\partial \vec{u}}{\partial t} + \vec{u}\cdot\nabla\vec{u} + \frac{\nabla p}{\rho} - \epsilon_f \nabla^2\vec{u} - \vec{B} = \vec{0} \tag{1}$$

$$\nabla\cdot\vec{u} = 0 \tag{2}$$

$$\frac{\partial \eta}{\partial t} + u_\eta \frac{\partial \eta}{\partial x} + v_\eta \frac{\partial \eta}{\partial y} - w_\eta = 0 \tag{3}$$

$$p = \rho g(\eta - z) \tag{4}$$

A simple closure scheme using the turbulent eddy viscosity law reported by Coleman (1981) and Van Rijn (1984) is adopted:

$$\begin{aligned} \epsilon_f &= 4\,\epsilon_m \frac{h}{h}\left(1 - \frac{h'}{h}\right), && \text{for } \frac{h'}{h} < 0.5; \\ \epsilon_f &= \epsilon_m = \frac{\kappa u^* h}{4}, && \text{for } \frac{h'}{h} > 0.5 \end{aligned} \tag{5}$$

with the variables defined below and vertical coordinates shown in Figure 1:

$h = \zeta + \eta$ = depth, u^* = shear velocity,
$h' = \zeta + z$ = elevation of any point, κ = Von Karman's coefficient.

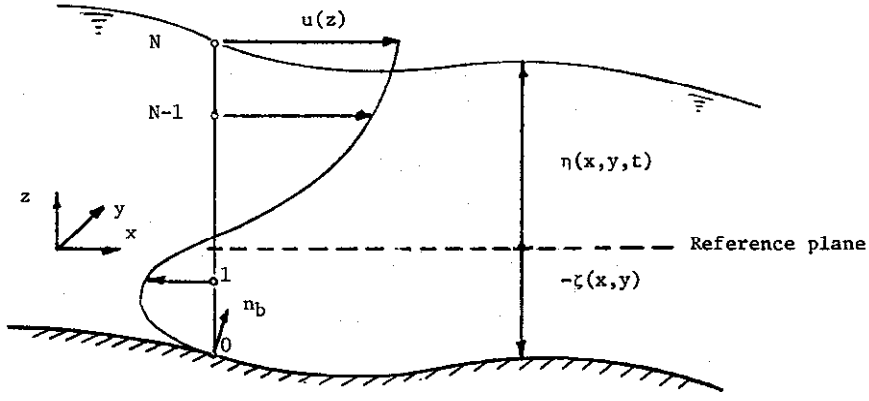

Figure 1: Vertical coordinates and velocity profile (u-component)

A nonslip boundary condition is adopted at all solid surfaces, but the friction forces at the bottom may be approximated by empirical functions, e.g.

$$\vec{B}_f = \frac{\vec{\tau}_f}{\rho} = -\ell^2_m \left(\left| \frac{\partial \vec{u}}{\partial n_b} \right| \frac{\partial \vec{u}}{\partial n_b} \right) \Big|_\zeta \tag{6}$$

with ℓ_m the Prandtl's mixing length and n_b the inward unit vector normal to the bottom. Forces on the free surface are equated to the wind shear forces; again, they are approximated empirically:

$$\vec{B}_w = \frac{\vec{\tau}_w}{\rho} = C_* \mid \vec{W}_d \mid \vec{W}_d \tag{7}$$

with W_d the wind speed and C_* a wind shear coefficient. Additional boundary conditions, such as discharge, velocity or stage, should be prescribed at the entrances and exits of the system, if any.

Sediment Transport Model

Sediment transport loads in flowing water may be classified as bed load and suspended load. The total sediment transport flux across any cross-section area may be estimated by summing the two. The mathematical model for describing the bed load has yet to be developed. Therefore, the numerical modelers have been adopting the well-established bed load empirical functions valid for the specific site of studies. However, the mathematical models for describing the suspended load have been developed by numerous authorities in the field. They include: Alonso/Wang (1980), Sheng/Butler (1982), Miller (1983), Wang/Adeff (1986), van Rijn/Meijer (1988), and others. Due to the impressive advancement of digital computer technology in terms of computing speed and memory storage size, research activities in the development of highly sophisticated 3-d sediment transport models have been accelerated in recent years.

The equation governing 3-d sediment transport in suspension is written as:

$$\frac{\partial c}{\partial t} - \nabla\cdot(\epsilon_s \nabla c) + \nabla\cdot(c\vec{u}) \frac{\partial}{\partial t}(w_s c) = 0 \tag{8}$$

where $c = c(x,y,z,t)$ the concentration, w_s is the particle fall velocity, and ϵ_s is the sediment diffusion coefficient, which is related to the turbulent eddy viscosity:

$$\epsilon_s = \beta\Phi\epsilon_f \tag{9}$$

where the β (constant over the depth) is the ratio between the maximum values of ϵ_s and ϵ_f, which may be calculated by:

$$\beta = 1 + 2\left(\frac{W_s}{u_*}\right), \qquad \text{for:} \quad 0.1 < \frac{W_s}{u_*} < 1 \tag{10}$$

and Φ expresses the damping of the turbulence due to the presence of sediment and can be estimated by:

$$\Phi = 1 + \left(\frac{c}{c_o}\right)^{.8} - 2\left(\frac{c}{c_o}\right)^{.4} \tag{11}$$

with $c_o = 0.65$, the maximum volumetric bed concentration. Van Rijn recommended the use of Φ as a fit parameter to reproduce measured concentration profiles. The Φ can also be used to compute a local Von Karman coefficient as affected by the presence of sediments, Yalin and Finlayson (1972):

$$\kappa_s = \Phi\ \kappa \tag{12}$$

The boundary concentration c_a at the reference level a may be computed by:

$$c_a = \frac{q_b}{u_b \delta_b} \tag{13}$$

where q_b is the bed-load transport, u_b is the particle velocity and δ_b is the thickness of bed-load layer. To complete the mathematical model for sediment transport simulation, one may also need the sediment transport fluxes (convective, diffusive and net or total flux) prescribed or free, bed and wall boundaries as well as imaginary surfaces across the entrances and exits, if any. The lack of understanding of the physical principles governing the water and sediment particle interactions has made the application of empirical functions a necessity in the development of computational simulation models. A detailed discussion on the flux boundary conditions is given by Van Rijn (1989).

Finally the Continuity equation for sediments may be written as:

$$(1 - P)\frac{\partial z_b}{\partial t} + \frac{\partial q_{ex}}{\partial x} + \frac{\partial q_{ey}}{\partial y} + \frac{\partial (h\bar{c})}{\partial t} = 0 \tag{14}$$

where P is the porosity, $\bar{c}$ is the depth-averaged concentration, and q_e is the effective sediment transport which includes both the bed-load transport, q_b, and the suspended-load transport q_s, $z_b = -\zeta$, represents the bed elevation, and q_{sx} and q_{sy} are obtained by computing:

$$q_{sx} = \int_{\delta_b}^{h} u\ c\ dz \quad ; \quad q_{sy} = \int_{\delta_b}^{h} v\ c\ dz \tag{15}$$

The different time scales in which the fluid flow changes and the sediment processes takes place permit to decouple the equations so that they can be solved separately. The fluid flow equations are solved first to yield, u,v,w and η; then the transport equation is solved for c and finally the sediment continuity equation for the new z_b.

EFFICIENT FINITE ELEMENT METHOD

This model was developed by combining the advantages of both the Finite Element and Finite Difference Methods. The solution domain is discretized into a system of several layers of 3-d elements using isoparametric interpolation functions (FE approach). The numerical equations are obtained one set at a node (FD approach) by a selected least square or collocation condition. This new model can be applied to simulate sedimentation processes in a highly irregular domain without the need of a complicated body-fitted coordinate transformation (as needed by FDM) and it can be formulated by sweep through the nodes rather than elements (as required by FEM). Therefore, more than 90% of the computing time required to formulate a FE Model can be saved. This is why this model is called Efficient Finite Element Model (EFEM), details are given by Wang/Hu, (1990). EFEM has included several refined schemes to enhance its accuracy and stability. The utilization of trigonometric functions as the interpolation functions has eliminated the errors in approximating the diffusion terms caused by the traditional Lagrangian interpolation functions. The introduction of convective shape functions augmented by the local flow velocity has accounted for the so-called upwinding effect locally (Figure 2).

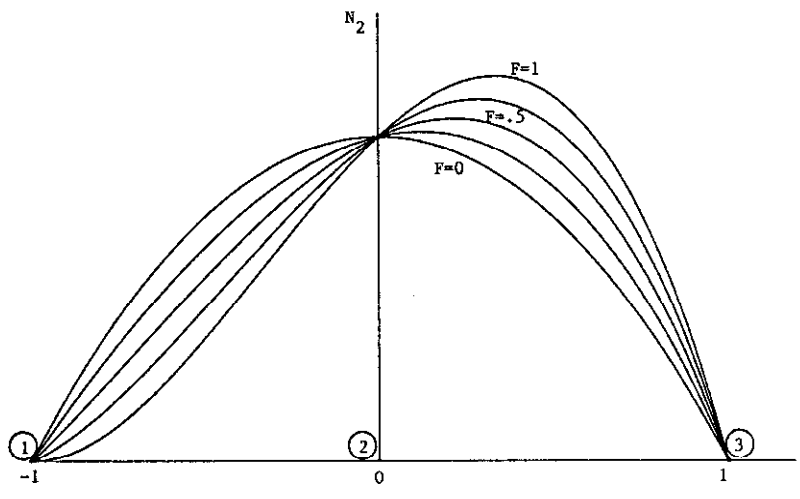

Figure 2: Convective shape function augumented locally by flow velocity to account for the upwinding effect.

The application of the least square condition to obtain the numerical equations at each and every node has effectively eliminated the spurious secondary waves;

and, thus, greatly improved the numerical stability. Due to the page limit, only one typical case is shown in Figure 3.

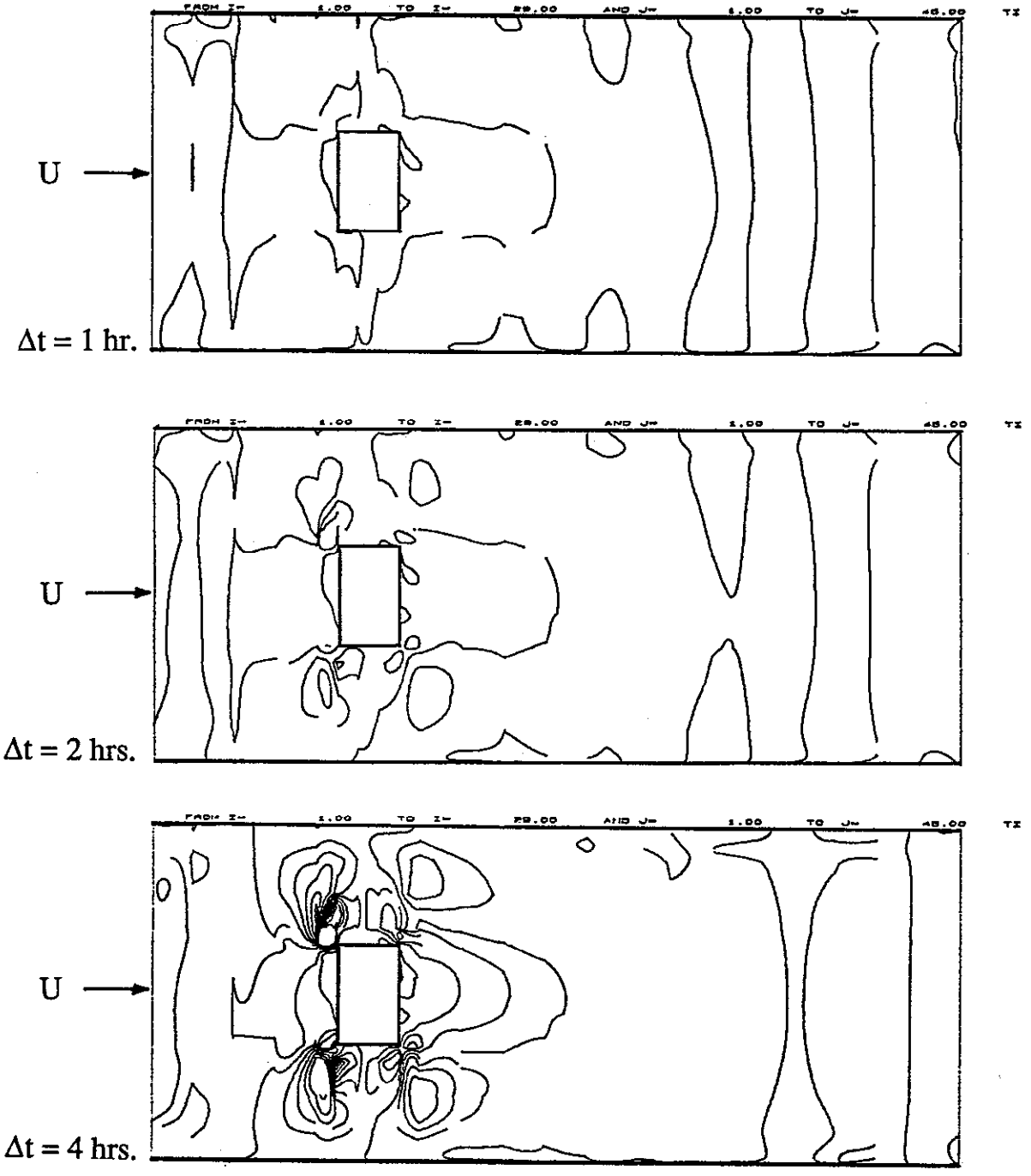

Figure 3: Morphological changes of an alluvial channel due to erosion and deposition around an obstruction.

CONCLUDING REMARKS

First, the EFEM utilizes the body-fitted coordinate transformation only to approximate a highly irregular solution domain by a finite element grid system. Since it is not used for transforming configuration of the solution domain, the governing differential equations are not complicated. By sweeping through all the nodes, one set of global finite element equations is derived at a node using a working element constructed around this node (node of attention). There is no need to derive many sets of local finite element equations and, then, to assemble them into a global set. Besides, the set of global algebraic equations derived by the EFEM has a narrow band width similar to that obtained by FDM. Therefore, it is more efficient than the traditional, FEM.

Secondly, the global finite element equations are obtained by the application of least square procedure to minimize the residual differential equations within the working element which is a generalized case of several Petrov or Dissipative Galerkin schemes. As a result, the new methodology is capable of elimination the spurious numerical oscillations so as to enhance the numerical stability.

Thirdly, the newly developed hybrid, convective and non-convective, shape functions can obtain more accurate interpolations. The local flow condition characterized by the Peclet (or Reynolds) number and/or the Froude number is used to control the degree of dominance of the convective terms. The skewness of the convective shape functions reflect the correct physics i.e. the hydrodynamic effects transmitted from upstream and downstream to the node of attention are not symmetric. The adoption of Fourier components or trigonometric functions to construct quadratic Lagrangrian Shape Functions has also found to be more realistic than those based on the polynomial Lagrangian type functions.

Finally, results of two complicated 3-d turbulent free-surface flows and sedimentation phenomena around hydraulic structures have demonstrated that the newly developed Efficient Finite Element Method is capable of producing accurate and reasonable simulation, eliminating spurious and node-to-node oscillation, and enhancing numerical stability and computing efficiency.

ACKNOWLEDGEMENT

This work is a result of studies sponsored by the USDA Agricultural Research Service, monitored by the National Sedimentation Laboratory under Specific Cooperative Agreement No. 58-4431-9-075; the U.S. Army, Corps of Engineers, Waterways Experiment Station, Hydraulics Laboratory, under Contract DACW 39-87-K-0088; and The University of Mississippi. Contributions of technical results by the research professionals and students of the CCHE at The University of Mississippi are also acknowledged.

REFERENCES

Adeff, S. and Wang, S. S.-Y., Hydrodynamic Model of River Flow on a Microcomputer, pp. 1017-1023, Proceedings of the ASCE Hydraulics Division Specialty Conference, Orlando, August, 1985.

Alonso, C.V. and Wang, S. S.-Y., Simulation of Local Scour and Fill in Sand Bed Stream, Finite Elements in Water Resources, Vol. III (6-57-68), University of Mississippi, October, 1980.

Anderson, O.H., Hedegaard, I.B., Deigaard, R., Girolamo, P. and Madsen, P., Model

for Morphological Changes under Waves and Current, IAHR Symposium, Copenhagen, Denmark, 1988.
Armanini, A. and Di Silvio, G., A One-Dimensional Model for the Transport of a Sediment Mixture in Non-Equilibrium Conditions, Journal of Hydr. Research, Vol. 26, No. 3, 1988.
Bechteler, W. and Schrimpf, W., Improved Numerical Model for Sedimentation, Journal of Hydr. Eng., ASCE, Vol. 110, No. 3, 1984.
Cunge, J.A., Holly, F.M., and Verwey, A., Practical Aspects of Computational River Hydraulics, Pitman, 1980.
Kerssens, P.J.M., Prins, A., Van Rijn, L.C., Model for Suspended Sediment Transport, Journal of the Hydraulics Division, ASCE, HY 5, 1979.
Miller, H.P., Three-Dimensional Free-Surface Suspended Particle Transport in the South Biscayne Bay, Florida, Int. Journal in Numerical Methods in Fluids, pp. 901-914, Vol. 4, 1983.
Sheng, Y.P. and Butler, H.L., Modeling Coastal Currents and Sediment Transport, Proceedings of 18th ICCE, Capte Town, South Africa, 1982.
Teisson, C. and Fritsch, D., Numerical Modelling of Suspended Sediment Transport in the Loire Estuary, IAHR Symposium, Copenhagen, Denmark, 1988.
Thomas, W.A., Mathematical Modelling of Sediment Movement, Gravel Bed Rivers, John Wiley and Sons, 1982.
Van Rijn, L.C., Mathematical Modelling of Morphological Processes in the Case of Suspended Sediment Transport, Thesis, Delft Tech. Univ., Delft, The Netherlands, 1987 (also Delft Hydraulics Communication, No. 382).
Van Rijn, L.C., The State of the Art in Sediment Transport Modeling, Proc. Int'l. Symp. on Sediment Transport Modeling, ASCE, pp. 13-32, 1989.
Van Rijn, L.C. and Meijer, K., Three-Dimensional Mathematical Modelling of Suspended Sediment Transport in Currents and Waves, IAHR Symposium, Copenhagen, Denmark, 1988.
Wang, S.S.-Y. and Adeff, S.E., Three-Dimensional Modelling of River Sedimentation Processes, Third Int. Symp. on River Sedimentation, University of Mississippi, 1986.
Wang, S.S.-Y. and Hu, K. K., Improved Methodology for Formulating Finite Element Hydrodynamic Models, to be published as a chapter in Finite Elements in Fluids, Vol. 8, Hemisphere Publishing Corp., 1990.
Wang, Z.B., Mathematical Modelling of Morphological Processes in Estuaries, Dissertation, Delft Univ. of Techn., Delft, The Netherlands, 1989.
Yalin, M.S. and Finlayson, G.D., On the Velocity Distribution of the Flow-Carrying Sediment in Suspension, Symposium to Honor Prof. H.A. Einstein, H.W. Shen, Editor, 1974.

MODELING OF SPATIALLY-VARYING VELOCITY DISTRIBUTION

By Chao-Lin Chiu, Professor of Civil Engineering, University of Pittsburgh, Pittsburgh, PA; Randy D. Crissman, Hydraulic Engineer, New York Power Authority, Niagara Falls, NY; and Weizu Yu, Graduate Student, Dept. of Civl Engineering, University of Pittsburgh, Pittsburgh, PA.

ABSTRACT

A method for simulating the spatially-varying velocity distribution along a channel is presented that can be used in multi-dimensional flow modeling and studying the transport of sediment and various pollutants in streams and rivers. The method employs a velocity distribution equation derived by entropy maximization. It enables determining the velocity distributions at various sections along a channel, from a given discharge and water-surface profile. An illustrative example is presented to describe the method and its applicability to natural channels.

INTRODUCTION

The velocity distribution is a basic flow property that affects the discharge, shear stress distribution, secondary currents, diffusion and various transport processes (transport of sediment and various pollutants). The flow in a natural stream or river is non-uniform in which the velocity distribution tends to vary from section to section along the channel. A feasible technique is, therefore, needed for modeling and simulation of the spatially varying velocity distribution along a river channel.

The water surface profile is related to the energy and momentum coefficients through the one-dimensional energy and momentum equations; the energy and momentum coefficients are related to the velocity distribution by definition; and the velocity distribution is in turn related to the shear stress. Therefore, it would be logical to make an attempt to develop a systematic approach that will use a water surface profile, along with the corresponding discharge and channel cross sectiions, etc., that are easily obtainable, to estimate the energy and momentum coefficients, velocity distribution and shear stress that are difficult to measure. The objective of this paper is to present an initial step towards the development of such an approach.

VELOCITY DISTRIBUTION EQUATION

Chiu(1989) derived a velocity distribution equation,

$$\frac{u}{u_{max}} = \frac{1}{M}\ln\left[1+(e^{M}-1)\frac{\xi-\xi_0}{\xi_{max}-\xi_0}\right] \quad \text{.....(1)}$$

in which u_{max} = the maximum velocity in a section; M= a parameter; ξ = an index variable with which u increases monotonically so that a one-to-one functional relationship may exist between u and ξ; and ξ_o and ξ_{max} = the minimum and maximum values of ξ, respectively.

While the expression for ξ may be many, an obvious one is

$$\xi = \frac{y}{D} \qquad \text{.....(2)}$$

in which D= the water depth along a vertical; and y = the vertical distance from the channel bed. Eq. 2 is suitable for a wide channel in which the velocity u increases monotonically with the vertical distance from the bed. Eq. 2 is not suitable as an approximation of ξ, however, for a channel which is not very wide and the maximum velocity occurs below the water surface, so that the same velocity occurs at two points, below and above the maximum velocity, respectively. In such a case, a suitable equation of ξ is

$$\xi = \frac{y}{D-h}\exp\left(1-\frac{y}{D-h}\right) \qquad \text{.....(3)}$$

in which h= the depth of maximum velocity below the water surface. According to Eq. 3, ξ_{max} and hence, u_{max} occur at y=D-h. The velocity at y=D is less than that at y=D-h. If a two-dimensional velocity distribution is required, the following equation (Chiu and Chiou 1986) may be used:

$$\xi = Y(1-Z)^{\beta_i}\exp(\beta_i Z - Y + 1) \qquad \text{.....(4)}$$

in which

$$Y = \frac{y+\delta_y}{D+\delta_y-h} \qquad \text{.....(5)}$$

and

$$Z = \frac{|z|}{B_i+\delta_i} \qquad \text{.....(6)}$$

δ_y and δ_i are parameters which, along with the y and z coordinates are defined in Fig. 1. β_i is a parameter in which i=1 or 2 represents the left or right side of the vertical y-axis which is defined as a vertical, passing through the point of maximum velocity. In a natural channel the velocity distribution tends to be asymmetric with respect to the y-axis, so that the β_1 and β_2 may be different. In a rectangular (or approximately rectangular)

channel δ_y and δ_i both approach zero. In Eqs. 5 and 6, h (>0) is the depth of maximum velocity below the water surface (Pattern II in Fig. 1). If h=0 the maximum velocity occurs on the water surface and isolvels are perpendicular to the water surface. If h<0 the maximum velocity occurs on the water surface but the isovels are not perpendicular to the water surface (Pattern I in Fig. 1). Eq. 1 is equivalent to

$$\frac{\xi-\xi_0}{\xi_{max}-\xi_0} = \int_0^u p(u)\,du \qquad \text{.....(7)}$$

in which p(u) is the probability density by function of u,

$$p(u) = \exp(a_1+a_2u) \qquad \text{.....(8)}$$

in which a_1, and a_2 are parameters. Eq. 7 means that if the value of ξ is randomly sampled between ξ_0 and ξ_{max}, and the corresponding value of velocity is obtained from its relation to ξ; then, the probability of velocity being between u and u+du is p(u)du. Eq. 8 was derived by maximizing the function,

$$H(u) = -\int_0^{u_{max}} p(u)\ln p(u)\,du \qquad \text{.....(9)}$$

subject to the constraints,

$$\int_0^{u_{max}} p(u)\ du = 1 \qquad \text{.....(10)}$$

and

$$\int_0^{u_{max}} up(u)\,du = \overline{u} = \frac{Q}{A} \qquad \text{.....(11)}$$

Eq. 10 is the condition of any probability density function, while Eq. 11 states the condition that p(u) must be such that the mean value of u must be Q/A where Q is the discharge, and A is the cross sectional area. H(u) in Eq. 9 is the (Shannon's) "entropy function" of u. The entropy maximization is widely used in information theory, statistical mechanics and statistics as a technique to determine a probability density function of a random variable (Goldman 1953, Rao 1965). Substitution of Eq. 8 into Eqs. 10 and 11 yields

$$u_{max}e^{a_1} = M(e^M - 1)^{-1} \qquad \text{.....(12)}$$

and

$$\frac{\bar{u}}{u_{max}} = e^{M}(e^{M}-1)^{-1} - \frac{1}{M} \qquad \text{.....(13)}$$

in which the parameter M, also appearing in Eq. 11, is defined as $M=a_2u_{max}$. For a wide channel (Chiu 1989),

$$e^{a_1} = \frac{\nu}{Du_*^2} \qquad \text{.....(14)}$$

Eqs. 12, 13, and 14 give

$$\bar{u} = \frac{Q}{A} = \frac{Du_*^2}{\nu F(M)} \qquad \text{.....(15)}$$

in which

$$F(M) = (e^{M}-1)\,[Me^{M}(e^{M}-1)^{-1}-1]^{-1} \qquad \text{.....(16)}$$

Eq. 15 can be used to obtain F(M) which in turn gives M through Eq. 16. This technique may be used to estimate the energy and momentum coefficients at a cross section through their relations to M. With Eq. 1 describing the velocity distribution, the energy coefficient can be expressed in terms of M as

$$\alpha = \frac{(e^{M}-1)^2\,[e^{M}(M^3-3M^2+6M-6)+6]}{[e^{M}(M-1)+1]^3} \qquad \text{.....(17)}$$

The momentum coefficient in terms of M is

$$\beta = \frac{(e^{M}-1)\,[e^{M}(M^2-2M+2)-2]}{[e^{M}(M-1)+1]^2} \qquad \text{.....(18)}$$

The value of M, along with $\bar{u}=Q/A$, can be used in Eq. 13 to determine the other parameter u_{max} in the velocity distribution equation (Eq. 1). Thus, the spatially varying velocity distribution along a non-uniform flow in a stream or river can be determined.

ILLUSTRATIVE EXAMPLE

Fig. 2 shows the Upper Niagara River situated between Lake Erie near Buffalo and the Niagara Falls. Fig. 3 shows the observed water surface profile along the the River, at 1 am, January 17, 1990 when the flow is in a fairly steady state. The corresponding Manning's n profile along the River estimated from the known discharge and the observed water surface profile is shown in Fig. 4. From the information in Figs. 3 and 4 the values of M along the

River were computed by using Eqs. 15 and 16, as shown in Fig. 5. The profiles of α and β were then computed by Eqs. 17 and 18, as shown in Figs. 6. Fig. 7 shows the distributions of mean and maximum velocities along the River, in which the mean velocity at each cross section was obtained by dividing the known discharge by the cross sectional area; and the maximum velocity given by Eq. 13 after obtaining the mean velocity and M. Note that the flow accelerates very rapidly after entering the River from the Lake, and attains very high velocities before being divided by the Grand Island into two parts, the flows in the East and West Channels. The rapid flow is associated with the steep slopes of the channel, water surface and energy grade line. Fig. 8 describes velocity distribution patterns (relation between u/u and y/D) given by Eq. 1 for various values of M. Note that for M greater than about 5 or 6 the mean velocity occurs at y/D= 0.368 (or e^{-1}). Fig. 9 describes the velocity distribution at the Black Creek section simulated by Eq. 1 with computed values of parameters (M and u_{max}) and ξ represented by Eq. 2 (ξ= y/D). The velocity distribution pattern may be refined by using Eq. 4 to represent ξ, to cope with the variability of velocity in the transverse direction.

SUMMARY AND CONCLUSION

This paper describes a technique for computing the energy and momentum coefficients and the velocity distribution along an open channel, from an observed water surface profile. The technique should have practical applications in various hydraulic studies, such as modeling of multi-dimensional flow and transport of sediment and pollutants in streams and rivers.

Figs. 4 through 9 only show some initial results. Additional tests must still be conducted and improvements could still be made.

ACKNOWLEDGMENTS

The Upper Niagara River data used in this paper were provided by the New York Power Authority.

REFERENCES

Chiu, Chao-Lin, 1989, Velocity Distributions in Open Channel Flow, Journal of Hydraulics Engineering, ASCE, 115 (5), 576-594.

Chiu, Chao-Lin, and Chiou, J.-D., 1986. Structure of 3-D Flow in Rectangular Open Channels, Journal of Hydraulic Engineering, ASCE, 112 (11), 1050-1068.

Goldman, S., 1953. Information Theory, Prentice-Hall, Inc., New York, N.Y.

Rao, C. R., 1965, Linear Statistical Inference and Its Applications, John Wiley & Sons, Inc., New York, NY.

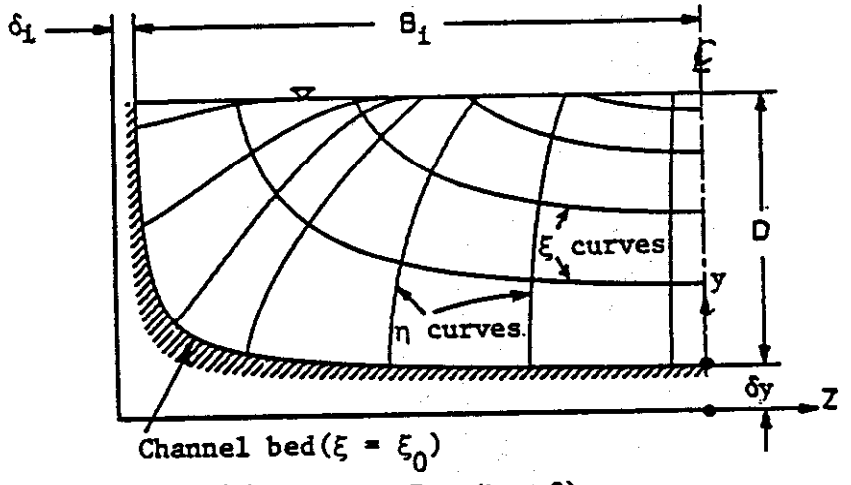

(a) Pattern I (h < 0)

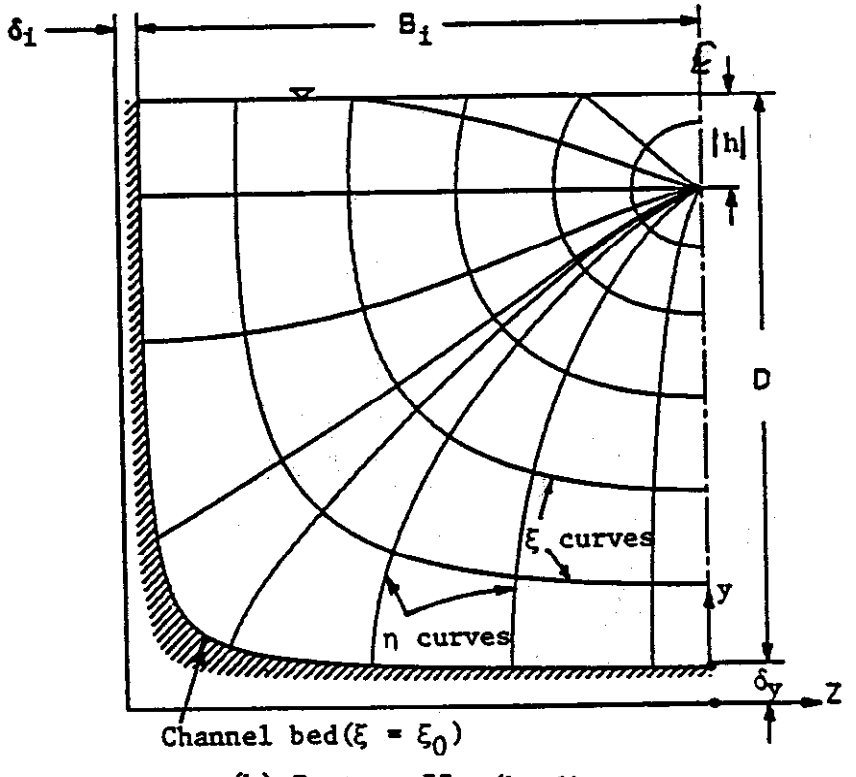

(b) Pattern II (h> 0)

FIG. 1.-Patterns of Velocity Distribution and Curvilinear Coordinate System

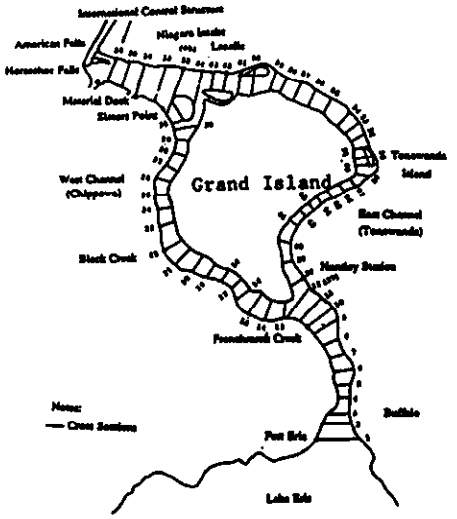

Fig.2.- Upper Niagara River

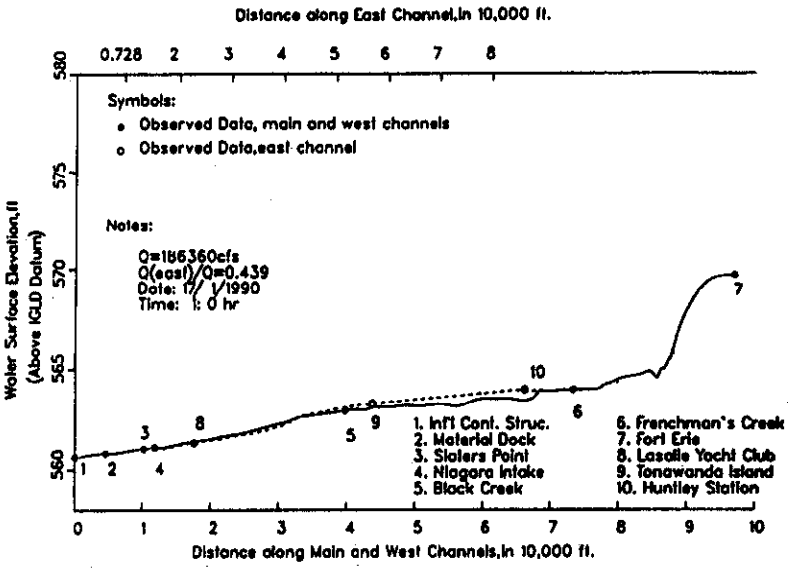

Fig.3.- Water Surface Profile along Upper Niagara River

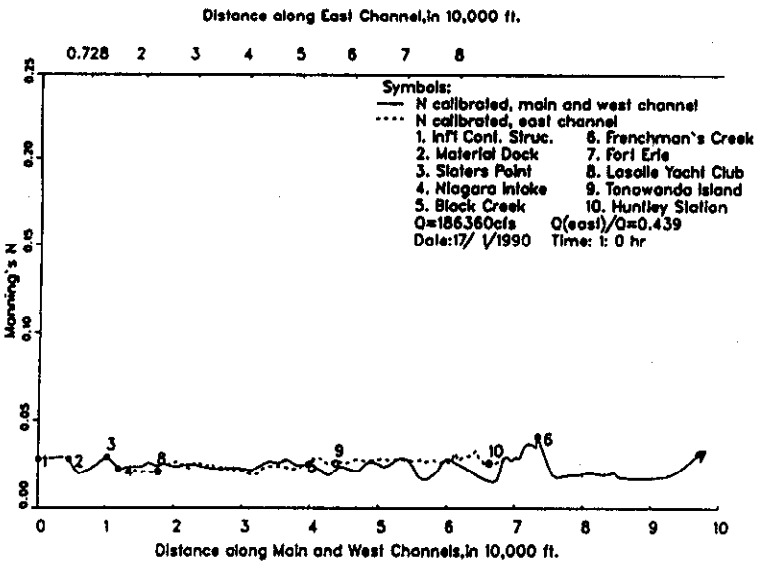

Fig.4.- Manning's N along Upper Niagara River

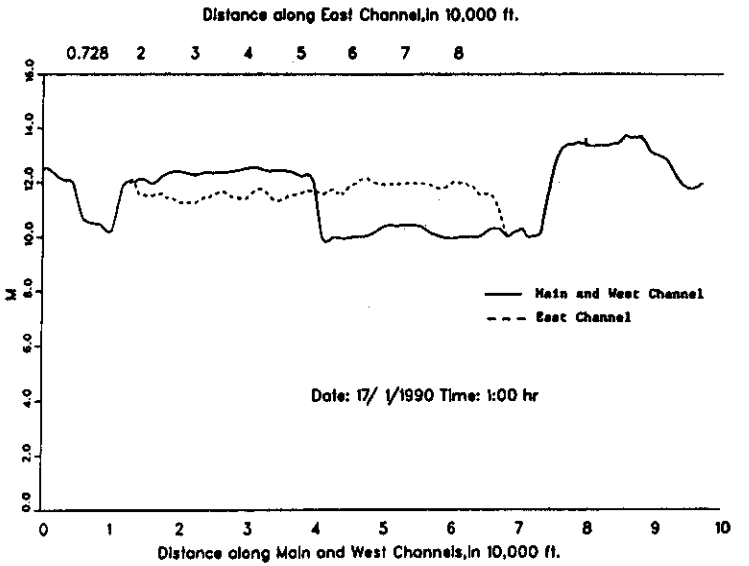

Fig.5.- M Value along Upper Niagara River

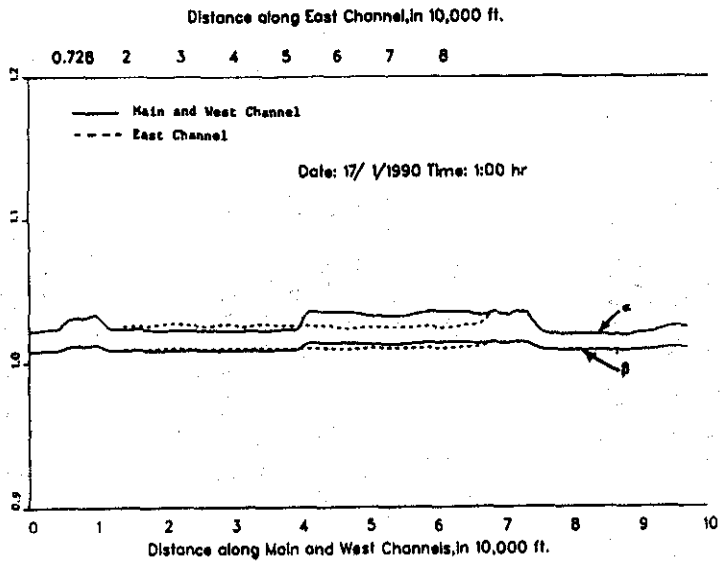

Fig.6.– Distribution of Energy and Momentum Coefficients

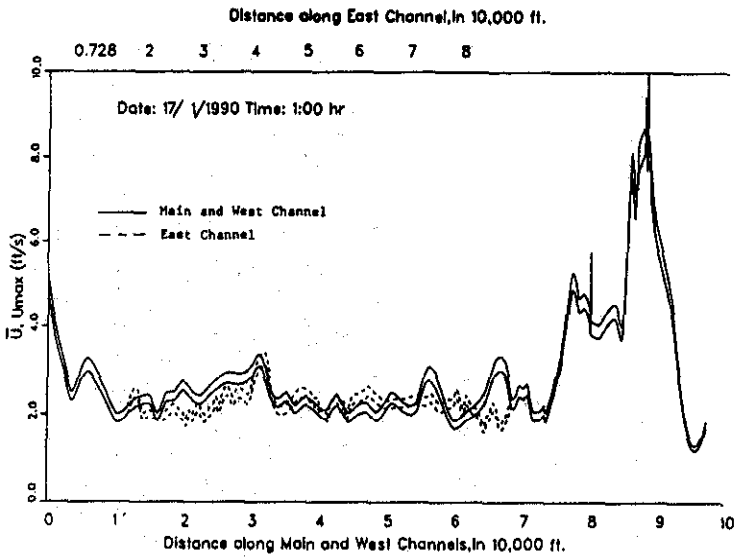

Fig.7.– Velocity along Upper Niagara River

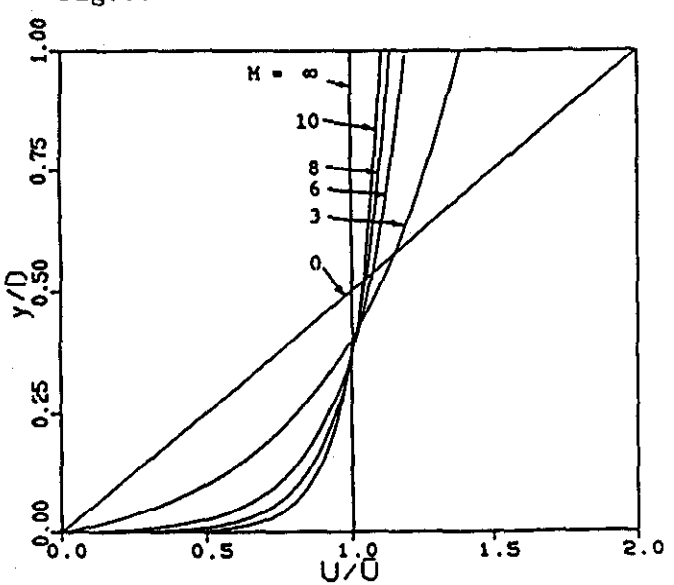

Fig.8.– Parameter M and Velocity Distribution

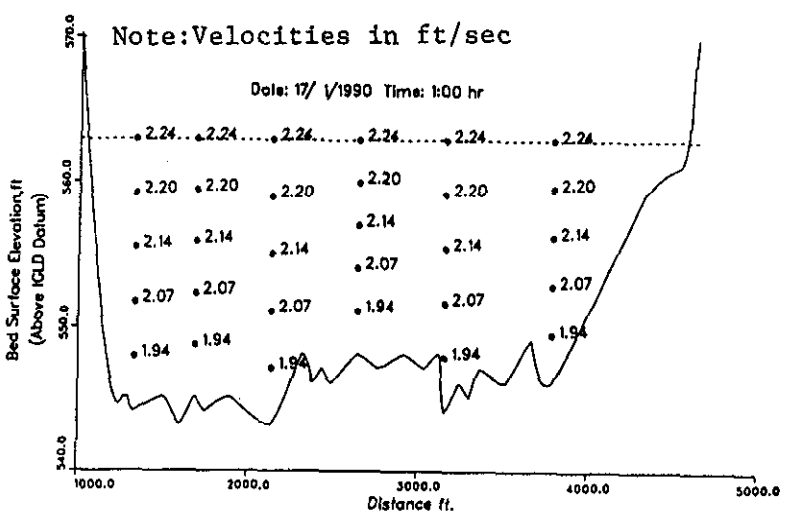

Fig.9.– Velocity Distribution at Black Creek Cross Section

BRI-STARS MODEL FOR ALLUVIAL RIVER SIMULATIONS

BY

Albert Molinas, Hydrau-Tech Engineering, Fort Collins, CO

and Roy Trent, Federal Highway Administration, McLean, VA

ABSTRACT

This paper is on the computation of alluvial river scouring/deposition using the BRI-STARS computer program. The BRIdge StreamTube Model for Alluvial River Simulation (BRI-STARS) which was developed under the National Cooperative Highway Research Program (NCHRP) is a semi-two-dimensional model capable of computing alluvial scour/deposition through subcritical, supercritical, and a combination of both flow conditions involving hydraulic jumps. The model is capable of computing scour/deposition for applications involving bridges not only along a study reach but also across the channel by the use of streamtubes. The BRI-STARS model runs on the IBM PC-AT or compatables. The paper presents the theoretical development behind the BRI-STARS model and describes various roughness, sediment transport, local scour, and other variable computations. Example model applications using laboratory data are presented. The computed results are compared with physical model experiments which were conducted at Colorado State University Hydraulics Laboratory.

I. MODEL DESCRIPTION

1.1 General

The BRIdge StreamTube Model for Alluvial River Simulation (BRI-STARS) which was developed under the National Cooperative Highway Research Program (NCHRP) is a semi-two-dimensional model capable of computing alluvial scour/deposition through subcritical, supercritical, and a combination of both flow conditions involving hydraulic jumps. This model, unlike the conventional water and sediment routing computer models, is capable of simulating channel widening/narrowing phenomenon as well as local scour due to highway encroachments.

The channel widening/narrowing is accomplished by coupling the stream tube computer model developed earlier by Molinas with a decision-making algorithm using rate of energy dissipation or total stream power minimization.

The first component, the fixed-width streamtube computer model, simulates the scouring/deposition process taking place in the vertical direction across the channel. The second component, the total stream power minimization algorithm, determines whether at a given cross-section the channel adjustments due to scour/deposition should take place in the lateral or vertical direction. It is this component that allows the lateral changes in channel geometries. Finally, the bridge component allows the computation of the hydraulic flow variables and the resulting scour due to highway encroachments. In the following sections each component will be elaborated.

1.2 StreamTube Model Component

The Stream Tube Computer Model was developed to simulate long-term streambed variations in rivers for which sediment and hydraulic data is limited. The computer model using stream tubes can be applied to a variety of river problems. It can be used as a fixed-bed model to compute water surface profiles for

subcritical, supercritical or the combination of both flow conditions involving hydraulic jumps. This capability allows the applications involving the flow profiles over spillways or flow profiles in natural river channels where the bed elevation changes are negligible. As a movable-bed model, the computer program can be applied to route water and sediment through natural river channels. The use of stream tubes allows the variation of hydraulic conditions and sediment activity not only in the longitudinal, but also in the lateral direction. With the selection of a single stream tube, the model becomes one-dimensional. Average channel response to changes in certain river flow or sediment conditions can be studied. With the selecition of multiple stream tubes the model becomes two-dimensional. The changes in the cross section geometries in the lateral direction can be simulated. Since the bed-elevation changes are not averaged over the entire active channel widths as in one-dimensional models, more realistic channel erosion or aggradation can be simulated. The use of streamtubes provides valuable information in model applications where the variation of flow variables across the channel is needed. The fixed width capabilities of **BRI-STARS** can also be used in bank stability problems in identifying expected regions of bank instabilities. The armouring process provided in the program allows the study of river sedimentation problems for longer periods of time.

The computer program is a semi-two-dimensional program with the third demension, depth, being intrinsically incorporated into the computations. As such, it has the basic limitations of every two-dimensional program: secondary flows cannot be simulated. The channel is divided into a preselected number of tubes. The bed elevation in each stream tube is allowed to move vertically up or down depending on the flow conditions. As a result, while one section of channel is eroding another might be aggrading. Depending on the number of stream tubes to be used, the channel cross section changes are averaged across different channel sections of different widths. Since the computer time and space is directly related to the number of stream tubes to be used, the user is required to decide upon the optimum number of tubes. Bed forms are not simulated due to the lack of a generally accepted mehtodology for determining them. Even though provisions are made to expand the program to include river confluences and middle islands, at this point these options are not available. The channel boundaries are fixed in the lateral direction and formation of meander bends cannot be simulated.

The Stream Tube Computer Model for routing water and sediment is composed of three major components: i) Backwater Computations, ii) Stream Tube Computations, iii) Sediment Routing Computations.

At each time step, first, Standard Step Method of water surface profile computations are carried out for the entire reach treating the channel as a single tube. Secondly, using the computed water surface elevations, lateral locations of stream tubes at each cross section are determined. Treating each stream tube as independent channels, new water surface profiles and hydraulic variables along them are computed. Thirdly, sediment is routed through each stream tube, satisfying the sediment continuity equation. At the end of these computations, bed material compositions are revised and channel bed elevations are updated. An armouring procedure is incorporated into the sediment routing computations. Computations are proceeded in time through defined water and sediment discharge hydrographs.

BACKWATER COMPUTATIONS

Water discharge hydrographs are appproximated by bursts of constant discharges. During each constant discharge time block, backwater computations are carried out without interruption for subcritical, supercritical, or a combination of both flow conditions modeling hydraulic jumps. The details of these computations are presented in several publicaitions (Molinas and Yang, 1985; Molinas, 1983). These uninterrupted water surface profile computations are one of the most significant features of the Stream Tube Computer Model. It is this unique component that makes the model applicable to water and sediment routing computations through complex flow conditions in bridge waterways.

STREAMTUBE COMPUTATIONS

Stream tubes are imaginary tubes bounded by stream lines. Since the discharge between stream lines is constant, each stream tube carries a constant discharge along its length. For steady, incompressible flows, it is possible to write

$$\frac{P}{\gamma} + \frac{V^2}{2g} + z = H_t$$

where H_t is a constant along the stream tube. When applied to real fluids, the total head is not a constant. Due to friction and other local losses, it is reduced in the direciton fo flow. Along a river it is possible to determine the variation of this quantity. This is the basic assumption in the Stream Tube computer Model.

The use of stream tubes in routing water and sediment through alluvial channels is another unique feature of the Stream Tube Computer Model. In the model, the total discharge carried through the channel is distributed equally among the preselected number of stream tubes. Along each stream tube the water discharge remains constant. Nonlateral inflow into individual stream tubes fron neighboring tubes is allowed. Due to the assumptions involved, at a given station water surface elevation across the channel should remain constant. Under these circumstances, the equal discharge location, and therefore lateral stream tube locations, correspond to equal channel conveyances. Following the initial backwater computations at each station, stream tube location across the channel which satisfy equal conveyance requirements are determined. Next, since total energy along each stream tube should remain constant, backwater computations are performed to establish the hydraulic conditions along individual tubes.

SEDIMENT ROUTING COMPUTATIONS

Sediment routing computations in each stream tube are performed by satisfying the sediment continuity equation, which is given as:

$$\frac{\partial Q_s}{\partial x} + \eta \frac{\partial A_d}{\partial t} = 0$$

where η is the volume of sediment in a unit bed layer volume or one minus porosity (in **BRI-STARS** it is set equal to a commonly used value of 0.6); A_d is the volume of sediment deposition per unit length; Q_s is the volumetric sediment discharge. The sediment continuity equation is discretized as follows:

$$\eta \frac{\partial A_d}{\partial t} = \eta \, (2W_i + W_{i+1} + W_{i-1}) \frac{\Delta Z_i}{4 \, \Delta t}$$

and

$$\frac{\partial Q_s}{\partial x} = 2 \frac{Q_{s\,i} - Q_{s\,i-1}}{\Delta x_i + \Delta x_{i-1}}$$

where W is the width of channel; ΔZ is the change in bed elevation and i is the cross-sectional index. The change in bed elevation, dz, can be obtained by staisfying the sediment continuity equation.

Sediment routing procedure is followed in the downstream direction. Starting from an upstream control station where the input sediment discharge hydrograph for different size classes is known, sediment discharge per size class, $Q_{si,k}$, is predicted using the selected sediment transport equation. The change in bed elevation for each size class is then computed.

Currently, several armouring procedures are being used by various mathematical models. Almost all these procedures divide the bed into several conceptual layers of different thicknesses. Also, almost all these procedures utilize the active and inactive layer concept. However, in each armouring procedure, the sediment accounting for individual layers is handled differently. In the Stream Tube Computer, one of the most recent armouring procedures has been used. This procedure has been presented been presented by Bennett and Nordin (1977) and Mengis (1981) from the U.S. Geological Survey. Due to the use of several stream tubes across the channel, the Bennett and Nordin method has been modified to accomodate stream tubes. The locations of stream tubes change with changing flow conditions and channel geometry.

To account for bed material composition, active and incative bed layer thicknesses for the stream tubes are transferred into point values across the channel. The sediment transport capacity computations in the present mathematical model can be carried out by the use of:

1. Yang's 1973 and 1984 equations

2. Ackers and White's equation

3. Engelund and Hansen's equation

4. Meyer-Peter and Muller's equation

5. User supplied generic equation

1.3 Total Stream Power Minimization Component

The second major component of the BRI-STARS is that of making decisions as to whether the channel adjustments taking place at a given cross section due to scouring/deposition should advance in the lateral or vertical directions.

The basic tool for this decision-making component is the "Minimum Rate of Energy Dissipation Theory" developed by Yang and Song and this general theory's special case "Minimum Stream Power Theory" which is used by Chang.

The Total Stream Power for a reach is defined as:

$$\Phi_t = \sum_{i=1}^{N-1} \frac{\gamma}{2}(Q_i S_i + Q_{i+1} S_{i+1}) \Delta X_i \text{ié} \qquad \text{ier.}$$

is the reach length, or distance between stations i and $i+1$; Q_i, S_i are discharge and slope at station i, respectively.

In the **BRI-STARS**, selecting directions for channel adjustmenst is accomplished by minimizing the integral expression for total stream power given above at different stations along the reach.

At a given time step, if altering the channel width at a given cross section results in lower total stream power than raising/lowering the channel, channel adjustments are progressed in the lateral direction. For the opposite case, the adjustments are made in the vertical direction.

At cross sections where sediment erosion is predicted by the sediment routing algorithm, channel adjustments can be made either by deepening or widening the existing channel. If both, the channel widening and the channel deepening, reduce the total stream power for the study reach, the selected mode of channel adjustment in the computer model is the one resulting in the minimum total stream power for the reach.

Similarly, at cross sections where sediment accumulation is predicted by the sediment routing algorithm, channel adjustments can proceed either by raising the channel bed or by narrowing the channel along the banks. In this case too the selected mode of channel adjustment in **BRI-STARS** is the one resulting in the minimum total stream power for the reach.

In both the aggrading and degrading channel cases, the sediment load is treated as a constriction in the minimization. In cases where geological/manmade restrictions are applied to the channel deepening/widening, computations are performed to accommodate these constrictions.

The amount of channel width adjustment during a time step is determined by the sediment continuity equation. Channel widening/narrowing computations are carried out only at the stream tubes neighboring the channel banks. In the stream tubes away from the banks, sediment routing computations are carried out by satisfying the sediment continuity equation. In these tubes the channel adjustments can proceed only in the vertical direction. The amount of sediment eroded from the banks in a given reach is treated as part of the sediment influx for the downstream cross sections to conserve the mass balance.

1.4 Bridge Component

BRI-STARS model contains the bridge hydraulics routines utilized in the **WSPRO** water surface profile compution program. The details of these computations are described in detail in the **WSPRO** User's Manual. A second option which utilizes user supplied local loss coefficients at the bridge sections is also available. In this "simple bridge" approach, the bridge loss coefficients can be calibrated with measured/computed water surface profiles for closer agreement with more accurate methods of computations. The "simple bridge" approach is applicable only for free surface bridge hydraulics computations since it treats the bridge piers as a part of the channel geometry.

The local scour due to bridge piers in the BRI-STARS model is computed utilizing the following methods:

1. Colorado State University equation
2. Jain and Fisher equation
3. Laursen equation
4. Froelich equations
5. User supplied generic equation

The model computes and lists the local scour at bridge piers separately from the computed general stream aggradation/degradation values.

II. MODEL INFORMATION

2.1 Program Documentation

The User's manual for the **BRI-STARS** model is available and presents the approaches utilized in the model as well as the necessary input/output information for a successful model execution.

2.2 Extent of Use/Acceptance by Engineering Community

The **BRI-STARS** model and its earlier versions reflecting various levels of development have been successfully used by the U.S. Corps of Engineers, U.S. Bureau of Reclamation and the University of Minnesota.

2.3 Hardware Requirements

The **BRI-STARS** model runs on an IBM PC-AT or compatable equipped with a minimum of 640K main memory, DOS 3.3, and EGA graphics capabilites.

2.4 Degree of Complexity of Use

Currently the **BRI-STARS** input/output is handled through the use of labeled "records". The input data to the model is entered through i) hydraulic; ii) hydrologic; iii) sediment transport; iv) channel widening option; and v) printout/plotting option records. Each input record contains specific fields for appropriate data entry as described in the User's Manual. A totally interactive environment is provided for data entry.

This environment is designed to reduce the learning curve of the model. However, the selection of input parameters and interpretation of computer results requires a certain degree of competency in the fields of sediment transport and river mechanics. Guidelines for usage are provided in appropriate detail in the User's Manual.

III. BRIDGE SCOUR EXPERIMENTS

A series of tests were conducted at the Engineering Research Center of Colorado State University using the 200 x 4 x 8 ft recirculating flume in the Hydraulics laboratory by C. V. Santoro. A model of a bridge pier was set in the flume, equidistant from both walls. The bed material consisted of pea gravel which rose to an elevation that covered the pier foundation. Three pumps of varying power were available to recirculate the water from the sump downstream of the flume. Combinations of one or more of the pumps were used, according to their power and the requested discharge.

IV. SIMULATION RESULTS

To demonstrate the capabilities of **BRI-STARS**, the bridge scour experiments conducted at Colorado State University Hydraulics Laboratory were simulated. The details of the facilities and experimental procedures are presented in detail by Santoro, 1989. Starting with known channel cross sections, sediment gradations, and downstream controlled water surface elevations, the experimental discharge hydrographs were routed numerically through the 8 hour duration of experiments. In order to avoid any model-to-prototype conversion problems, all the computations were carried out using physical model dimensions. The two test cases presented in this paper correspond to the straight pier experiments for Q = 16 cfs and Q = 24 cfs. The model Froude numbers corresponding to these test cases were 0.35 and 0.53 (subcritical). The computed thalweg profile corresponding to Q = 16 cfs experiment is presented in Figure 1. Also in

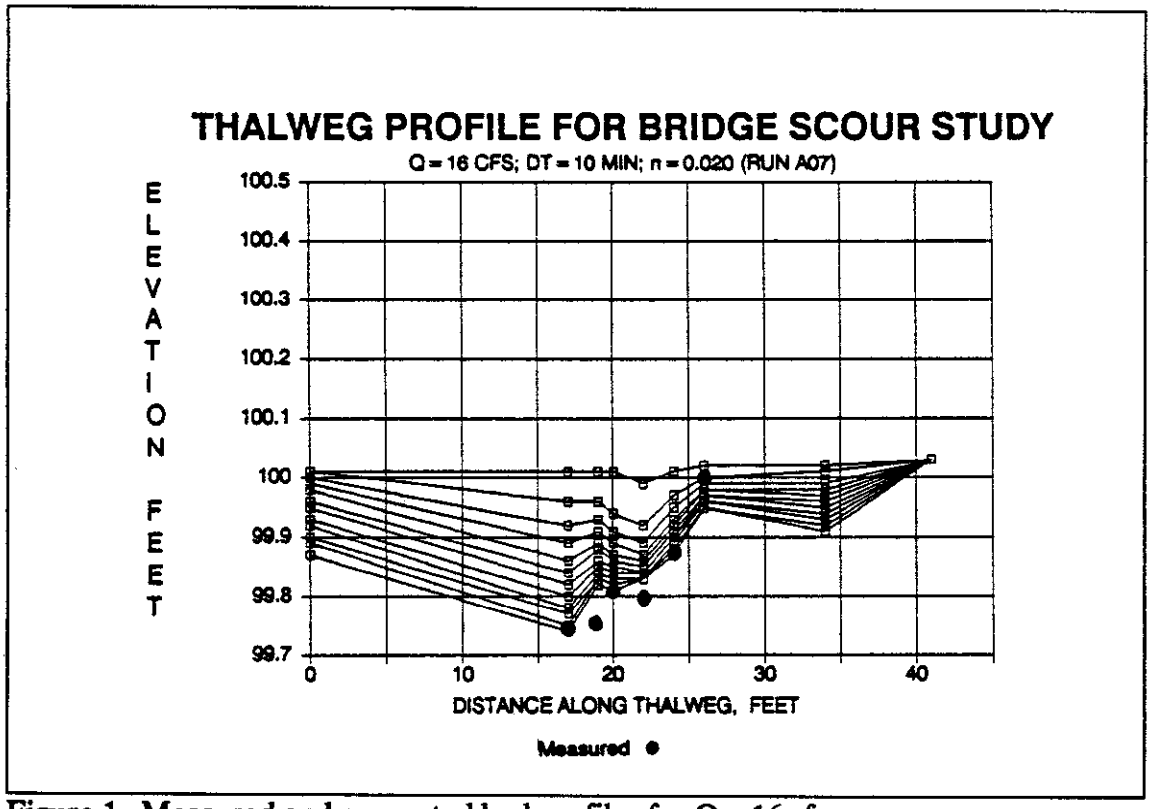

Figure 1. Measured and computed bed profiles for Q = 16 cfs.

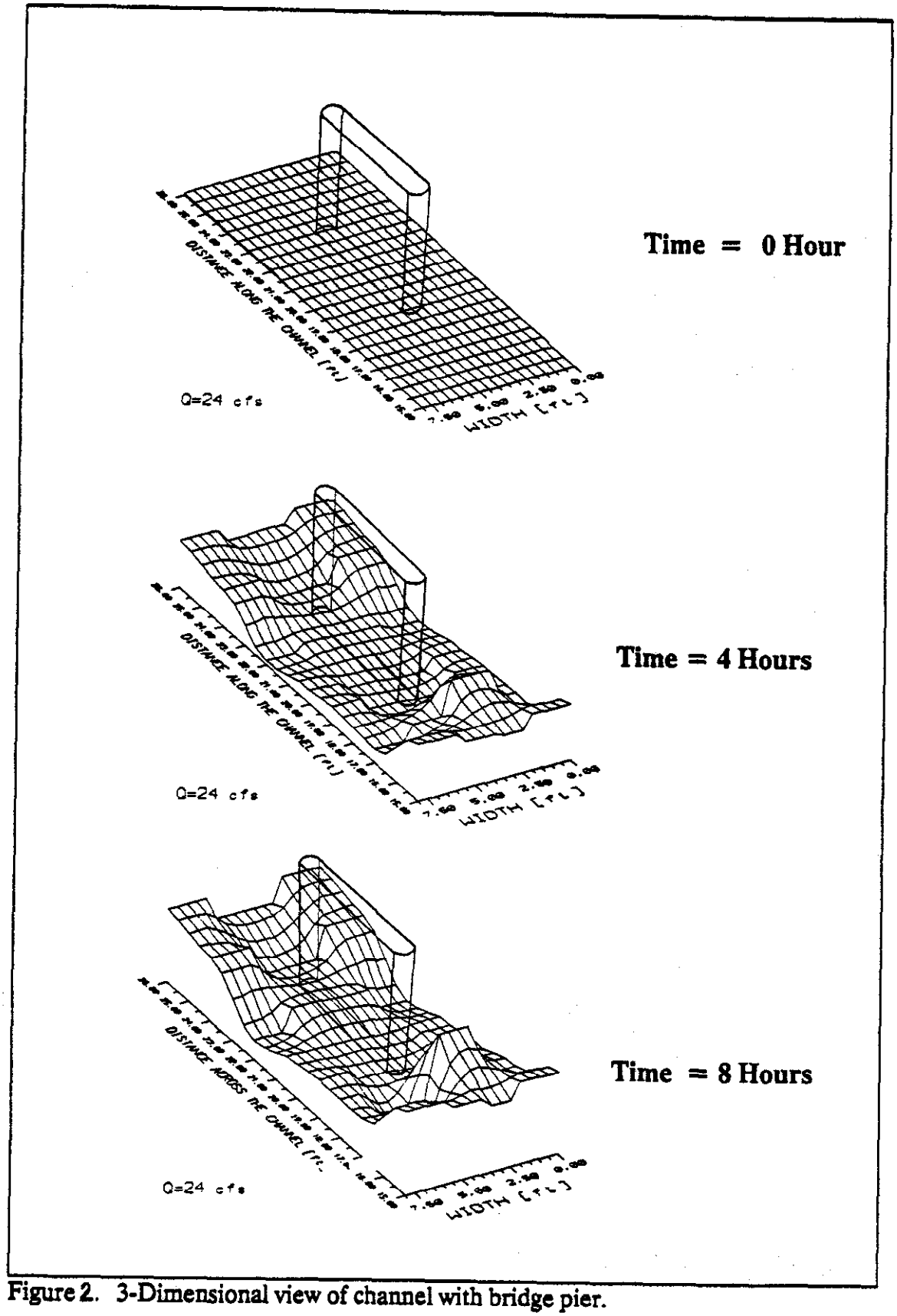

Figure 2. 3-Dimensional view of channel with bridge pier.

figure 1 the measured thalweg elevation values are indicated. The computed results are presented in 3-dimensional form in figure 2.

V. SUMMARY AND CONCLUSIONS

In this paper the **BRI-STARS** model which was developed under the National Cooperative Highway Research Program (NCHRP) Project No. 15-11 was presented. This model was applied to simulate the laboratory bridge scour experiments conducted at Colorado State University Hydraulics Laboratory. The agreement between measured and computed scour patterns and values are very encouraging. Work on model development to simulate more complex flow conditions continues.

ACKNOWLEDGEMENTS

The development of **BRI-STARS** model is funded through the **NCHRP** Project No. 15-11. The funding for the experimental work was provided through the Colorado State University Hydraulics Laboratory.

MODELING SEDIMENT TRANSPORT IN AN EPHEMERAL RIVER

By David W. Hyndman, Hydrologist, Department of Applied Earth Sciences, Stanford University, Stanford, CA 94305; Richard A. Roberts, Civil Engineer, Department of Civil Engineering, University of Arizona, Tucson, AZ 85721; and Robert H. Webb, Hydrologist, U.S. Geological Survey, 300 W. Congress Street, Tucson, AZ 85701.

ABSTRACT

Flow in ephemeral rivers is typically characterized by a rapid increase in discharge from a virtually dry channel to peak discharge, followed by a recession to low-discharge levels over several hours. These rapidly varying flows, which can cause extensive channel change and transport most of the sediment that moves in ephemeral rivers, provide a challenge to sediment-transport modeling. The Santa Cruz River is an ephemeral river with a long history of flash flooding and channel change. In 1988 and 1989, suspended-sediment concentrations and bedload-transport rates were sampled for 11 of 13 flows exceeding 400 ft^3/s in the Santa Cruz River at Tucson, Arizona. Peak discharges for these flows ranged from 400-9,580 ft^3/s and typically lasted 1-15 hrs. Suspended-sediment concentrations in single verticals ranged from 3,100 to 64,000 ppm and concentrations did not vary significantly from other verticals in the cross section for a given discharge. Bedload ranged from 5 to 1,900 tons/day and was approximately 17 percent of the bed-material transport rate. Bed-material transport rates were estimated, using several techniques, to be approximately 22 percent of measured total sediment-transport rates. Bed-material transport rate was modeled for two flows using GFLUVIAL, a 1 1/2-dimensional transport model. Preliminary results indicate that, although the order of magnitude of bed-material transport rate was modeled, timing of the peak transport rates, transport during the rising limb of the hydrograph, and the hysteretic relation between discharge and transport rate were not modeled accurately.

INTRODUCTION

"Flash floods," or rapidly varying flows that occur in response to high-intensity precipitation, are common in ephemeral rivers of the southwestern United States. Channel change during rapidly varying flows is one of the greatest hazards to urban development along ephemeral rivers in southern Arizona. For example, a large flood in October 1983 resulted in widespread failure of bridge abutments and approach sections and destruction of structures adjacent to channels as a result of lateral erosion (Saarinen and others, 1984). Flows of more frequent nature also can cause channel change, although changes may be heavily influenced by site-specific factors (Parker, 1990).

As a result of historic lateral channel change, channelization is becoming a common practice along rivers in the Southwest. Channelization without hydraulic structures can result in extensive channel erosion (Rhoads, 1990), which exacerbates flood-plain management problems. Computer modeling of sediment transport is used in the design of bank protection and hydraulic structures required for effective bank protection (Chang and Osmolski, 1988). Most models are based on the concept of equilibrium sediment transport and are usually driven by steady-flow hydraulics (Fan, 1988). These assumptions may not be valid for the highly unsteady flow conditions that characterize rapidly varying flows.

Sediment transport has rarely been measured during rapidly varying flows in ephemeral rivers. The purpose of this study is to present data on sediment transport during several rapidly varying flows of 1988-89 in the Santa Cruz River at Tucson, Arizona, and to attempt to verify aspects of a sediment transport model that is commonly-used in the design of bank protection and hydraulic structures along ephemeral rivers.

DATA COLLECTION AND ANALYSIS

Sediment transport was measured and bed-material transport rates were estimated for partial verification of a commonly used sediment-transport model. Sediment transport was measured at the Santa Cruz River at Tucson (09482500) gaging station in southern Arizona. The Santa Cruz River flows northward to Tucson from its headwaters in southern Arizona and northern Mexico (fig. 1). The drainage area above the gaging station is 2,222 mi^2, but only part of this area contributes runoff to most flows. The average discharge from 1906-81 at Tucson is 23 ft^3/s, but the river is dry more than 300 days per year. Stage for only those flows larger than 400 ft^3/s was recorded at 5-min intervals in 1988, whereas stage was recorded for flows larger than 200 ft^3/s in 1989. Direct measurement of most flows was made 295 ft upstream of the gaging station from a 230-ft-long bridge that has one set of four round piers in its center and is parallel to the channel. Flows less than 400 ft^3/s were measured by wading near the gaging station. The reach in the vicinity of the gaging station is laterally stabilized with soil-cemented banks, forming essentially a trapezoidal channel without a flood plain, and concrete sills that are approximately 1,000 ft upstream and 900 ft downstream of the bridge limit general scour in the measurement reach.

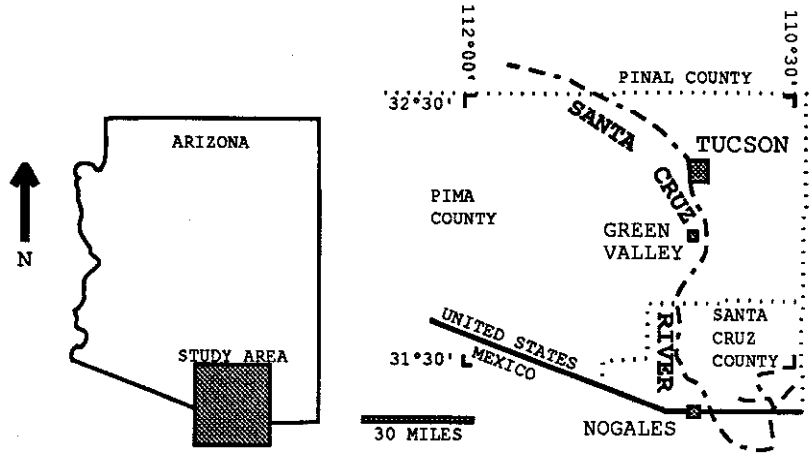

Figure 1. The Santa Cruz River basin.

Suspended-sediment and (or) bedload samples were collected during 11 of 13 flows in the summer and fall of 1988-89 (Table 1). The duration of flows ranged from 1-15 hrs with peak discharges of 400-9,600 ft^3/s. Most of the flows were caused by isolated summer thunderstorms over the southern part of Tucson, but flows in October 1989 were related to the dissipation of Hurricane Raymond from the Pacific Ocean, which originated over a larger but unknown part of the drainage area. Only one flow, that of October 6, 1989, originated as far south as Nogales (fig. 1). The magnitude of the flows are typical for summer months in the Santa Cruz River.

Bed-material samples were collected from the measurement reach in June 1989 and February 1990 when the channel was dry. Attempts to collect bed-material samples using a BM-54 sampler (see Edwards and Glysson, 1988, for sampler description) failed during flows. Particle-size distributions of all bed-material, bedload, and selected suspended-sediment samples were measured by sieving or visual accumulation tubes for sand fractions and by pipette analysis for silt and clay fractions. The median diameter of bed material in

Table 1.--Flows in the Santa Cruz River at Tucson that were sampled for sediment transport, 1988-89.

Date	Peak discharge (ft^3/s)	Time of flow (hrs)[1]	Storm type[2]	Contributing area[3]	Date	Peak discharge (ft^3/s)	Time of flow (hrs)[1]	Storm type[2]	Contributing area[3]
07-26-88	700	8.2	T	TM	07-09-89	500	1.1	T	TM
07-27-88	930	2.2	T	TM	08-02-89	400	1.1	T	TM
08-01-88	<400	1.5	T	TM	08-17-89	1,100	3.0	T	TM
08-23-88	9,600	13.9	T	TM	10-05-89	900	5.8	H	LB
08-27-88	2,700	16.8	T	LB	10-06-89	1,200	10.1	H	UB
10-20-88	3,000	11.8	C	LB					

1. Before June 1, 1989, the minimum discharge recorded was 400 ft^3/s. After this time, the minimum discharge recorded was 200 ft^3/s.
2. T -- summer thunderstorm, H -- Hurricane Raymond, C -- cutoff low.
3. TM -- Tucson metropolitan area, LB -- area between Green Valley and Tucson (fig. 1), UB -- area upstream of Green Valley.

the reach was 4 mm with only 3 percent finer than 0.063 mm. Scattered cobbles were found in the reach but were not present in a significant quantity except between the gaging station and the downstream concrete sill.

Suspended sediment was sampled using D-49 and D-74 samplers suspended from the bridge or, during low flow, with hand-held DH-48 and DH-75 samplers (see Edwards and Glysson, 1988, for descriptions of samplers and general methodology). During flows in 1988, suspended sediment was sampled in equal-width increments (EWI) of 20 ft at the bridge or 10 ft at the wading section. Because the rapid change in discharge during EWI measurements, suspended sediment was sampled at single verticals at 5-min intervals in 1989 with equal-discharge increment (EDI) samples collected only during periods of relatively constant discharge. The locations of the single verticals were chosen on the basis of flow depth and position relative to the central bridge piers.

Measured suspended-sediment concentrations (fig. 2) have a large amount of scatter with respect to discharge that appears to be related to source areas of the individual flows. Hysteretic loops on concentration-discharge

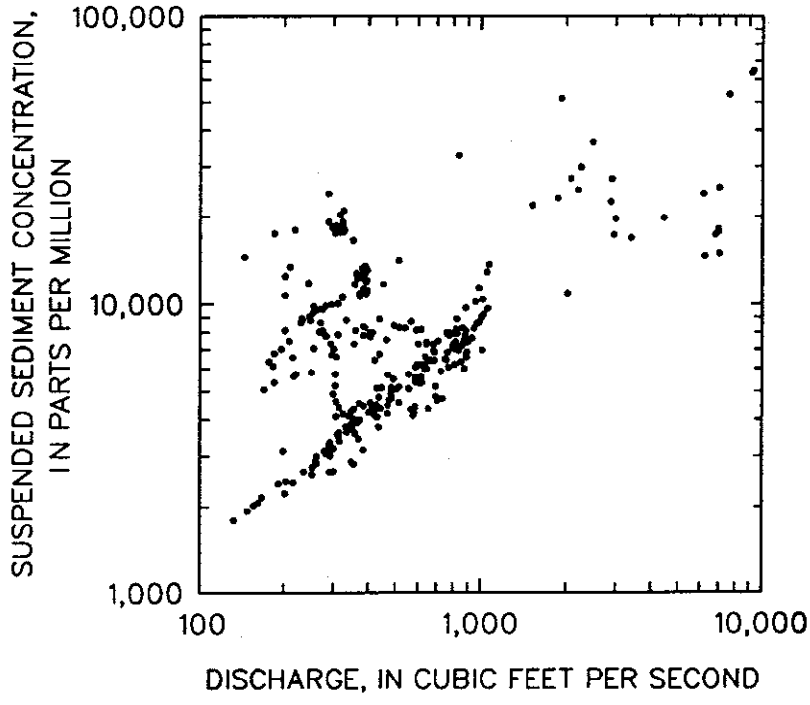

Figure 2.-- Suspended-sediment concentrations for all flows measured in 1988-89 at the Santa Cruz River at Tucson.

graphs (C-Q relations), usually clockwise loops (Williams, 1989), commonly occurred over individual hydrographs. Comparison of concentrations at single verticals with EDI measurements suggests no significant variation over the cross section. Because a large number of samples (170) was collected, particle size was determined for only 40 selected samples spaced over the hydrographs. The percentage of silt and clay for measured samples generally decreased from 99 to 67 percent as discharge increased from 200 to 2,400 ft^3/s (Roberts, 1990). Particle size for other samples was determined by linear interpolation between the measured samples.

The bed-material component of suspended sediment, needed for modeling purposes, was determined using two methods (Woo and others, 1986). In the first method, particles finer than 0.063 mm were assumed to be wash load and was subtracted from the suspended-sediment concentration. In the second method, all sediment finer than the 10-percent fraction of bed material (D10) was subtracted from suspended sediment. The results of the second method were rejected because only 5 percent of suspended sediment remained after wash load was removed (Roberts, 1990). This small amount, which would be the only fraction of suspended sediment that could be modeled, is unrealistically low.

Bedload was sampled from the bridge using a Helley-Smith sampler with a 3 in. square nozzle, 3.22 flare ratio, and 250 micron bag (see Edwards and Glysson, 1988, p. 30). In 1988, bedload transport ranged from 300 to 1,900 tons/day (fig. 3) for five cross sections measured over the active bed, which was determined by cross-sectional measurements. The transport rate was fit to a base-10 log-log equation by the method of least squares, and the resulting equation is $\log(Q_{BL}) = 1.2 + 0.5 \log(Q)$, where Q_{BL} = bedload transport rate in tons per day and Q = discharge in ft^3/s (fig. 3). In 1989, bedload in single verticals ranged from 5 to 900 tons/day for 13 bedload samples collected in the approximate center of the active channel bed (fig. 3). The average particle size of bedload is approximately 0.8 mm.

The large scatter in individual bedload transport rates and the small number of bedload cross sections (5) suggested that a theoretical approach was needed to estimate bedload. Bedload was estimated using the Meyer-Peter and Muller equation incorporated in the GFLUVIAL model (Chang, 1988, 1990; see next

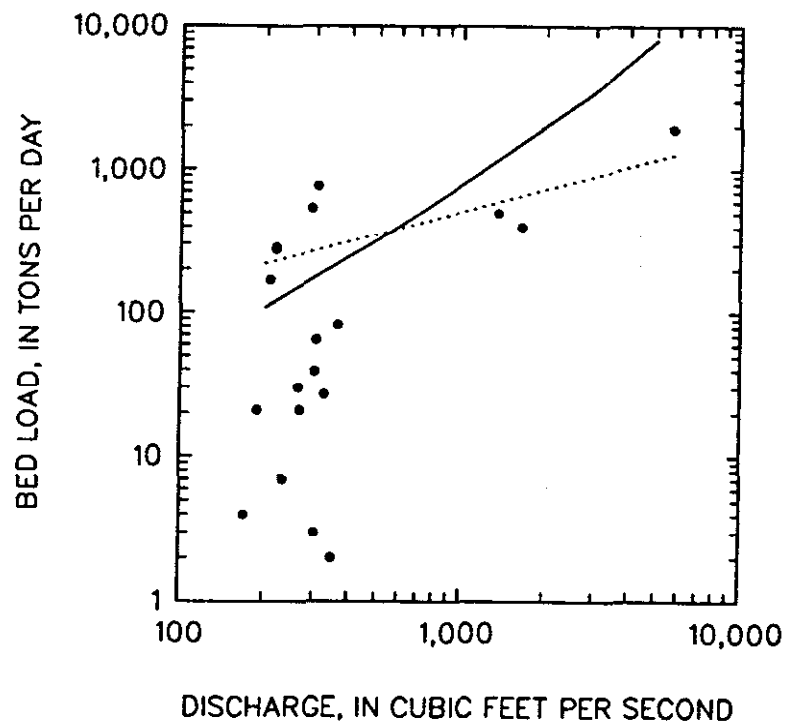

Figure 3. -- Bedload transport rates for all flows measured in 1988-89 at the Santa Cruz River at Tucson. Solid dots indicate bedload data, solid line indicates bedload estimated using Meyer-Peter and Muller equation, dashed line indicates best fit line through cross-section bedload transport rates.

section for more discussion of this model). Modeled bedload transport (fig. 3) adequately represents measured bedload transport below about 5,000 ft^3/s. Bed-material transport rates were then determined by adding bedload calculated using the Meyer-Peter and Muller equation to the bed-material component of suspended sediment.

Data for two small flows indicate some of the challenges of modeling sediment transport during rapidly varying flow. First, peak sediment transport is not consistently related to peak discharge. Peak sediment transport preceded peak discharge during the flow of August 17, 1989, whereas peak sediment transport lagged peak discharge during the flow of October 5, 1989 (fig. 4). Secondly, hysteretic C-Q relations are a major feature of sediment transport in ephemeral rivers (fig. 5). Finally, the flows are highly unsteady, although the flow from Hurricane Raymond (October 5, 1989) varied less rapidly than the flow that resulted from an isolated summer thunderstorm (August 17) (fig. 4).

MODELING SEDIMENT TRANSPORT

Sediment transport in the Santa Cruz River was modeled using GFLUVIAL, a 1 1/2-dimensional model (Chang, 1988, 1990). GFLUVIAL is based on a 1-dimensional solution of continuity and momentum equations using a flow-resistance equation

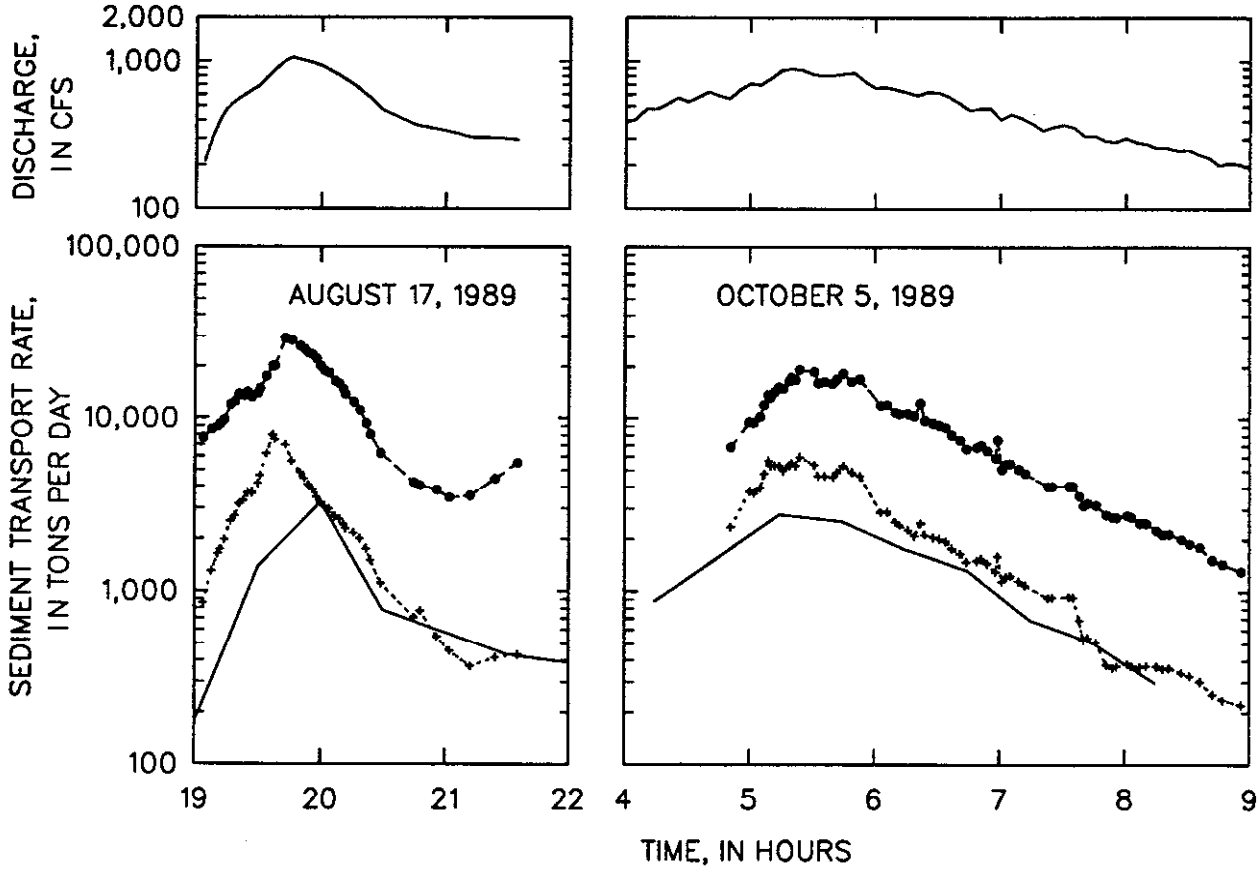

Figure 4. -- Hydrographs and total and bed-material transport rates for two flows in 1989 at the Santa Cruz River at Tucson. Solid lines in lower graphs indicate modeled bed-material transport rate using the model GFLUVIAL, dotted lines and crosses indicate bed-material transport rate, and dashed lines and solid circles represent total transport rate.

(e.g., Manning equation; Chang, 1990), and hydrographs are simulated by changing discharge in discrete time steps and assuming steady flow. GFLUVIAL allows a choice of five sediment-transport equations and the Meyer-Peter and Muller bedload equation. The Engelund-Hanson sediment-transport equation was used because it predicts bed-material transport better than most equations in sand-bed rivers (Brownlie, 1981; Chang, 1988). Roughness during flow was varied using the flow-resistance equation of Brownlie (1981, 1983), which in turn was used to estimate flow depth from discharge, slope, and bed-material size. The Brownlie method allows roughness to vary depending on scour, deposition, or bedforms that are modeled during simulated flow. Although GFLUVIAL also estimates lateral channel change, lateral erosion was not estimated because of soil-cemented banks. Therefore, only 1-dimensional model capability was used to model sediment transport in the Santa Cruz River.

To model sediment transport at the gaging station, twelve benchmarked cross sections were established over an 1,800-ft, nearly straight reach downstream from the bridge. A fixed-bed step-backwater model was calibrated for this reach by adjusting Manning n-values until the modeled stage-discharge relation approximated the stage-discharge rating curve for the gaging station. Low-flow Manning-n values (0.022-0.029) were reasonable for the channel conditions, but the low-flow values had to decrease 0.004 units as the depth increased from 1 to 7 ft (300-10,000 ft^3/s) to match the rating curve.

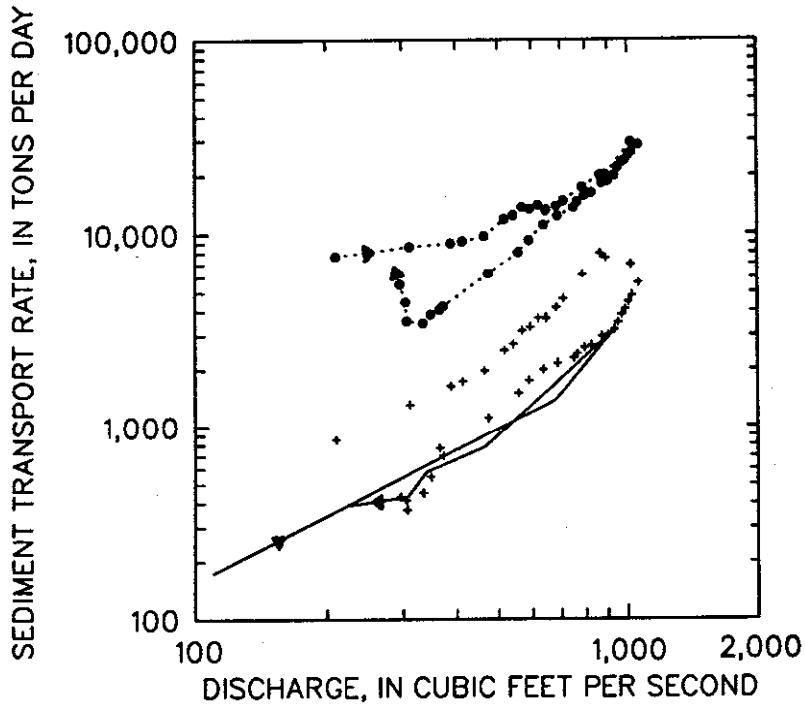

Figure 5. -- Discharges and total and bed-material transport rates for a flash flood on August 17, 1989. Solid line indicates modeled bed material transport rate using the model GFLUVIAL, crosses indicate bed-material transport rate, dotted lines and solid circles represent total transport rate, and arrows indicate the direction of change with time.

Bed topography, Manning n-values, hydrographs, and bed-material characteristics were used as inputs to GFLUVIAL. Most of the preliminary modeling effort was concentrated on two small flows in 1989 for which abundant data was available for verification of the sediment transport model. Despite small discharges (less than 1,100 ft^3/s), temporal change in sediment transport during these flows is typical of the larger floods that were measured less intensively.

Bed-material transport rates were modeled for the August 17 and October 5, 1989, flows using GFLUVIAL (fig. 4). Modeled and measured bed-material transport rates were within the same order of magnitude for both flows. However, modeled sediment transport was less than measured transport during the rising limb of the hydrograph and the modeled peak transport rate did not

correspond with the measured peak in time. The magnitude of hysteresis and the clockwise C-Q relation also were not modeled correctly (fig. 5), although the model results indicate that hysteresis should occur. For the August 17 flow, hysteresis was modeled as a figure-8 pattern instead of a simple clockwise rotation.

DISCUSSION AND CONCLUSIONS

Data collected from the Santa Cruz River at Tucson, Arizona, suggest that only about 22 percent of total sediment moving past the gaging station can be modeled using existing sediment-transport relations. The low percentage of sediment that can be modeled indicates that models based on bed-material transport relations cannot be used for sediment mass-balance estimates in ephemeral rivers unless particles larger than silt size are the only interest or only size being transported. However, the sediment transport that can be modeled may be of more interest for estimates of scour and lateral channel change.

Source area is an important factor in total sediment transport in ephemeral rivers. Only one storm (October 6, 1989) in the two-year study period caused runoff from the Nogales area to reach the gage (fig. 1). Suspended-sediment concentrations were higher for this flow than for most of the flows caused by local thunderstorms in the Tucson area. Each flow has a fairly well-defined hysteretic relation between sediment concentration and discharge (C-Q relation), whereas only a weak relation is apparent for all data. Flows generally have a rapid rise in suspended-sediment concentration up to peak discharge, followed by a decrease in concentration with a clockwise C-Q relation. This indicates that less total sediment is transported at a given discharge on the falling limb compared with the rising limb of the hydrograph.

The preliminary modeling results suggest that sediment-transport modeling based on steady-state hydraulics adequately estimates the magnitude of bed-material transport rates, but the model that was used may not be able to mimic some details of transport over the course of a flow hydrograph. For two small flows for which considerable data are available, GFLUVIAL was used to estimate the order of magnitude of peak bed-material transport rates but did not model timing of peak rates nor hysteretic C-Q relations well. The fact that hysteretic relations could be modeled at all is related to use of the Brownlie method for estimating roughness combined with predicted fining of bed material. The Brownlie method correctly indicated that roughness should decrease with increasing stage, which was already determined using a fixed-bed step-backwater model.

Future data collection efforts may be directed at obtaining detailed, high-frequency sediment-transport measurements for larger discharges than the two flows modeled in this study. Measurement of bed elevation during flows would allow an evaluation of the predicted scour from flows. Although bed-material sampling has been unsuccessful, bed-material samples are needed during flow to verify predicted changes in bed roughness and particle size. Verification of a model as complex as GFLUVIAL would necessarily involve simultaneous, high-frequency measurements of bed elevation, bed material, discharge, and sediment transport, which are extremely difficult to make during rapidly varying flows in ephemeral rivers.

ACKNOWLEDGMENTS

This study was funded by Pima County Department of Transportation and Flood Control District. John R. Gray and John T.C. Parker, U.S. Geological Survey, helped plan the study and collect samples from the Santa Cruz River. Gray and Julie B. Graf, U.S. Geological Survey, reviewed the manuscript.

REFERENCES

Brownlie, W.R., 1981, Prediction of flow depth and sediment discharge in open channels. Pasadena, Calif., Calif. Inst. Tech., W.M. Keck Lab. Hydr. Water Res. Rept No. KH-R-43A, 232 p.

Brownlie, W.R., 1983, Flow depth in sand-bed channels. J. Hydr. Engr. 109, 959-990.

Chang, H.H., 1988, Fluvial processes in river engineering. New York, John Wiley and Sons, 432 p.

Chang, H.H., 1990, Users manual, generalized computer program GFLUVIAL, mathematical model for erodible channels. San Diego, California, Department of Civil Engineering, San Diego State University, 47 p.

Chang, H.H., and Osmolski, Z., 1988, Computer-aided design for channelization. J. Hydr. Engr. 114, 1377-1389.

Edwards, T.K., and Glysson, G.D., 1988, Field methods for measurement of fluvial sediment: U.S. Geological Survey Open-File Report 86-531, 118 p.

Fan, S.S. (ed.), 1988, Twelve selected computer stream sedimentation models developed in the United States. Washington, D.C., Federal Energy Regulatory Commission, Interagency Advisory Committee on Water Data, Subcommittee on Sedimentation Report, 552 p.

Parker, J.T.C., 1990, Channel-changing processes on the Santa Cruz River, Pima County, Arizona, 1936-86. San Diego, CA, ASCE, Proc. Intl. Sym. Hydraul./Hydrol. Arid Lands, p. 441-446.

Rhoads, B.L., 1990, The impact of stream channelization on the geomorphic stability of an arid-region river. Natl. Geogr. Res. 6, 157-177.

Roberts, R.A., 1990, Analysis of sediment transport in an ephemeral stream. Tucson, Univ. Ariz. M.S. thesis, 45 p.

Saarinen, T.F., Baker, V.R., Durrenberger, R., and Maddock, T., Jr., 1984, The Tucson, Arizona, flood of October 1983. Washington, D.C., National Academy Press, 112 p.

Williams, G.P., 1989, Sediment concentration versus water discharge during single hydrologic events in rivers. J. Hydrol. 111, 89-106.

Woo, H.S., Julien, P.Y., and Richardson, E.V., 1986, Washload and fine sediment load. J. Hydr. Engr 112, 541-545.

ESTIMATING VELOCITIES AND SCOUR DEPTH IN RIVER CHANNEL BENDS

By Drew C. Baird, Chief River Assessment Branch, USBR, Albq. NM and David G. Achterberg, Senior Dam Safety Program Coordinator, USBR, Denver CO.

ABSTRACT

The scour of a pool on the outside of a meander bend can cause failure of riprap stabilization blankets. Estimating future bend velocities, and scour potential, therefore; are critical parameters for designing the size of the riprap stones and the thickness of the riprap toe section.

A one-dimensional, steady-state stream tube model has been used to vary the hydraulic characteristics across a cross section. This enables computation of higher velocities on the outside and lower velocities on the inside of a meander bend. Good agreement has been found between the measured longitudinal channel velocities and those computed by the model.

A modified application of the Blench scour equation, together with the computed channel velocities across the cross section were used to estimate scoured cross sections at 7,000 ft^3/s from cross sections measured at 4,000 ft^3/s. The computed cross sections compared favorably with the measured sections at 7,000 ft^3/s.

The model was then used to compute channel velocities across the cross section for the bankfull discharge. Using the bankfull longitudinal velocities and the Blench equation, scour across the cross section was computed and new cross sections were developed for the design scour case, at 10,000 ft^3/s.

INTRODUCTION

The velocity structure, sediment transport characteristics, and associated bed topography in alluvial channel bends has been studied by Yen (1970), Kikkawa et. al. (1976), Odgaard (1984,1986), Chang (1988), and others. In a channel bend there is a transverse bed slope, and a mass shift of flow towards the outside bank (Odgaard, 1986), due to both the point bar and a radial centrifugal force component. This results in higher outside bank and lower inside bank velocities. Secondary currents in the transverse direction have magnitudes of about 15 percent of the average channel velocity (Simons, 1971). The secondary currents play a major role in the development of point bars and the shape of the transverse bed slope. The shape of the transverse bed slope influences the depth of scour along the outside bank of a meander bend. Much of the recent research effort has been to analytically address the difficulties of estimating the transverse bed slope and associated pool scour. Previous research empirically related scour depth to one-dimensional hydraulics, bed material size, and an appropriate adjustment for increased scour in bend ways. The flow velocities along the concave bank cause pool scour that can result in failure of riprap stabilization blankets. Therefore, estimating the lateral variation of bend velocities and the depth of scour, is necessary to design the size of riprap stones and toe protection.

This paper describes an estimating technique that successfully models the lateral velocity variation in a channel bend and can be economically used by designers to predict scour under design flow conditions. In addition a comparison has been made of the scour estimates using several scour computation proceedures. A modified application of the Blench scour equation (Pemberton and Lara, 1984) was used together with the lateral velocity variation to compute scour across the cross section and to develop new cross sections for the design scour case.

FLOW MODEL

The flow conditions described above are quite different than those computed by a one-dimensional water and sediment routing model, which cannot simulate non-uniform velocity distributions, and scour and depositional processes. A model was developed by the U.S. Bureau of Reclamation (Orvis and Randle, 1986, 1987) called STARS (Sediment Transport and River Simulation). STARS utilizes a one dimensional steady state stream tube approach to simulate the lateral variation of hydraulic properties across a cross section. The STARS model can be used as a fixed or moveable bed simulator. The model utilizes a standard step method backwater procedure which solves the energy equation, and includes a contraction and expansion eddy loss term, an energy correction coefficient for each cross section, and varying channel lengths across a cross section for use in channel bends. The model can also handle critical and incremental discharges.

Once the model converges on an upstream section water surface, the conveyance for each stream tube is found by dividing the total conveyance by the number of stream tubes (10 maximum). The model then computes the hydraulic properties for each tube (Randle, personal conversation 1989). The conveyance for the area between each coordinate pair is computed and summed as the procedure moves from the lowest to the highest position coordinate . When the summed conveyance equals that for each stream tube, the velocity for the tube is computed. The process is repeated until the properties for each stream tube across the cross section have been computed. A scheme is included to find the width of each tube when the tube boundary does not lie on a coordinate point.

The equation to compute the conveyance K is:

$$K = \sum_{\substack{i=1 \\ j=1}}^{\substack{n \\ m}} \frac{1.486}{N_j} A_i R_i^{2/3} \qquad (1)$$

Where; i denotes the coordinate points, m is the number of coordinate pairs for a cross section (200 maximum), j denotes the number of roughness segments, n is the number of roughness segments across the cross section (10 maximum), N is Manning's roughness coefficient, A is the area, and R is the hydraulic radius.

It is the change in hydraulic radius R, across the cross section which results in the computation of variable velocity for each stream tube. Therefore, the shape of the modeled cross section must be similar to the estimated future section to provide a valid velocity simulation.

SCOUR ESTIMATING

The Blench scour equation from Pemberton and Lara (1984) is a regime equation which relates the design flow discharge per unit width to the Blench "zero bed factor". Both hydraulic and bed material size data are required for this method. The Blench equation is as follows:

$$d_{fo} = \frac{q_f^{2/3}}{F_{bo}^{1/3}} \qquad (2)$$

Where; d_{fo} = depth for zero bed sediment transport, ft., q_f = the design flood discharge per unit width, ft^3/s, and F_{bo} = Blench's "zero bed factor", ft/s^2.

The depth of scour is then found from the equation:

$$d_s = Z \; d_{fo} \qquad (3)$$

Where; d_s = the depth of scour below the measured stream bed, Z = a multiplication factor, equal to 0.6 for straight reaches, and moderate and severe bends. Right angle bends have values of 1.25, implying that Z values larger than 0.6 may be applicable for more severe bend.

SIMULATION OF FLOW HYDRAULICS

The simulation of flow hydraulics through the Santo Domingo reach of the Rio Grande in New Mexico has been previously reported (Baird and Achterberg, 1989) and is briefly summarized here. The simulation was based on two sets of field data collected in 1985, with additional data collected in 1986 and 1988. The 1985 data was collected for discharges ranging from 4,150 to 5,000 ft^3/s, and the second set from 5500 to 7,000 ft^3/s. The data sets were calibrated to determine the average reach Manning's roughness coefficient which was 0.032. Using 10 stream tubes the average velocities across each section were computed. Figure 1 shows the average stream tube velocity plotted at the mid point of each tube, the measured depth, and the measured depth averaged velocities. Figure 1 also shows how the simulation was improved when the roughness was varied across the section. The Manning's roughness was varied from the inside to the outside of the main channel in the following fashion: 0.022, - 0.029, - 0.032, - 0.035, - 0.045. For crossing sections, the simulated velocities computed with a uniform roughness compared well with the measurements. Therefore, the need to vary the roughness across a section is

unique to bends. The increased roughness on the outside of the bend simulates the influence of bed form roughness (i.e. greater wetted perimeter) and greater turbulence due to higher velocities and secondary currents.

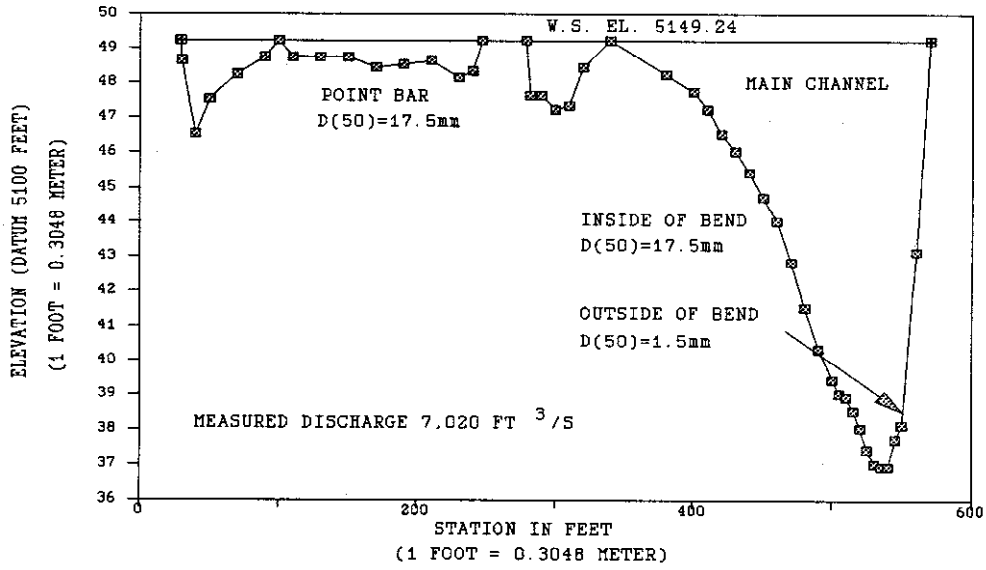

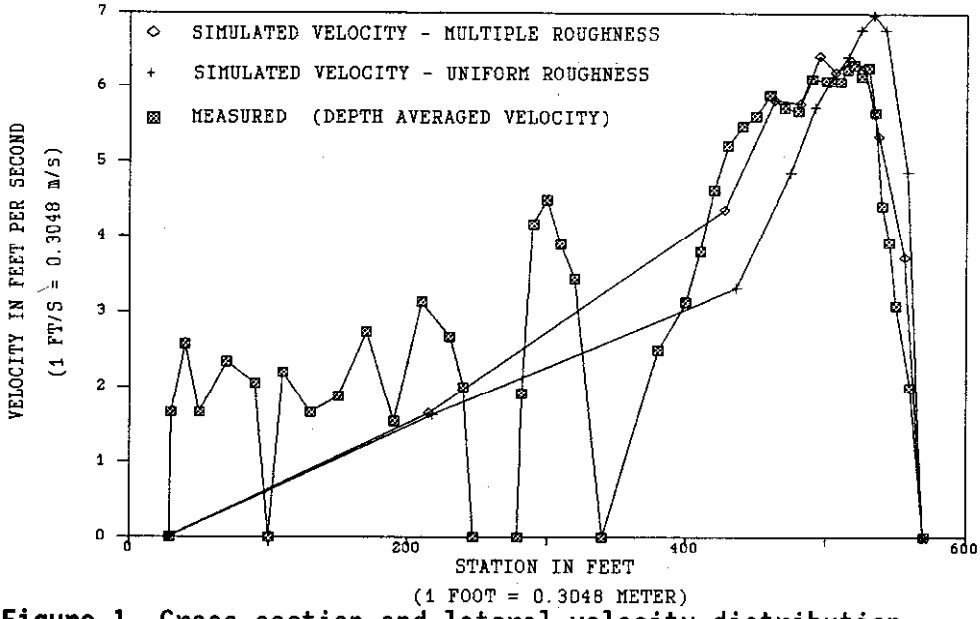

Figure 1 Cross section and lateral velocity distribution

CROSS SECTION COMPUTATIONS

The stream tube hydraulics were applied with the Blench scour equation to find the scour bed elevation. By using the unit discharge q, for each of ten stream tubes, it was found that the Blench equation's depth for zero bed sediment transport d_{fo} was equal to the measured depth in the channel. Therefore, the Blench equation (equation 2) could be used directly to compute the scoured channel depth without using the Z multiplication factor as defined in equation 3. Figure 2 shows the main channel cross section computed from the Blench equation and the stream tube hydraulics together with the measured cross section (measured at 7,000 ft^3/s.)

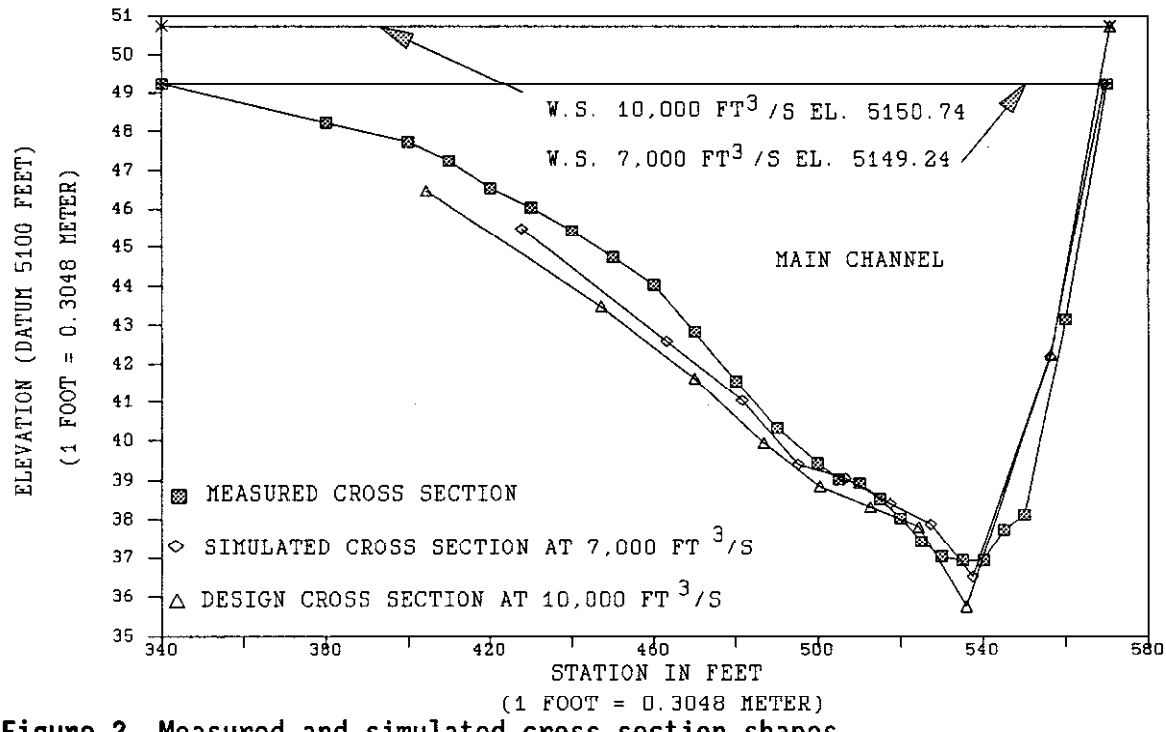

Figure 2 Measured and simulated cross section shapes

The scour simulation technique was verified by using cross sections measured at 4,000 cfs to estimate the cross section shapes measured at 7,000 ft^3/s. The stream tube hydraulics at 7,000 ft^3/s were computed using the cross sections measured at 4,000 cfs. The Blench depth for zero bed transport d_{fo} was computed for each tube and compared to the measured cross section at 7,000 ft^3/s. Figure 3 shows a plot of the measured cross section at 4,000 ft^3/s and 7,000 ft^3/s together with the computed cross section for 7,000 ft^3/s simulated from the measured 4,000 ft^3/s cross section. The Blench equation compares favorably with the measured data; therefore, this method was used to predict the scour and cross section shape for other discharges.

The initial simulation of scour at 10,000 ft^3/s predicted a greater scour depth than at 7,000 ft^3/s in the maximum section. However, due to the higher water surface elevation, the predicted bed elevation was above the bed

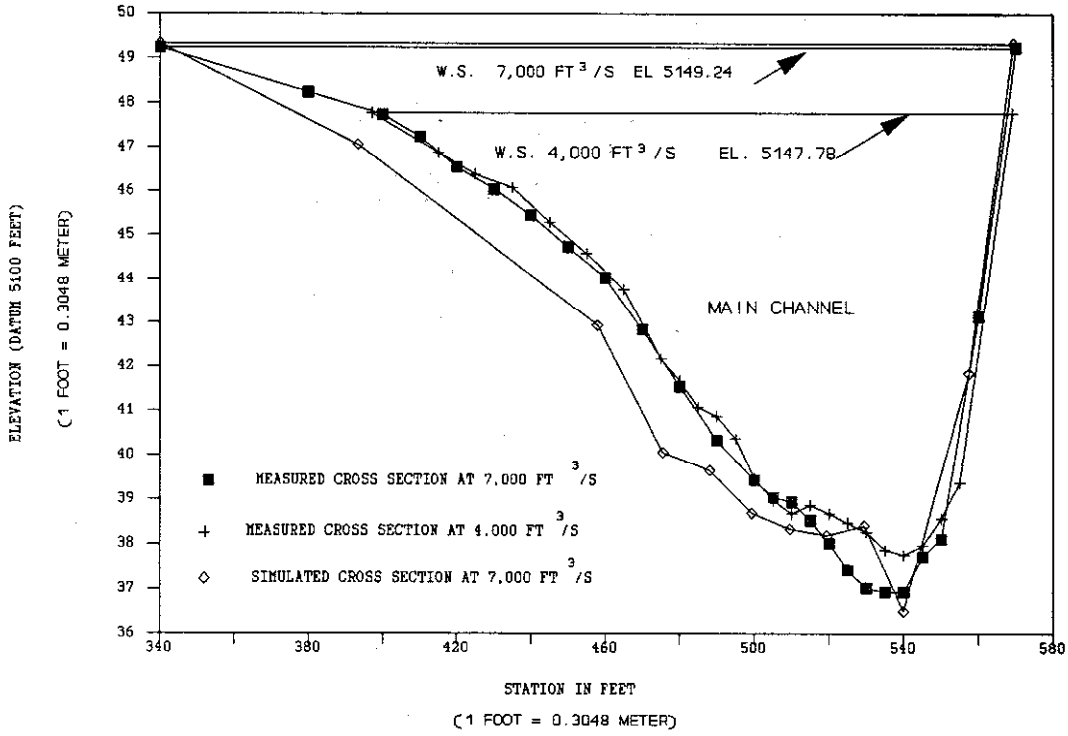

Figure 3 Comparison of simulated and measured cross sections at 7,000 ft^3/s

predicted in the 7,000 ft^3/s simulation. The 10,000 cfs simulation also indicated that deposition should be occurring on the bar. Bar deposition has been observed at high discharges in this reach. Therefore, the bar was transformed to reflect deposition. The average scour depth predicted was compared to the average stream tube depth to determine deposition. The deposition for each stream tube was added to the elevation coordinate, and another scour prediction computed. Several iterations of this procedure were required until the simulation no longer predicted significant bar deposition. Figure 2 shows the main channel scour which would be used for design of riprap bank protection at 10,000 ft^3/s.

SCOUR COMPUTATION COMPARISON

The Blench and Lacey methods of scour computations were applied in the recommended way (Pemberton and Lara, 1984). For the 1988 Santo Domingo reach design data set the scour depth using the STARS model and the modified application of the Blench equation was compared to both the usual Blench and Lacey approaches. The Blench and Lacey Z values used were 0.6, and 0.75, respectively. The average of the Blench and Lacey equations was 2.6 ft. lower than the stream tube approach. This reduced scour depth of 2.6 ft. results in an estimated savings of 0.53 cubic yards per lineal foot of riprap or $ 17.00 per lineal foot based on a cost estimate of $33.00/cubic yard for riprap development and installation.

METHOD LIMITATIONS

The modified application of the Blench scour equation together with stream tube hydraulics successfully modeled scour in the Santo Domingo reach for the available data. This methodology has also been used in the Espanola reach of the Rio Grande. Good agreement was found between the measured and computed channel cross sections using the bank full discharge. The Espanola and the Santo Domingo channels have similar characteristics. Both have well defined pools and riffles, gravel point bars, fine bank materials, and the sediment transport rates are supply limited. River reaches where this approach may not apply are those with; 1) high bed load transport rates of sand sized materials, 2) wide channels with a shifting thalweg, and 3) upper regime sediment transport conditions.

CONCLUSIONS

The one-dimensional, steady-state, stream tube model, STARS, produced good simulation of the lateral variation in velocity in a cross section. Uniform roughnesses were used in the model to simulate the lateral change in velocity for crossing section and multiple roughnesses were used to simulate the lateral change in velocities in bends. The stream tube hydraulics could then be used with empirical local scour equations to economically predict scour for designing riprap bank stabilization.

REFERENCES

Baird,D.C., and Achterberg,D.G., (1989) "Estimating Velocity and Scour in River Bends", Proceedings of the International Symposium on Sediment Transport Modeling, Wang, Sam S.Y. Editor, ASCE, New York, NY.

Chang, H.H., (1988), "Fluvial Processes in River Engineering", John Wiley and Sons, New York.

Kikkawa, H., Ikeda, S., and Kitagawa, A. (1976), "Flow and Bed Topography in Curved Open Channels", Journal of Hydraulic Engineering, ASCE 102(HY9), 1317-1342.

Odgaard, A.J. (1984), "Flow and Bed Topography in Alluvial Channel Bend", Journal of Hydraulic Engineering, ASCE 110(HY4), 521-536.

Odgaard, A.J. (1986), "Meander Flow Model. I: Development", Journal of Hydraulic Engineering, ASCE 112(HY12), 1117-1136.

Orvis, C.J. and Randle, T.J. (1986), "Sediment Transport and River Simulation Model", Proceedings of the Fourth Federal Interagency Sedimentation Conference, Las Vegas, Nevada.

Orvis, C.J. and Randle, T.J. (1987), "Stars: Sediment Transport and River Simulation", Technical Guideline, U.S. Bureau of Reclamation, Denver Colorado.

Pemberton, E.L. and Lara, J.M. (1984), "Computing Degradation and Local Scour", Technical guideline, U.S. Bureau of Reclamation, Denver, Colorado.

Randle, T.J. (1989) personal conversation, Hydraulic Engineer, Earth Sciences Division, Surface Water Branch, Sedimentation and River Hydraulics Section, U.S. Bureau of Reclamation, Denver, Colorado.

Simons, D.B. (1972), "River and Canal Morphology", River Mechanics Vol. II, Shen, H.W. Editor, Water Resources Publications, Fort Collins, Colorado.

Yen, C.L. (1970), "Bed Topography Effect on Flow in a Meander", Journal of Hydraulic Engineering, ASCE 96(HY1), 57-73.

NUMERICAL SIMULATION OF TRANSIENT SEDIMENT LADEN FLOW IN AN ALLUVIAL CHANNEL

Jinn–Chuang Yang, Associate Professor
Kuan–Ping Chiu, Graduate Student
Department of Civil Engineering
National Chiao Tung University
Hsinchu, Taiwan, 30050

ABSTRACT

This article introduces a sediment transport model which is especially suitable for simulating the bed evolution along the downstream channel of reservoir in Taiwan under the peaky flood condition. The governing equations used for this model consist of a set of three partial differential equations — the sediment continuity equation and equations of continuity and motion for sediment–laden flow. These equations where transformed into three pairs of characteristic and compatibility equations. The method of characteristics with the fixed time–space grid system is used to solve these equations. Since the fixed grid system is used, the interpolation for the solution is always inevitable. In this article, instead of the commonly–used linear interpolation, the cubic interpolation technique is used. In addition, the reach–back scheme is used for the bed wave characteristics, which is expected to give the better results.

INTRODUCTION

The construction of a dam at the upstream of stream can always induce a progressive change of the channel bed elevation. This bed–level change, or degradation/aggradation will cause numerous environmental and structural problems including potential undermining of bank protection works and bridge foundations, and reduce efficiency of water intake works etc. For performing the future planning for the river system development and management, it is necessary to predict the future course of bed–level change affected by the build–up of a dam. For Taiwan's rivers, the construction of a dam has also caused the river stability problems. The major cause for the river bed change in Taiwan's river is not the sediment cutoff by the dam, but the large amount of sediment evacuated from the reservoir. In Taiwan, most streams carry very little water except the floods occurring two or three times in a year. The sediment evacuation is conducted during the flood period to use the large amount of water to flush the deposited sediment out of the reservoir. Nevertheless, the large amount of sediment carried by the flood transmitting to the downstream channel can cause serious change of the river pattern. The prediction of such impact caused by the sediment evacuation from the reservoir to the downstream channel has become an important issue to be investigated in Taiwan. In order to be able to accurately simulate the movement of the sediment carried by the peaky flood for most of Taiwan's streams with a steep slope, a sediment transport model has been developed. This model is expected to be capable of simulating the sediment movement along the downstream channel of reservoir under the unsteady condition. The characteristics method is tentatively used for this model to simultaneously solve the three governing equations consisting of water continuity and momentum equations and the sediment continuity equation. The set of governing equations will be transformed into a set of characteristics equations, three distinct characteristics are obtained. Two of the characteristics represent

the propagation of hydrodynamic waves which in fact are similar to the case of unsteady water flow computation, and the third represents the propagation of bed deformation. For solving these three characteristic equations, one can apply the method of characteristics with specific time intervals(MOC) in combination with linear spatial interpolation at the present time level(Chang & Wang, 1972; Wu, 1973). However, with the use of this kind of model, the time step is severely limited by the courant constraint, and the coupling of hydrodynamic and transport processes is not so effective due to the great disparity between the speeds of surface and bed–deformation waves. Lai(1988) has proposed a multimode scheme which can simultaneously solve unknowns by the implicit mode along the rapidly traveling hydrodynamic characteristics, as well as by temporal of spatial reachback scheme along the slowly moving bed–deformation characteristics. However, for these methods mentioned above the interpolation is always needed since the fixed grid system is used. Usually, the linear interpolation technique is used, which can cause a tremendous extent of errors to the solution. This may overwhelm the benefit from the multimode technique. In this article, the cubic interpolation technique is used to incorporate with the characteristics method to tentatively reduce the errors induced by the interpolation. This article will introduce the mathematical formulations for this new method for the mobile bed modeling. The expected difficulties and problems are also stated. This model will be applied to the study of bed evolution along the downstream channel of reservoir in Taiwan.

GOVERNING EQUATIONS

For sediment–laden flow in a unit width of cross section of an alluvial channel, the governing equations can be written as follows [Lai, 1988]:

$$\frac{\partial h}{\partial t} + \frac{\partial uh}{\partial x} + \frac{\partial z}{\partial t} = 0 \tag{1}$$

$$\frac{\partial hC}{\partial t} + \frac{\partial uhC}{\partial x} + (1-P)\frac{\partial z}{\partial t} = 0 \tag{2}$$

$$\frac{\partial u}{\partial t} + u\frac{\partial u}{\partial x} + g\frac{\partial h}{\partial x} + g\frac{\partial z}{\partial x} + \left[\frac{\gamma_s - \gamma_w}{\gamma_m}\right]\frac{gh}{2}\frac{\partial C}{\partial x} - \frac{[(1-P)\gamma_s + P\gamma_w]}{\gamma_m}\frac{u}{h}\frac{\partial z}{\partial t} = g(S_o - S_f) \tag{3}$$

in which P = porosity; g = gravitational acceleration; u = flow velocity; C = sediment concentration; h = flow depth; z = active sediment layer; γ_s = sediment specific gravity; γ_w = water specific gravity; γ_m = specific weight of sediment–laden water; S_o = bed slope; S_f = energy slope; t = time; x = distance. In the above equations, Eq. (1) is the sediment–laden flow continuity; Eq. (2) is the sediment continuity; Eq. (3) is the momentum equation for sediment–laden flow.

With the use of a simple power relation, $C = ku^a h^b$ for the sediment transport capacity, appearing in Eqs (2) & (3), the system of Eqs (1) to (3) can be reduced to three unknowns (u,h,z).

The characteristic equation and compatibility equation for the above equations have been derived by Lai [1988], which can be restated as follows:

$$\lambda_i = \left[\frac{dx}{dt}\right]_i = y_i + \frac{2}{3}u \qquad i = 1,2,3 \tag{4}$$

$$L_i = S_i\frac{Dh}{Dt} + T_i\frac{Du}{Dt} + P_i\frac{Dz}{Dt} + F_i = 0 \tag{5}$$

in which

$$S_i = \mu_i + \psi;\ T_i = \omega h + \nu_i;$$

$$P_i = \mu_i + (1-P)\ ;F_i = \nu_i g(S_f - S_o);$$

$$\psi = \frac{\partial C}{\partial h};\ \omega = \frac{\partial C}{\partial u}\ ;$$

$$\mu_i = [\frac{\varphi}{\mu}]\lambda_i - \psi\ ;\ \nu_i = [\frac{\varphi}{g}]\lambda_i[\frac{\lambda_i}{\mu} - 1];$$

$$\varphi = \psi - (1-P);\ y_1 = 2\sqrt{-P/3}\cos\theta/3;$$

$$y_{2,3} = -2\sqrt{-P/3}\cos\frac{\theta+\tau_1}{3}\ ;\ \theta = \cos^{-1}[\frac{-q}{2\sqrt{-(P/3)^3}}]$$

Lai and Chang [1987] have indicated that $\lambda_1\lambda_2\lambda_3 < 0$. This result leads to that there must be an odd number of negative–valued characteristic roots. For subcritical flow, it is known that $\lambda_1 \approx \mu+c > 0$ and $\lambda_2 \approx \mu-c < 0$, in which $c = \sqrt{gh}$. Therefore, for a subcritical flow λ_3 must be positive, $\lambda_3 > 0$; and for a supercritical flow $\lambda_3 < 0$. The characteristic direction for these water wave propagation and bed deformation can be shown in the following schematic space–time figures, Figs.1 & 2.

REVIEW OF MULTIMODE SCHEME

In order to better handle the great disparity between the magnitudes of λ_3 and λ_1 , λ_2 in maintaining a coupled computational algorithm, Lai [1988] has proposed the multimode scheme which combines the implicit & reachback schemes together. The schematic diagrams for the characteristics trajectories of this scheme are shown in Figs. 3 & 4.

As shown in Fig. 3, the characteristics λ_1 & λ_2 intersect the adjacent time line at 1 & 2 within the present time step. To interpolate quantities at 1 & 2 from adjacent grid points, involves additional unknowns at points S and Q. Therefore this scheme is usually referred to as implicit scheme.

The value for λ_3 is always small. Therefore, the characteristics may be projected back beyond the present time level for temporal interpolation at the adjacent time tine, as shown in Fig. 3. This is so called temporal reachback scheme.

However, for mobile problem, λ_3 is so small that it always needs a very large reachback time steps to apply the temporal reachback scheme. In order to present the number of reachback time steps from growing too large, a limit can be set for λ_3 at which a spatial interpolation can be used instead of temporal interpolation, as shown in Fig. 4.

Lai has combined the aforementioned three schemes, with the classical scheme as a special case, into one scheme for affording better coupling of hydrodynamic and bed–deformation waves.

For the above–mentioned computational scheme, Eqs. (4) & (5) can be converted to the corresponding finite–difference expressions:

$$x_p - x_i = \lambda_{ip}(t_p - t_i) \tag{6}$$

$$S_{ip}(h_p - h_i) + T_{ip}(u_p - u_i) + P_{ip}(z_p - z_i) + F_{ip}(t_p - t_i) = 0 \tag{7}$$

Lai used the time/space linear interpolation technique to solve the variables ϕ = (h,u,z).

$$\phi_1 = \xi_1\phi_{j-1}^{k} + \xi_1'\phi_{j-1}^{k+1}; \quad \phi_2 = \xi_2\phi_{j+1}^{k} + \xi_2'\phi_{j+1}^{k+1};$$
$$\phi_3 = \xi_3\phi_{j-1}^{k-m} + \xi_3'\phi_{j-1}^{k+1-m}; \quad \phi_4 = \xi_4\phi_{j-1}^{k+1-m} + \xi_4'\phi_{j}^{k+1-m}; \tag{8}$$

The factors ξ_1 , ξ_2 , and ξ_3 or $\xi 4$ can be calculated from Eq.(6) as :

$$\xi_1 = [\frac{\Delta x_j}{\Delta t}]/[\frac{dx}{dt}]_{1p} = \frac{r_j}{\lambda_{1p}}$$
$$\xi_2 = -[\frac{\Delta x_{j+1}}{\Delta t}]/[\frac{dx}{dt}]_{2p} = \frac{-r_{j+1}}{\lambda_2}$$
$$m_3 + \xi_3 = [\frac{\Delta x_j}{\Delta t}]/[\frac{dx}{dt}]_{3p} = \frac{r_j}{\lambda_{3p}} \tag{9}$$
$$\xi_4 = [\frac{M\Delta t}{\Delta x_j}]/[\frac{dx}{dt}]_{4p} = \frac{M\lambda_{4p}}{r_j}$$

in which M is the maximum reach–back number; $r = \Delta x/\Delta t$
The compatibility equations along the characteristics C_i can be written from Eq. (7) with h_i , u_i , and ξ_i replaced by the corresponding expressions given in Eq. (8).

With two upstream boundary conditions and one downstream boundary condition, one can close the system of equations to construct a matrix equation of the form AZ = B. Here A is the coefficient matrix, Z is the column unknown vector, and B is the column known quantities. This can be solved by any matrix solution technique.

CUBIC INTERPOLATION TECHNIQUE

However, it is known that the linear interpolation can cause a great numerical damping and phase errors. In this paper, instead of the linear interpolation technique described above the cubic interpolation technique is used to compute the variables ϕ_i . In fact, the cubic interpolation technique has been used to solve the dispersion equation which was proposed by Holly & Preissmann [1977].

The key of Holly–Preissmann method is to use the dependent variables and its derivatives at the adjacent two points as the parameters to construct the interpolation polynomials. When the cubic interpolation is used, Eq. (8) has to be written as follows:

$$\phi_1 = a_{11}\phi_{j-1}^{k} + a_{12}\phi T_{j-1}^{k} + a_{13}\phi_{j-1}^{k+1} + a_{14}\phi T_{j-1}^{k+1}$$
$$\phi_2 = a_{21}\phi_{j+1}^{k} + a_{22}\phi T_{j+1}^{k} + a_{23}\phi_{j+1}^{k+1} + a_{24}\phi T_{j+1}^{k+1} \tag{10}$$

$$\phi_3 = a_{31}\phi_{j-1}^{k-m} + a_{32}\phi T_{j-1}^{k-m} + a_{33}\phi_{j-1}^{k+1-m} + a_{34}\phi T_{j-1}^{k+1-m}$$

$$\phi_4 = a_{41}\phi_{j-1}^{k+1-m} + a_{42}\phi X_{j-1}^{k+1-m} + a_{43}\phi_{j}^{k+1-m} + a_{44}\phi X_{j}^{k+1-m}$$

in which a_{11} , a_{12} , ..., a_{44} are the coefficients which can be derived by following Holly & Preissmann's idea[1977] ; ϕT is the time derivative of ϕ, $\frac{\partial \phi}{\partial t}$; ϕX is the space derivative of ϕ, $\frac{\partial \phi}{\partial X}$.

The use of Holly–Preissmann's method introduces uT, hT, zx or zT as new dependent variables. Therefore, four additional equations are required to evaluate ux, hx and zx or zT. These four equations can be obtained by taking the derivation of Eq. (7) with respect to x or t.

This method may have the potential to improve the accuracy over that of the linear interpolation method but the complexity of the mathematical formulation and the additional variables may cause program coding problem and some other difficulties which are described in the following section.

DIFFICULTIES EXPECTED

Several difficulties in practical use of this method can be identified at the outset. The first problem is in the treatment of boundary values of ux, hx, zx or zT. The evaluation of these boundary values is very difficult since no analytical values are available. The error induced at the boundary point for the mobile bed problem can retain for a very long time and propagate downstream due to the fact of the slow bed wave motion. Hence, the unsuitable evaluation for these derivatives of dependent variables may make the accuracy of computation rather poor.

The second problem is in the approximate integration of the characteristic equations. First–order integration is easy and commonly used but not adequate for accurate computation. When the strong nonlinearity appears, faithful integration along the trajectory is especially important. However, accurate integration of the energy term seems extremely difficult, which may make it difficult to achieve good accuracy in computed values of uT, hT, zx or zT.

The third problem is in the coding of program. Since the reachback technique is used for the bed deformation equation, one needs to determine the values of reachback number for each computation point at time step. In addition, the program has to be so designed to memorize the values of dependent variables at the reach–back time level.

CONCLUSION

The evacuation of sediment from reservoir during the flood period, which occurs very often for Taiwan's reservoirs, has caused severe change of channel pattern. In order to study how the downstream channel of the reservoir is affected by the sediment carried by a peaky flood flow, a numerical model has been tentatively developed. The multimode scheme which has been verified by Lai to be the most suitable method for the highly unsteady sediment transport problem, is used for this model. In addition, for the purpose of avoiding the excessive error induced by the interpolation procedure used for the fixed grid characteristics method, the cubic interpolation technique is used. This article briefly introduces the mathematical formulations of this newly–developed model. By the time of writing this paper, no solid results has been obtained yet. Therefore, no analysis can be presented in this paper. However, in principle, it is expected that the better results should

be able to be obtained with the use of cubic interpolation technique.

ACKNOWLEDGEMENTS

The writers would like to express their appreciations to Dr. C.T. Lai who provided his papers related to this article, and gave many valuable suggestions. Partial support by the National Science Council of Taiwan under the grant number NSC78–0414–P009–01B is gratefully acknowledged.

REFERENCES

1. Chang, F.F.M., and Wang, T.W., "Scour and Fill in the Missouri River as related to the Water Resources Planning", Completion Rep. for Proj. No.B–008–SDAK, South Dakota State Univ., Brookings, S.D., 1972.
2. Lai, C.T., "Numerical Modeling of Unsteady Alluvial–Channel Flow Using the Multimode Method of Characteristics", 14th Southeastern Conference on Theoretical and Applied Mechanics, Biloxi, Mississippi, 1988.
3. Holly, F.M. Jr. and Preissmann, A., "Accurate Calculation of Transport in Two Dimensions", JHYD, ASCE, Vol.103, No. HY11, PP.1259–1277,1977.
4. Wu, C.M., "Unsteady Flow in Open Channel With Movable Bed", Proc. Int. Symp. River Mechanics, IAHR, Bangkok, Thailand, 3,447–488, 1973.

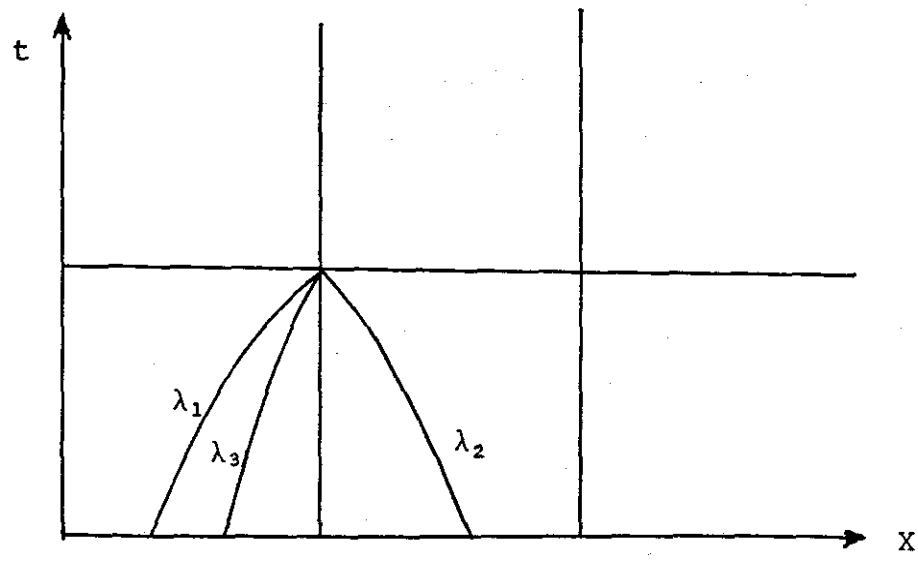

Fig. 1 Characteristics for subcritical flow

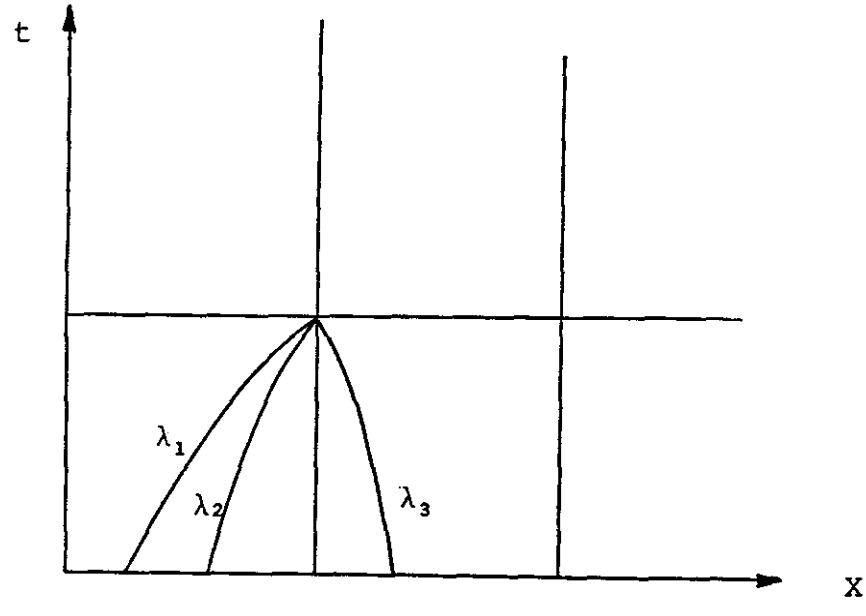

Fig. 2 Characteristics for supercritical flow

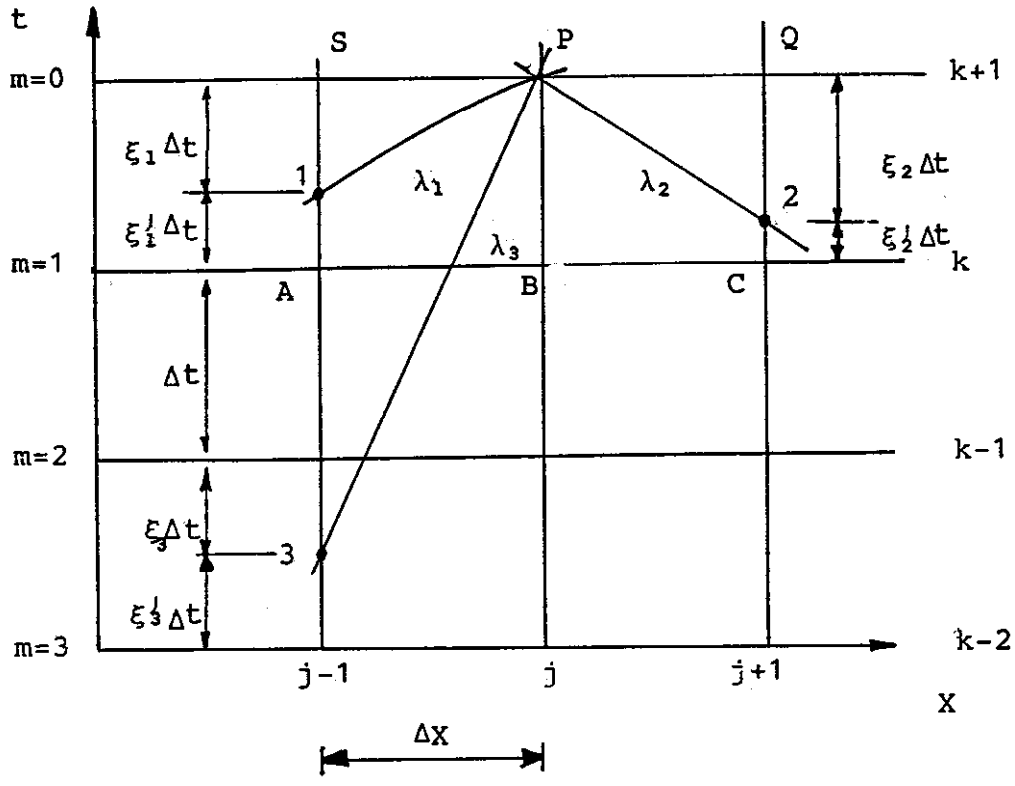

Fig. 3 Temporal reachback scheme

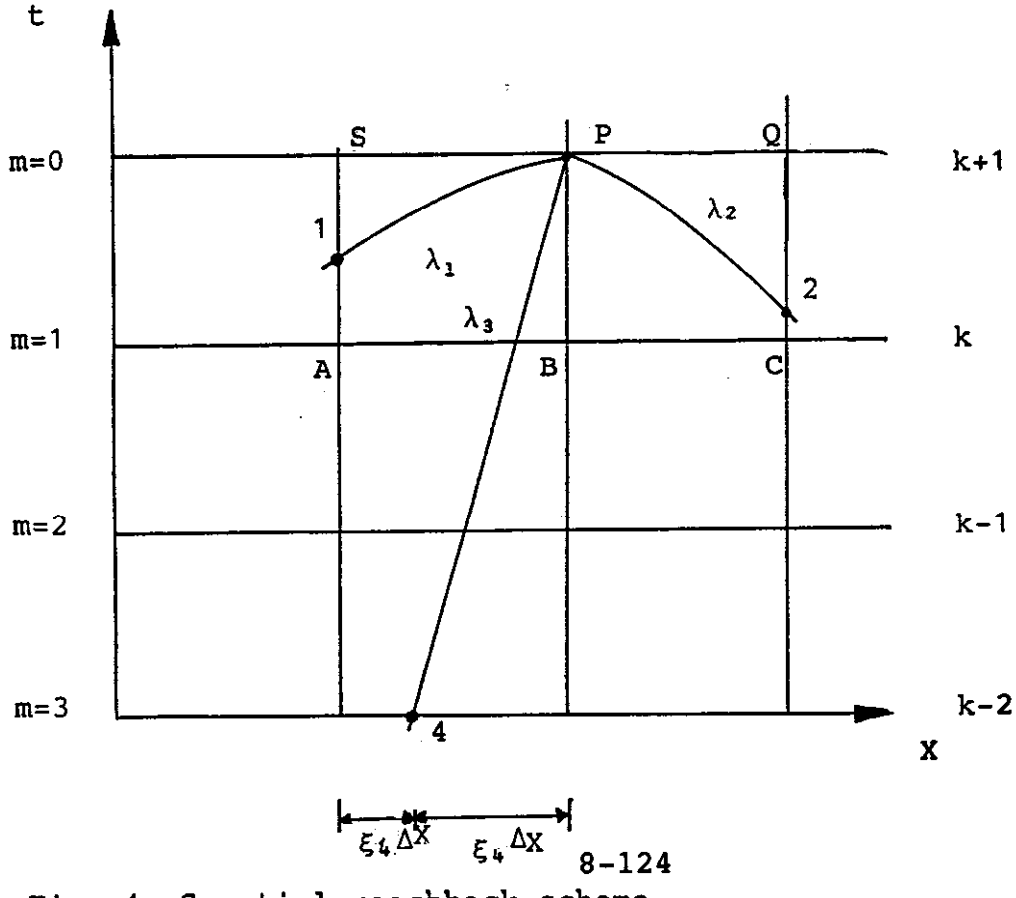

Fig. 4 Sepatial reachback scheme